TOWARDS A BETTER UNDERSTANDING OF COCHLEAR MECHANICS: A New Cochlear Model

A Thesis presented for the Degree of
Doctor of Philosophy
in
Electrical and Electronic Engineering
at the
University of Canterbury,
Christchurch,
New Zealand.

by

Paul Johannes Kolston
BE (Hons 1)

February 1989

Abstract

Improving our understanding of cochlear mechanics requires the analysis of cochlear models. In the formulation of such models, it is necessary to make assumptions as to the relative importance of the many structures which comprise the cochlear partition. Data on the relative motion of these structures are virtually non-existent, and so the accuracy of many of the assumptions made is questionable. The bulk of the content of this thesis relates to the formulation and analysis of a new type of linear mechanical cochlear model. The new assumptions made in the formulation of the model are justified on the basis of the structure of the cochlear partition. The apparent realism of the model (both its structure and certain features of its response) seriously questions the hypothesis that response tuning and changes in response resulting from trauma prove the existence of active processes in the cochlea. Furthermore, arguments are presented that question the validity of using the presence of spontaneous otoacoustic emissions to justify the existence of active processes in cochlear tuning. The new model suggests that the complicated structural geometry of the cochlear partition (particularly the organ of Corti) must be incorporated in a model before conclusions relating to real cochlear behaviour can be drawn from it. In particular, the model suggests that a mechanical second filter exists in the cochlea, from rather broad tuning in the pectinate zone of the basilar membrane to sharper, neural-like tuning in the arcuate zone. It is concluded that the only way to properly check the validity of cochlear models is to obtain more experimental data pertaining to the relative motions of the various components that constitute the cochlear partition. Before this is done, we should not place too much faith in our present (alleged) understanding of cochlear mechanics. Also presented in this thesis are new modelling techniques for improving the realism of electrical transmission line cochlear models: the ability to include longitudinal and radial mechanical coupling, multidimensional fluid motion and stick-slip friction. It is shown that the inclusion of mechanical coupling and two-dimensional fluid motion in the new cochlear model has a predictable (and trivial) effect on its response. The use of the stick-slip friction modelling technique is illustrated by means of two simple examples.

Acknowledgements

I am very grateful to Dr. Peter T. Gough for allowing me the freedom to pursue this field of research. I am indebted to Prof.dr. Egbert de Boer and Prof.dr.ir. Max A. Viergever for showing an interest in my work and for enabling me to undertake part of my studies in The Netherlands.

Thanks are due to those members of staff and postgraduate students in the Department of Electrical and Electronic Engineering, University of Canterbury, and in the Vakgroep Toegepaste Analyse, Faculteit Technische Wiskunde en Informatica, Technische Universiteit Delft, who provided me with technical help, companionship and amusement.

This work was financially supported by the Vakgroep Toegepaste Analyse, Faculteit Technische Wiskunde en Informatica, Technische Universiteit Delft, and by a Postgraduate Scholarship from the New Zealand University Grants Committee.

Preface

For at least the last five years virtually all literature on cochlear mechanics has made mention of an "active process" being necessary within the cochlea in order for it to produce the sharply-tuned mechanical response curves that have been recently observed experimentally. I believe that the evidence cited (to date) in support of the existence of such an energy-producing process is not convincing. In support of this conclusion, I have developed a passive cochlear model that exhibits certain features of cochlear response which previously required the incorporation of active processes in cochlear models.

Considering the anatomy of the cochlear partition (CP), it seems odd that few descriptions of cochlear mechanics have taken into account the gross radial structural differences of the CP. I have found that the division of the CP radially into two zones, combined with a few other assumptions, results in a passive cochlear model with realistic parameters being able to exhibit a sharply-tuned mechanical response, a realistic phase response, and show realistic response changes as a result of trauma. Even so, I do not believe that the new cochlear model described in this thesis is an accurate representation of the cochlea, since it ignores most of the structural features of the organ of Corti. However, all other cochlear models are (at best) equally deficient and so I believe that we must be more sceptical in our interpretations of modelling studies.

This thesis does not present an overview of cochlear mechanics. Topics such as non-linearities, electrophysiology, transduction, and mechanics of non-mammalian cochleae are completely ignored, since they do not contribute to the conclusions that can be drawn from the work described herein. A chapter-by-chapter description of the thesis contents now follows.

- The Introduction presents justifications for pursuing this field of research. A few definitions and abbreviations are also provided.
- In Chapter 2 the anatomy of the ear is briefly summarized. Obvious features of cochlear anatomy that seem to have been largely overlooked by other modellers are described in more detail. In particular, the gross structural differences between the arcuate and pectinate zones of the CP are emphasized.
- Chapter 3 includes a non-mathematical description of the formation of the travelling wave. Also presented in Chapter 3 is an overview of recent measurements of the mechanical response of the cochlea.

- Chapter 4 includes a critical review of the assumptions made in the formulation of cochlear models. Considering these assumptions in the light of cochlear anatomy and response (as described in Chapters 2 and 3), I conclude that *all* cochlear models may not represent those features of cochlear mechanics that are responsible for the cochlea's exquisite tuning. Active models are briefly reviewed and the formulation of transmission line cochlear models is described in detail.

- The new type of cochlear model that I have proposed is described in Chapter 5. This model has been the subject of a number of papers: Kolston (1988a,c), Kolston and Viergever (1989a), Kolston *et al.* (1989). In the formulation of this model, the CP is divided radially into its two zones, and the presence of the outer hair cells greatly alters the mechanics of the arcuate zone. The model simulates realistic selectivity and phase response, and realistic changes in response as a result of trauma, without needing to incorporate active processes. The model's response is evaluated on the basis of recent experimental mechanical response data.

- Electrical transmission line (ETL) cochlear models have a number of unique advantages over other modelling techniques. The most obvious is that when an ETL model is realized as a physical circuit, its response is available in real time to real inputs (e.g. speech), thereby enabling direct observations of its operation and response. Until now, such models have been deficient in that they did not include mechanical coupling in the CP nor, more importantly, multi-dimensional fluid motion. Chapter 6 describes two new modelling techniques which enable incorporation of these two features in an ETL model. The effect of adding mechanical coupling and two-dimensional fluid motion to the new cochlear model (described in Chapter 5) is assessed.

- The Discussion presents an appraisal of the new model, and the Conclusion comments on the model's significance and makes suggestions on how best to further improve our understanding of cochlear mechanics.

- The Appendix presents a new technique for modelling stick-slip friction, a form of friction that may play a role in cochlear micromechanical fluid motion. The technique enables incorporation of stick-slip friction in an ETL cochlear model, but this has not been attempted. Instead, two test examples are used to illustrate the validity of the technique.

Some of the work contained in this thesis has appeared (or will appear) in published form:

Kolston, P.J. (1988a). Sharp mechanical tuning in a cochlear model without negative damping. Journal of the Acoustical Society of America, Vol. 83, pp 1481-1487.

Kolston, P.J. (1988b). Modeling stick-slip friction using electrical circuit analysis. ASME Journal of Dynamic Systems, Measurement and Control, Vol. 110, pp 440-443.

Kolston, P.J. (1988c). Micromechanics remove the need for active processes in cochlear tuning. In *Basic Issues in Hearing*, edited by H. Duifhuis, J.W. Horst and H.P. Wit, (Academic Press, London), pp 74-79.

Kolston, P.J. and Viergever, M.A. (1989a). Realistic basilar membrane tuning does not require active processes. In *Cochlear Mechanisms - Structure, Function and Models*, edited by J.P. Wilson and D.T. Kemp, (Plenum Press, London), pp 415-424.

Kolston, P.J. and Viergever, M.A. (1989b). How do the outer hair cells influence cochlear mechanics? Submitted for publication.

Kolston, P.J., Viergever, M.A., de Boer, E., and Diependaal, R.J. (1989). Realistic mechanical tuning in a micromechanical cochlear model. Journal of the Acoustical Society of America, Vol. 86 (In Press).

I was fortunate to have been able to attend (and present papers at) the following conferences:

8th International Conference on Hearing (Paterswolde, The Netherlands, 5-9 April, 1988).
Mechanics of Hearing 1988 (Keele, England, 4-8 July, 1988).

During the periods June 1985 to May 1987, and August 1988 to February 1989, the work for this thesis was undertaken in the Department of Electrical and Electronic Engineering, University of Canterbury, Christchurch, New Zealand. From June 1987 to July 1988 the work was undertaken in the Department of Technical Mathematics and Informatics, Delft University of Technology, Delft, The Netherlands.

Paul Kolston
February 1989.

Contents

List of Figures

The shaking air rattled Lord Edward's membrana tympani;
the interlocked malleus, incus and stirrup bones were set in motion
so as to agitate the membrane of the oval window
and raise an infinitesimal storm in the fluid of the labyrinth.
The hairy endings of the auditory nerve
shuddered like weeds in a rough sea;
a vast number of obscure miracles were performed in the brain,
and Lord Edward ecstatically whispered
'Bach!'

from
"Point Counter Point"
Aldous L. Huxley

Chapter 1

Introduction

This chapter outlines some of the reasons for investigating the operation of the cochlea; including an explanation of the role that the formulation and analysis of cochlear models plays in improving our understanding of cochlear mechanics. Also included are definitions for a number of technical terms used throughout the thesis. It should be noted that only the mammalian cochlea is considered in this thesis.

1.1 Aim of the Thesis

A proper understanding of cochlear mechanics can only be obtained by combining information gained from three quite different areas of research: observations of cochlear anatomy; psychophysical, electrophysiological and mechanical measurements of cochlear response; and analysis of cochlear models. The main aim of the work undertaken for this thesis is to improve our understanding of cochlear mechanics by the formulation and analysis of cochlear models. The most valuable contribution of this work is the description of a new model of the linear mechanical motion of the cochlea, a model that has prompted the author to question the present state of our understanding of cochlear mechanics.

1.2 Why Cochlear Research?

The air pressure variations generated by, for example, a voice, a musical instrument, or an environmental disturbance, enter our ears and undergo complicated signal-processing procedures before we can perceive them as sound. However, what we hear is largely determined by what we listen to, in that the last part of this analysis process occurs at a conscious level within the higher centres of the brain. The ear, or in more formal language the *peripheral auditory system*, consists of the first part of the hearing chain

that takes the air pressure variations and converts them into nerve pulses which travel to the brain. Irrespective of what we choose to listen to, the ear always senses the air pressure variations and sends the processed information to the brain.

Although a large amount of the signal processing in our sense of hearing takes place after the ear, the ear performs important initial processing. Most of this initial processing occurs within the cochlea. The cochlea is that part of the ear that functions as a microphone, converting mechanical motion into nerve pulses. It acts as an interface between the acoustic environment and the neural environment, and constitutes one of the more accessible stages of our hearing process. Furthermore, hearing disorders are often the result of a malfunctioning cochlea and so a greater understanding of its operation should improve our ability to alleviate the suffering of the deaf and hearing-impaired.

To better understand the operation of the human cochlea, it is necessary to know both its structure and its response. Humans are able to prevent destructive irreversible experiments being performed on their bodies and therefore much of our understanding of human cochlea function is derived from experiments performed on animal cochleae. Fortunately, the basic structure of all mammalian cochleae is very similar and so it is assumed that the response measured in animal cochleae reflects that of human cochleae.

1.3 Why Cochlear Modelling?

The purpose of modelling cochlear mechanics is to gain a better understanding of the operation of the real cochlea by the formulation and analysis of models that reflect the structure and mechanical response (see Section 1.4) of the real cochlea. When a model is found that conforms with these criteria, it can be assumed that the model is an accurate representation of the real thing. Observing the effects of changing the parameter values or altering the structure of the model can be helpful in determining the important (abnormal) features characterizing damaged cochleae. This information can be used to minimize damage caused by harmful influences on normal cochleae.

In order to formulate an accurate cochlear model, it is necessary to know both the structure and the response of the real cochlea. Much of what we know about the mammalian cochlea is the result of the experiments conducted on *post mortem* specimens by von Békésy. A book describing these experiments (von Békésy, 1960) makes for fascinating reading, and acquaints the reader with the difficulties associated with the experimental side of cochlear research. These difficulties, arising from the relative inaccessibility of the cochlea (which is small and embedded in temporal bone), mean that accurately measuring either its structural parameters or its response is very difficult. More recent experiments have shown that the cochlea is highly sensitive to trauma; the response of a dead (or traumatized) cochlea is different from that of a normally functioning cochlea. Because of the scarcity of accurate structural parameter and response measurement data, cochlear modellers have a responsibility to explicitly state the underlying reasons behind the assumptions made in the formulation of a cochlear model, so that experimenters can

check if these assumptions are valid.

In the formulation of a cochlear model certain structures can be disregarded, enabling study of only those variables which govern the particular phenomenon of interest. For example, the first variable considered essential to the response of cochlea was the elasticity variation observed along the length of the cochlear partition. Therefore, this was the first structural parameter measured in the human cochlea and was the main feature of the first cochlear models investigated by von Békésy. Cochlear modellers are very reliant on experimental studies to determine which variables should be included and which can be disregarded. Unfortunately, all cochlear models require considerable assumptions to be made in their formulation and so they seldom reflect the microstructure of the cochlea to any realistic extent.

The importance of following an iterative process cannot be overemphasized: using structural observations to formulate a model, analysing its response, comparing this with that observed in the real cochlea, and using this comparison to improve the model and to suggest new observations. An accurate cochlear model must be consistent with the structure and the response of the cochlea. It is the author's opinion that there is *no* current model which satisfies both these criteria.

1.4 Definitions and Symbols

As is usual in highly-specialized fields of research, cochlear mechanics nomenclature plays an important role in communicating specific ideas. To ensure that the nomenclature used in this thesis has the same meaning to all readers, it is appropriate to include here a list of terms which have possible ambiguities in their meanings.

Motile/active processes

In the author's opinion, the term *active process* is applied incorrectly and inconsistently by many investigators in the field of cochlear mechanics. It is the current trend to use this term to describe the metabolically-sensitive process that exerts forces on the structures within the cochlea. In an engineering sense, the word "active" implies that these forces involve the injection of mechanical energy into the cochlea. However, many elements within a mechanical system generate forces without adding energy to the system. The direction (or phase) in which an element exerts a force, in relation to the controlling signal, determines whether the element adds energy or dissipates energy. For example, a dashpot (an element which exerts resistive forces in a mechanical system) can be replaced by a force generator whose output is directly proportional to an input velocity (with the correct phase relationship). Both the dashpot and the generator have *exactly* the same effect on the system, so to call one "passive" (the dashpot) and the other "active" (the generator) is misleading.

It is necessary to adopt a different convention for the description of the metabolically-

sensitive process present in the cochlea. The convention adopted here is to describe such a process as a *motile* process, a convention tying in nicely with the description of hair cell motility, a likely source of such a process within the cochlea. The term *active process* is reserved for a motile process that injects mechanical energy into the cochlea.

Symbols and other definitions

The *cochlear partition* (CP) is defined as encompassing *all* of the flexible structure that mechanically divides the cochlea into two scalae; the basilar membrane (BM) is just one component (albeit a very important one). The mechanical response of the cochlea refers to the motion of the BM for a certain stapes (or eardrum) excitation. The BM motion is influenced by the mechanics of the CP. With reference to the latter, the terms *stiffness* and *compliance* are used interchangeably (one is the inverse of the other).

With reference to a cross-section of the cochlea, that part of the CP extending from the edge of the spiral lamina to the edge of the outer pillar of Corti is defined as the *arcuate zone.* The remainder of the CP, extending out to the spiral ligament, is defined as the *pectinate zone.*

Selectivity is defined as the shape of the tuning curve (the *relative* amplitude of motion as a function of frequency or place), and *sensitivity* is defined as the absolute position of the tuning curve (the actual magnitude of vibration of the BM for a certain magnitude of stapes (or eardrum) excitation).

Realistic means "pertaining to real life". Therefore, if a model exhibits a realistic response it means that the response is similar to that measured in the real cochlea. The same definition is used for a realistic cochlear model - the model truly represents the real cochlea, in terms of its structure and its response. It is implicitly assumed that the experimentally-observed structure and response accurately reflects that of the cochlea.

Chapter 2

Anatomy

This chapter presents a summary of those aspects of cochlear anatomy that are directly relevant to the formulation of a linear mechanical model of the cochlea. The chapter begins with a brief description of outer ear and middle ear anatomy. It is concluded that the arcuate and pectinate zones of the CP have gross (and mechanically important) structural differences which *must* be taken into account when considering basic aspects of cochlear mechanics.

Much of the material in this chapter comes from the reviews of Yost and Nielsen (1977) and Lim (1980, 1986); extra references are added where appropriate. The dimensions quoted here are approximate. Where there is considerable variation of dimensions (e.g. in different animal species) an average value is quoted. Most of the dimensions and descriptions relate to the human ear.

2.1 Outer and Middle Ear

Figures 2.1 and 2.2 show, respectively, a drawing and a schematic of the human ear. The ear is nominally divided into three functional units: outer, middle, and inner ear. The most obvious component of this chain, the outer ear, consists of the pinna, the external auditory meatus (ear canal), and the tympanic membrane (eardrum). The main purposes of the outer ear are the "collection" of sound (to maximize sensitivity) and the improvement of spatial localization by causing the spectral content of the sound entering the ear canal to be a function of source position. In humans, localization performance is further enhanced by the effects of reflections from shoulders and diffraction around the head.

On the other side of the eardrum is the middle ear, an air-filled cavity that contains the ossicular bones; the malleus, incus and stapes. Attached to the middle of the eardrum is one end of the malleus bone. The malleus is connected to the incus which is, in turn, connected to the stapes. The stapes is located in the oval window of the inner ear. The only other opening to the inner ear is the round window, which is covered by a thin, flexible membrane. Through this combination of bones, a vibration of the eardrum (caused by air pressure vibrations in the ear canal) results in piston-like motion of the stapes, and

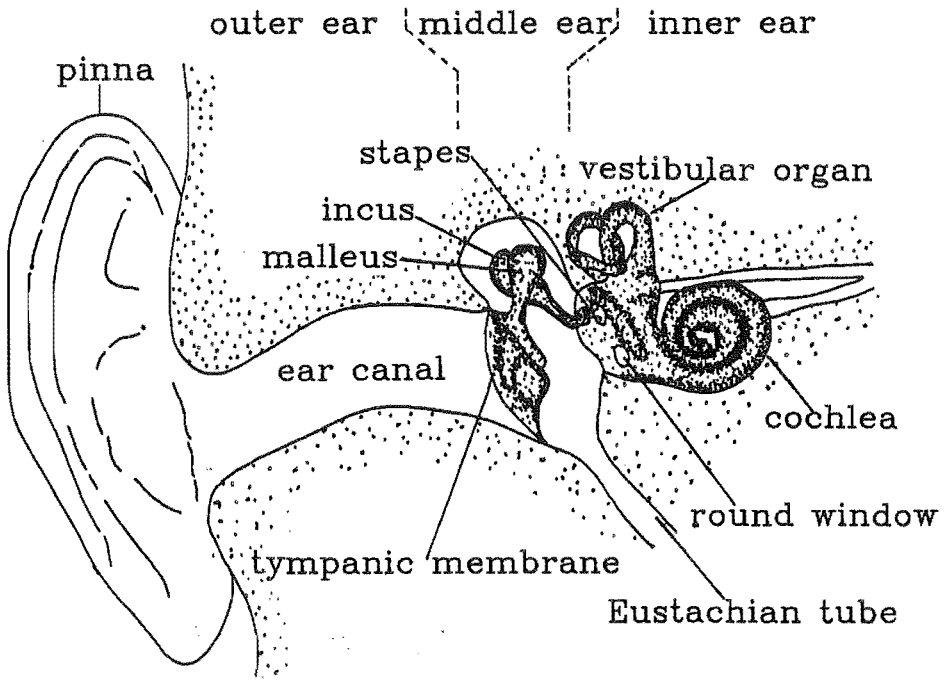

Figure 2.1: Drawing of the human outer, middle and inner ear. The outer ear comprises the pinna and ear canal, which act to direct incident sound waves towards the tympanic membrane (eardrum). Vibration of this membrane is transmitted to the inner ear by the bones of the middle ear; the malleus, incus and stapes. This excites the fluids contained within that region of the inner ear which is involved with audition (i.e. the cochlea) .

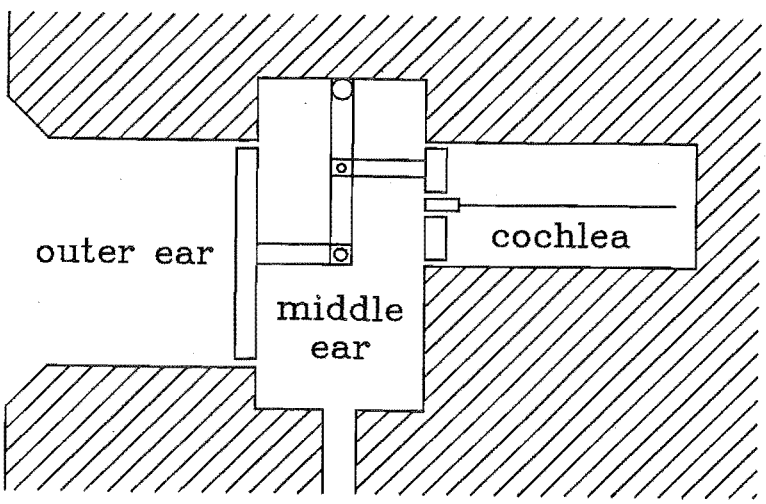

Figure 2.2: Simplified schematic of the ear, showing the lever action of the ossicular bones which effects an impedance match between the air and the cochlear fluids .

hence excites the fluids of the inner ear. The inner ear comprises the vestibular organ (the organ of balance) and the cochlea (the organ of hearing). Although they contain the same fluid, the two organs operate quite independently. Only the cochlea is considered in this thesis.

The area of the stapes footplate is 17 times less than that of the eardrum. This feature, combined with a 1.3-fold ratio in the malleus-incus lever system, effects an impedance transformation between the (low impedance) air and the (high impedance) fluids of the cochlea. The resulting impedance match effects an efficient transfer of energy (50-75 % from 0.3-3 *kHz*) from sound waves to fluid waves. Sound can also enter the cochlea by bone conduction, but the threshold for this is approximately 80 *dB* higher than that for eardrum vibration.

The middle ear protects the cochlea from damage by loud sounds by the contraction of muscles which impedes the transmission of sound from the eardrum to the cochlea. The amount of contraction increases with sound intensity, thereby preventing the ossicles from bouncing out of contact and causing excessive distortion at high levels. The Eustachian tube, connecting the middle ear cavity to the throat, ensures a constant operating position for the eardrum by equalizing the pressure in the middle ear cavity with the environmental pressure. This is achieved by the tube opening (e.g. by swallowing or yawning).

The transmission of sound through the middle ear is frequency dependent. The middle ear acts as a lowpass filter, with a corner frequency of 1-2 *kHz*. However, this outer ear-to-cochlea transfer function is insignificant compared to the filtering performed by the cochlea, and so the middle ear is ignored in this thesis (except when comparisons are made between cochlear model responses and experimental data; for the latter a reference of eardrum pressure is often used).

2.2 Cochlear Anatomy

Most of the signal analysis performed by the ear occurs within the cochlea. The cochlea acts as a transducer, converting stapes motion into nerve pulses that are sent to the brain.

2.2.1 Cross-sectional structure

A diagram showing a cross-section of the cochlea appears in Fig. 2.3. The cochlea consists of three turns of an approximately circular canal, wound in a very similar manner to that of a snail shell (hence the name, from the Greek word *kochlias*). When stretched out, the cochlea is 25-35 *mm* long and has a cross-sectional area of 2 mm^2.

Figure 2.4 is a diagram of a cross-section of the cochlear canal, showing its division into three scalae by two flexible boundaries: the CP (the BM plus additional structures) and Reissner's membrane. The scala media constitutes 10% of the cross-sectional area. The stapes is positioned at the *basal* end of the scala vestibuli, whilst the round window is situated at the basal end of the scala tympani. The scalae vestibuli and tympani are filled

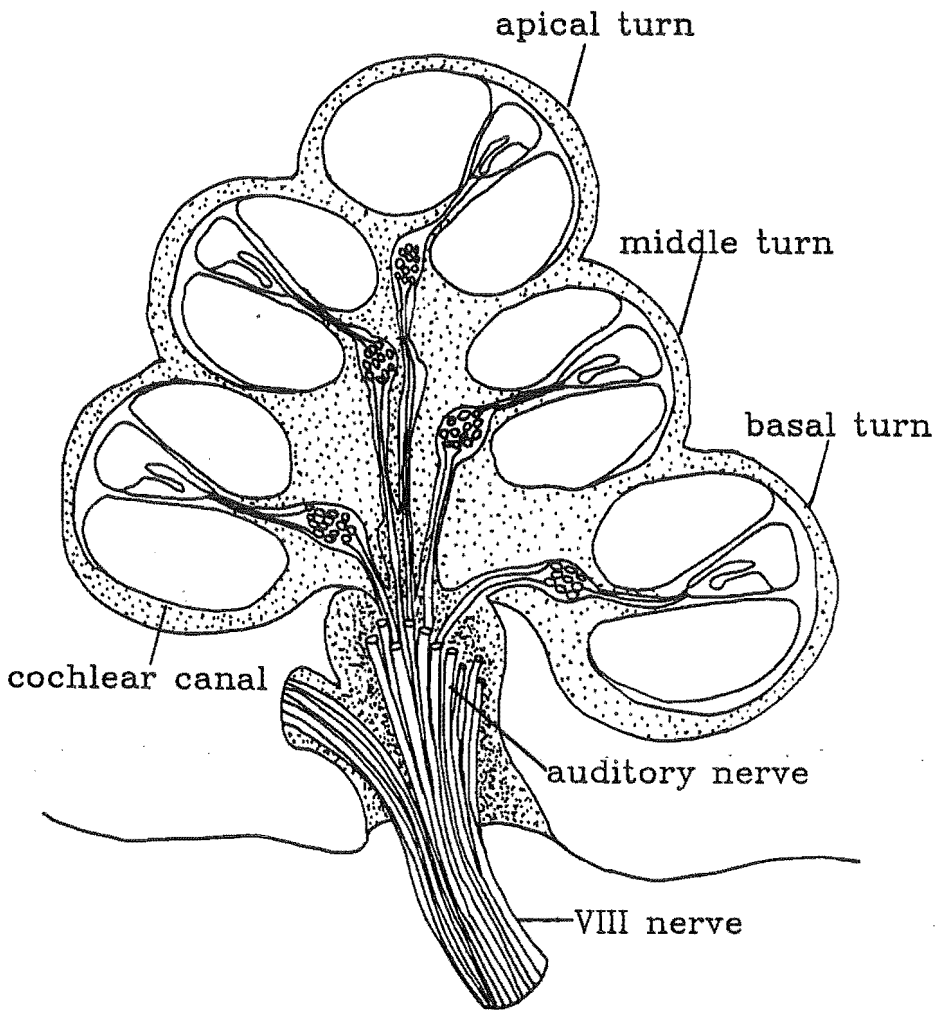

Figure 2.3: Diagram of a cross-section of the cochlea, showing its spiral shape embedded in the temporal bone. The stapes is positioned in the basal turn. The acoustic nerve projects down the centre of the cochlea which, together with the vestibular nerve bundle, forms the VIII nerve to the brain.

with perilymph, and the scala media is filled with endolymph. The density of both of these fluids is similar to that of water. Reissner's membrane acts as an electrical insulator to the potential that exists between the perilymph and endolymph. The mechanical impedance of the BM is much greater than that of Reissner's membrane, which results in only the BM affecting the mechanics of the travelling wave. Therefore, when considering the mechanical response of the cochlea, Reissner's membrane can be disregarded and the scala media can be combined with the scala vestibuli. For

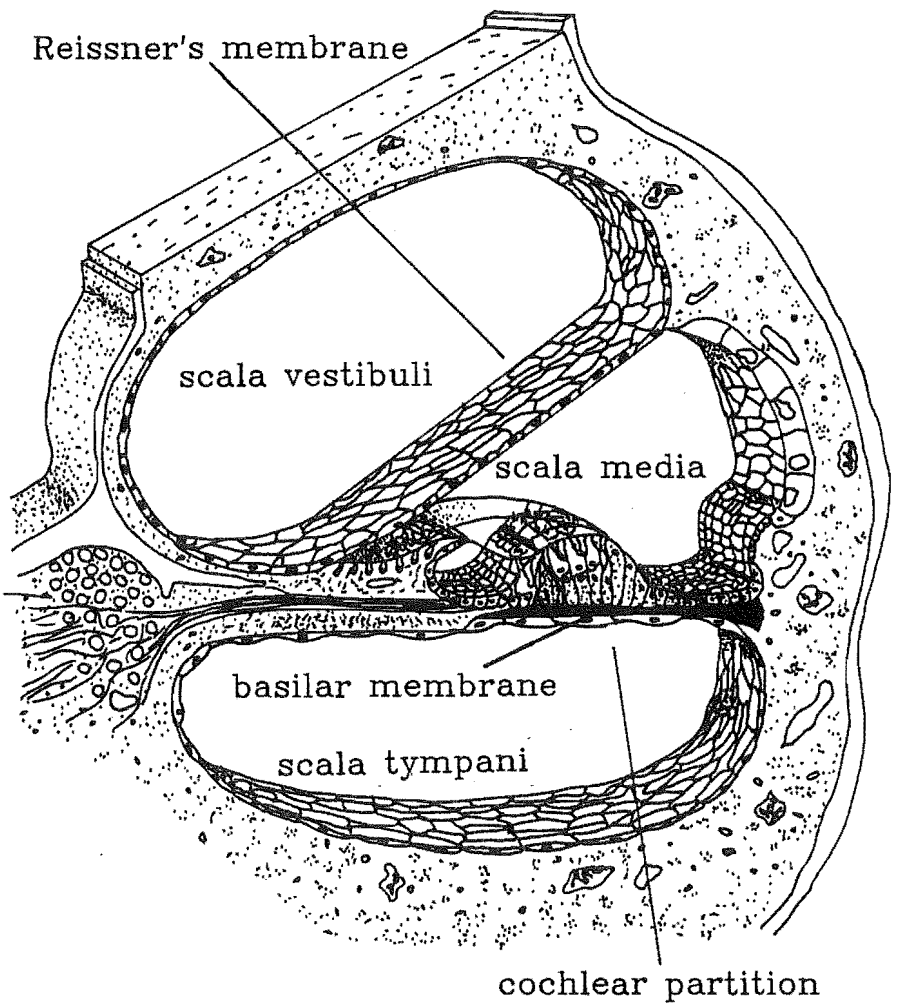

Figure 2.4: Diagram of a cross-section of the cochlear canal. The cochlea is divided into three scalae, but only the cochlear partition (CP) affects the mechanical motion of the fluid. The stapes is positioned at the basal end of the scala vestibuli, and communicates with the round window via motion of the basilar membrane (BM). The variation of BM width and thickness along the length of the cochlea is responsible for a large stiffness gradient in the CP This results in the formation of a transverse travelling wave on the BM, that propagates from base to apex.

all audible stimulus frequencies the fluids in the two scalae interact via the motion of the BM. This motion stimulates sensory hair cells, resulting in information being sent to the brain. The equilibrium position of the BM is maintained by a small hole (the helicotrema) at the *apical* end of the cochlea.

Certain features of the CP structure necessitate a detailed description, since they play

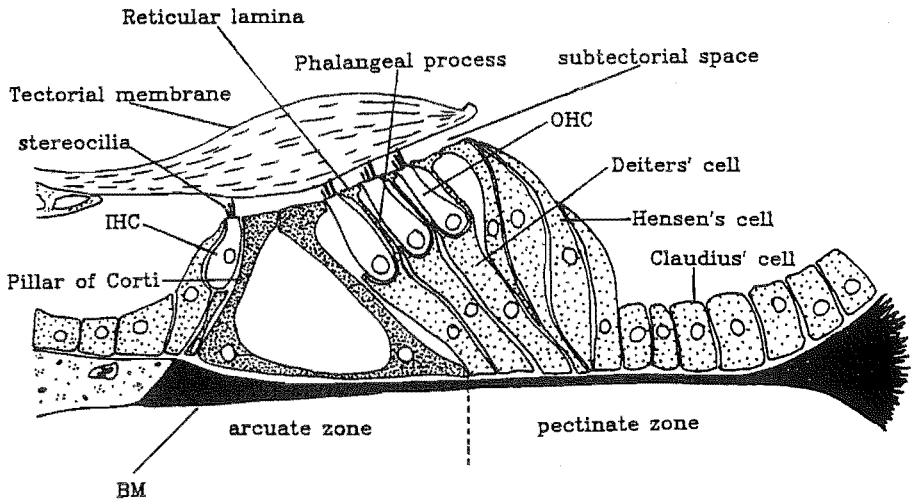

Figure 2.5: Diagram of the CP. The BM is divided into its two zones. The sensory hair cells, pillars of Corti, and Deiters', Hensen's and Claudius' cells constitute the organ of Corti. The hair cells are divided into two distinct groups: inner hair cells (IHCs) and outer hair cells (OHCs). Vertical motion of the arcuate zone results in shear motion in the subtectorial space, bending the hair cell stereocilia and thereby causing excitation of the hair cells.

an important role in the development of the new cochlear model described in Chapter 5. In particular, the need for a clear differentiation of the CP into its arcuate and pectinate zones can be justified on the bases of anatomical structure and experimental observations.

Figure 2.5 is a diagram of the CP, showing its three main structural components: the BM, the tectorial membrane, and the organ of Corti. The BM and the tectorial membrane are attached at different points, so that vertical motion of the BM arcuate zone results in shear motion in the subtectorial space. It is likely that this directly stimulates the sensory hair cells, by the bending of their stereocilia. This is known as the forward transduction process, with information concerning the form of the stimulus (at the BM and hence at the eardrum) being sent to the brain.

The organ of Corti comprises the sensory hair cells, pillars of Corti, and supporting (Deiters', Hensen's and Claudius') cells. The sensory hair cells are divided into two distinct groups: inner hair cells (IHCs) and outer hair cells (OHCs). The IHCs are supported by the inner pillar of Corti. Projections from the top of the outer pillars extend out in a radial direction. These projections, along with the ends of phalangeal processes from the Deiters' cells, form the reticular lamina. The reticular lamina supports the top of each OHC, which hangs down to be further supported by the top of a Deiters' cell. The Deiters cells rest on the edge of the BM pectinate zone.

The most obvious anatomical distinction between the two types of hair cells is that there are three rows of OHCs but only one row of IHCs at each position along the cochlear length. The IHCs are innervated by 90-95% of the afferent nerve fibres (Spoendlin, 1969), and so are largely responsible for the information that is sent to the brain (i.e. the forward transduction process). The OHCs, on the other hand, are mainly innervated by efferent nerve fibres (from the brain). The response of the cochlea is altered when the efferent fibres are stimulated electrically (Mountain, 1985). Furthermore, the selectivity and sensitivity of the cochlear response decrease when the condition of the OHCs deteriorates (Khanna and Leonard, 1986). These observations suggest that a reverse transduction process exists within in the cochlea, in which forces generated by the OHCs affect the mechanics of the BM. The OHCs are located in the arcuate zone of the BM (see Fig. 2.5), and so it is assumed that such a reverse transduction process will directly affect the arcuate zone only; the pectinate zone will be affected via its coupling to the arcuate zone provided by the BM fibres and the cochlear fluid.

The tops of the OHC stereocilia are embedded in the underside of the tectorial membrane. It is uncertain whether or not the IHC stereocilia are embedded (Lim, 1980; Steel, 1983). If they are not, then it is likely that the IHCs would respond to the velocity of the subtectorial fluid motion, and hence to the velocity of the BM arcuate zone. This is supported by experimental measurements (Sellick *et al.*, 1983a - see Section 3.2.3).

In each hair cell the stereocilia are arranged into three distinct rows. In each row the stereocilia are approximately the same height, but the heights are graded between the three rows. In the IHC the rows run parallel to the longitudinal axis of the cochlea, whereas in the OHCs the rows form a very distinct "V" shape, pointing away from the IHC. The tallest stereocilia of each hair cell are longest for those cells near the apex, and it has been shown that this height gradation along the cochlear length could result in a stereocilia stiffness gradient which closely matches that of the BM (Wright, 1984). Strelioff and Flock (1984) measured a smaller variation of stereocilia stiffness than proposed by Wright. However, allowing for changes in the dimensions of the tectorial membrane and the organ of Corti, they concluded that OHC stereocilia stiffness could significantly influence BM mechanics. Since the actual means by which the OHCs alter BM mechanics is still uncertain (e.g. Zenner *et al.*, 1988), it is merely *assumed* in this thesis that the presence of the OHCs does indeed alter BM (arcuate) mechanics.

The width and thickness of the BM vary along the cochlear length, both increasing towards the apex. The associated stiffness gradient (from 10^9 *dyn·cm*$^{-3}$ to 10^5 *dyn·cm*$^{-3}$ - these are specific acoustic stiffness parameters (see Section 4.4.1)) gives rise to a travelling wave on the BM (see Chapter 3). The structure of the BM is shown in Fig. 2.6. The two cross-sectional diagrams in Fig. 2.6 show that in the pectinate zone the BM consists of three layers: a supporting layer of BM cells, an intracellular layer and the covering epithelium layer of tympanic cells (Iurato, 1962). The cell layers do not affect the mechanical properties of the BM. The intracellular layer, having neither cells nor vessels, consists of an amorphous ground substance in which small proteinaceous fibres (approximately 10 *nm* in diameter) are embedded. These fibres, which run in a radial direction spanning the full width of the cochlea, determine the mechanical properties of the BM.

along the cochlear length, a number that closely matches the number of hair cell rows.

There are appreciable differences in the arrangement of the BM fibres and the ground substance in the arcuate and pectinate zones. The geometric arrangement of the BM fibres

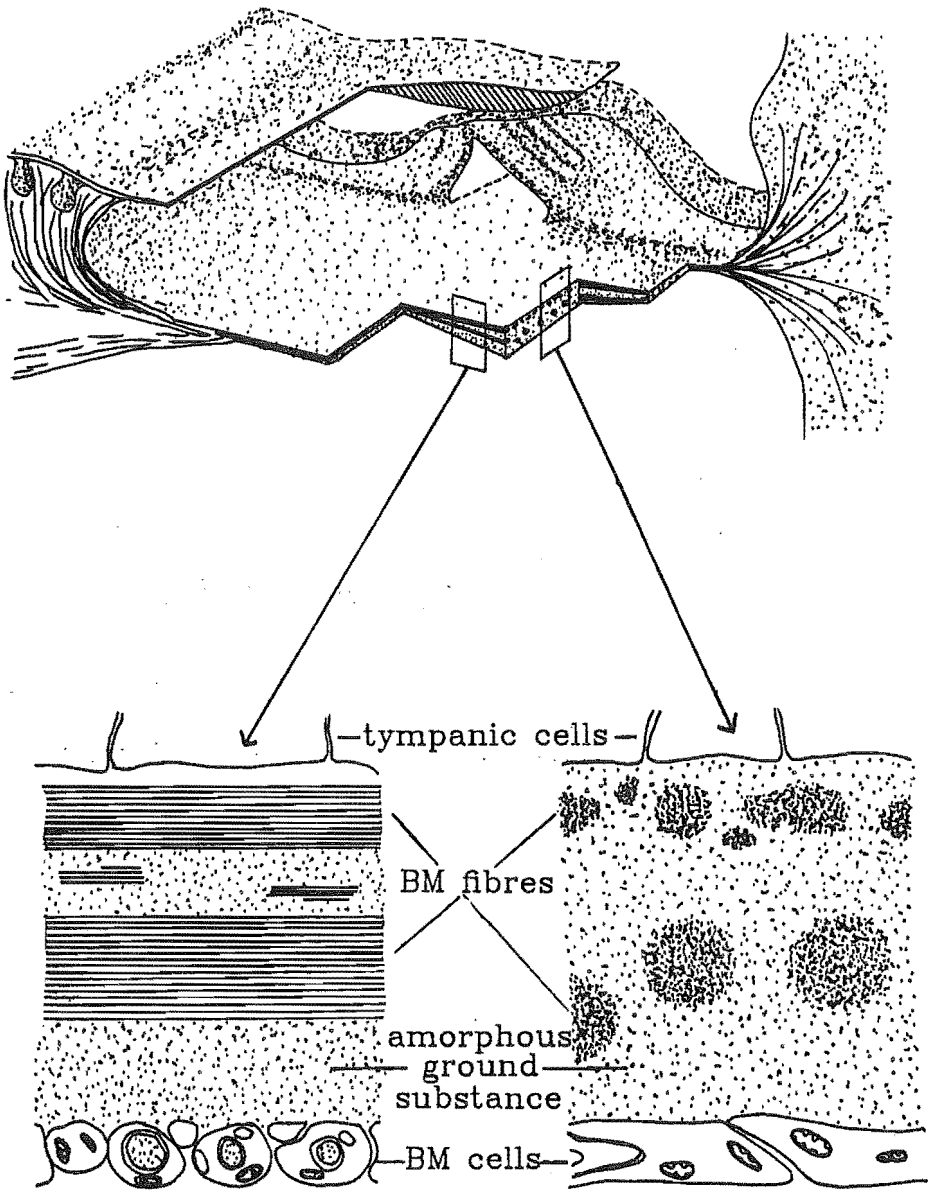

Figure 2.6: Structure of the BM (adapted from Iurato, 1962). In the pectinate zone, the BM fibres are formed into distinct fibre bundles embedded in an amorphous ground substance sandwiched between the BM and the epithelium of the organ of Corti. In the arcuate zone the fibres form a dense mat.

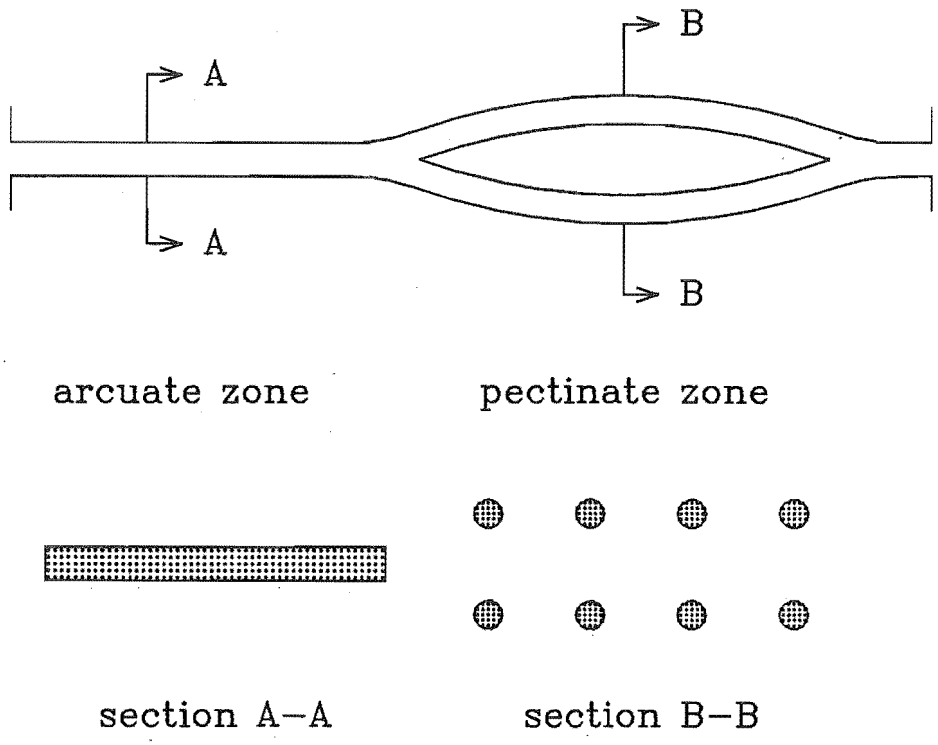

Figure 2.7: BM fibre geometry in arcuate and pectinate zones (adapted from Miller, 1985). The dense fibre mat probably results in an isotropic arcuate zone. However, the distinct BM fibre bundles in the pectinate zone result in little longitudinal rigidity and so the pectinate zone is highly anisotropic.

in the two zones is shown in Fig. 2.7. In the arcuate zone the fibres form a continuous mat, suggesting that this zone has isotropic mechanical properties. In the pectinate zone the fibres are grouped into bundles which lie in two distinct layers. The ground substance in which the fibre bundles are embedded has a very low shear modulus and so it provides very little longitudinal coupling between adjacent bundles. There is a significant change in fibre geometry at the transition point between the arcuate and pectinate zones. This geometry change would allow for significantly different motion in the two zones.

2.2.2 Longitudinal structure

The longitudinal geometric arrangement of the OHCs, the Deiters cells, their phalangeal processes and the pillars of Corti is shown in Fig. 2.8. Longitudinal coupling is provided by the triangular arrangement of the OHCs and the phalangeal processes of the Deiters

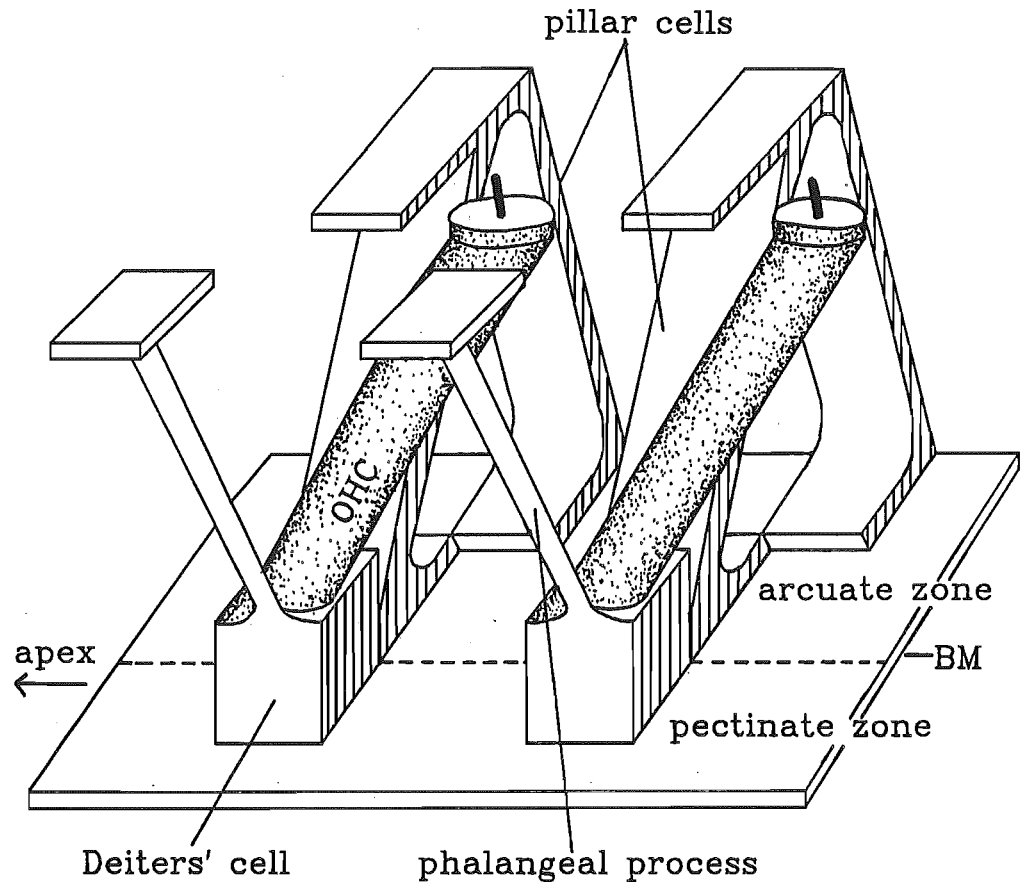

Figure 2.8: Diagram of the organ of Corti's longitudinal structure, showing the geometric arrangement of the OHCs, the Deiters cells, their phalangeal processes, and the pillars of Corti (adapted from Voldrich, 1983).

cells. The top of each OHC is in close proximity to a phalangeal process from an adjacent (more basal) Deiters' cell. The reason for this structural geometry is not known. The triangular arch formed by the pillars of Corti, being two slender rods connected only at the ends, is a flimsy structure compared to the BM. However, the longitudinal connections that are present between the heads of adjacent inner and outer pillar cells, and between phalangeal processes, restrain the pillars from rotation at one location relative to one another and thus increase the stiffness in the arcuate zone (Miller, 1985). Von Békésy (1960) measured differences in stiffness of up to 50 times between the two BM zones. Miller (1985) measured a difference of only 5-10 times, but in her experiments only the pillars of Corti were present - the presence of the complete organ of Corti would substantially increase the arcuate stiffness. In Chapter 5, a cochlear model is described which utilizes these structural features in order to obtain a realistic response.

The accepted amount of anisotropy in the BM has varied over the years, with more recent studies having lead to the general acceptance of a highly anisotropic BM. However, the greatly differing structure of the BM in its two zones can be helpful in providing an explanation for the contradictory observations of its mechanical properties. Von Békésy (1960) observed that the BM displayed isotropic elastic properties under light pressures and anisotropic properties under much stronger forces. Voldrich (1978) found that freshly prepared samples exhibited anisotropic properties, whereas physically or chemically damaged (or *post mortem*) preparations were always isotropic. He attributed von Békésy's observations to the fact that the earlier experiments were conducted on *post mortem* specimens. However, von Békésy also observed similar results in living animals. Since descriptions of the experimental data are not explicit about in which zone the observations were made, it is suggested that the measured amount of (an)isotropy (and hence longitudinal coupling) will be affected by the radial position of measurement position. This conclusion can be justified by considering both the greatly differing structure of the BM fibres in the arcuate and pectinate zones, and the longitudinal coupling afforded by the pillars of Corti and the phalangeal processes of the Deiters cells.

Chapter 3

Response

This chapter describes the mechanical response of the cochlea. The formation of the travelling wave is qualitatively described, and the form of the mechanical response measured experimentally is outlined. It is concluded that the response of the BM is probably quite different in its arcuate and pectinate zones.

3.1 Formation of the Travelling Wave

Some important aspects of cochlear anatomy are outlined in Chapter 2. The most important feature of this, in terms of the gross mechanical (*macro*mechanical) response of the cochlea, is that the cochlea is a canal divided lengthwise into two scalae by a flexible partition that possesses a substantial stiffness gradient. For all forms of stapes stimulus, this anatomical feature results in the formation of a travelling wave on the BM.

3.1.1 Historical

The formation of the travelling wave, which travels from the base to the apex of the cochlea, is one of the (few) aspects of cochlear response that is universally accepted today. However, at the time of von Békésy's (1928) observations there was considerable controversy concerning the form of BM motion. One of the more famous theories was the resonance theory, proposed by Helmholtz (1863). He assumed that the CP was comprised of a series of resonators tuned to different frequencies, with the cochlear fluid acting only to lower the resonant frequency of these resonators. Therefore, when the sound stimulus contained several frequencies, each would produce a separate vibration maximum at a different location on the BM, corresponding to a crude (spatial) Fourier analysis. The problem with this theory was the paradox it generated. For a resonator to be effective in fine frequency analysis, as our pitch perception abilities require, it must have very low damping. However, if the cochlea was equipped with such underdamped resonators we would have difficulty comprehending the rapidly-changing events in music and speech (since the resonators would exhibit prolonged ringing during the transients). The actual

analysis performed by the cochlea is still uncertain, but it has been suggested that the response to sine signals approaches a pure Fourier analysis, the response to transients approaches a pure waveform (time) analysis.

Von Békésy's observations were initially in a physical model of the cochlea, and later in *post mortem* (and a few live) specimens. When fine metallic particles were added to the cochlea fluid, they were seen (using a light microscope) to move from base to apex, indicating the presence of a travelling wave. Eddies of fluid motion were also seen in the region of maximum response. The presence of a travelling wave was later confirmed in the cochleae of various animals in a fresh state and in the living guinea pig.

3.1.2 A qualitative description

A diagram of the unrolled cochlea is shown in Fig. 3.1. It is generally considered that the coiled nature of the cochlea has little affect on its mechanical response (as suggested by the analyses of Viergever (1978a), Loh (1983), and Steele and Zais (1985)). Consider a pulse-type stimulus to the cochlea, consisting of a force applied to the stapes tending to cause it to move inwards. This produces a compressional wave that propagates away from the stapes travelling at the speed of sound in the fluid (approximately 1500 $m \cdot s^{-1}$). For such a compressional wave the BM appears transparent and so the wave invades both scalae. The only other opening to the cochlea is the round window, which normally has the middle ear air pressure keeping it at an equilibrium position. The compressional wave causes an unequal pressure to be exerted on the round window, which tends to make it bulge outwards. The (potential) movement of the round window results in the formation of a pressure differential across the BM.

Conservation of fluid mass dictates that the fluid displacement of the stapes and the round window must equal the integrated volume displacement of the BM. The BM constitutes the membrane with the largest impedance, and hence neither the stapes nor the round window will bulge outwards until the *response time* of the BM has passed. The response time is defined as the time taken for the BM to begin moving after the application of a force. It can be estimated by considering the BM to be an assemblage of independent masses and springs, each tuned to a frequency determined by the point values of mass and stiffness at that location. The response time of any such spring-mass system is governed by the system's *bandwidth* (defined as the frequency range over which the system can absorb energy). If the bandwidth is large, this implies that the system is capable of absorbing energy from the stimulus over a wide frequency range and hence will tend to respond to that stimulus more rapidly (and vice versa for a system with a small bandwidth).

The most basal region of the BM has the widest bandwidth and hence it is this region that deflects first (together with the stapes and the round window). The potential energy in the deflected BM then causes it to move back towards its resting position. Owing to the fluid coupling between adjacent sections, the energy begins to be transmitted to more apical parts of the BM, causing the appearance of the travelling wave. As the wave propagates toward the apex it slows down until, at a position that is dependent on

11. (page 18, para. 3 - page 20, para. 1) "Author's explanation":

"The description of the formation of the travelling wave is derived from basic physical principles as understood by the author. That is, the text is not gleaned from any reference material - it is the author's own description of a physical process."

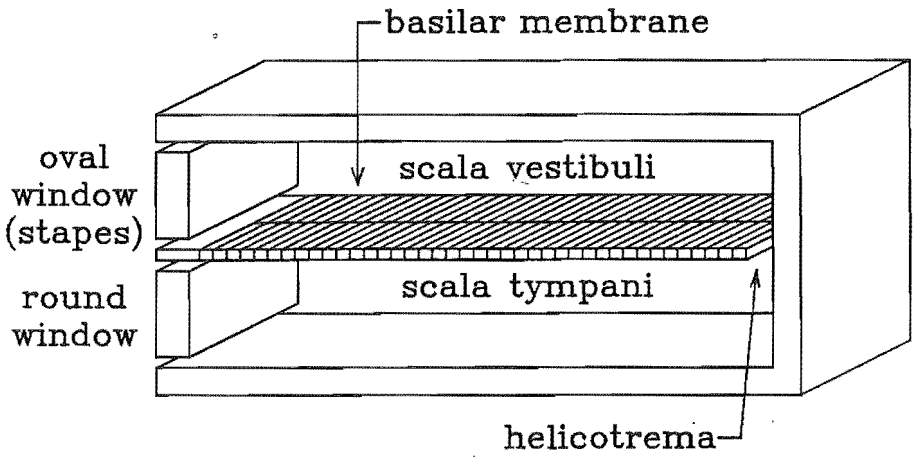

Figure 3.1: Diagram of longitudinal section of the cochlea. When a force is applied to the stapes it will not move until the response time of the BM has passed. Instead, a compressional wave invades both scalae (since the BM is transparent for such waves). The unequal pressure on the round window causes it to bulge outwards. Conservation of fluid mass means that the stapes moves inwards and the BM bulges downwards with the same volume displacement. The most basal region of the BM deflects first, since it has the largest bandwidth and hence the smallest response time. The BM deflection heralds the beginning a transverse wave which travels towards the apex. The travelling wave propagates as far as the (lessening) BM bandwidth will allow, at which point the wave reaches a peak, thereafter being rapidly attenuated. The point of resonance is near the base for high frequency stimuli and near the apex for low frequency stimuli.

frequency, it effectively stops and the energy contained in the wave is absorbed by the local BM resistance. Points beyond this position receive no excitation from the travelling wave; instead they are excited (at a very low level) by the initial pressure in the scala vestibuli, resulting in the characteristic phase plateau (at a multiple of π radians) for all positions beyond the point of resonance.

The usual stimulation to the cochlea is more complicated than the pulse-type stimulus considered above. However, no matter how complicated the stimulus, it always causes the formation of waves travelling from base to apex. At the basal end, the BM follows the time waveform of the stimulus. In the travelling wave, each frequency component approaches a maximum, slows down, and is absorbed by the BM damping at a position characteristic of that frequency. This mode of operation is akin to that of "critical layer absorption", as identified by Lighthill (1981). The frequency at which the peak occurs for each position is termed the "characteristic frequency" (CF). Likewise, for a given

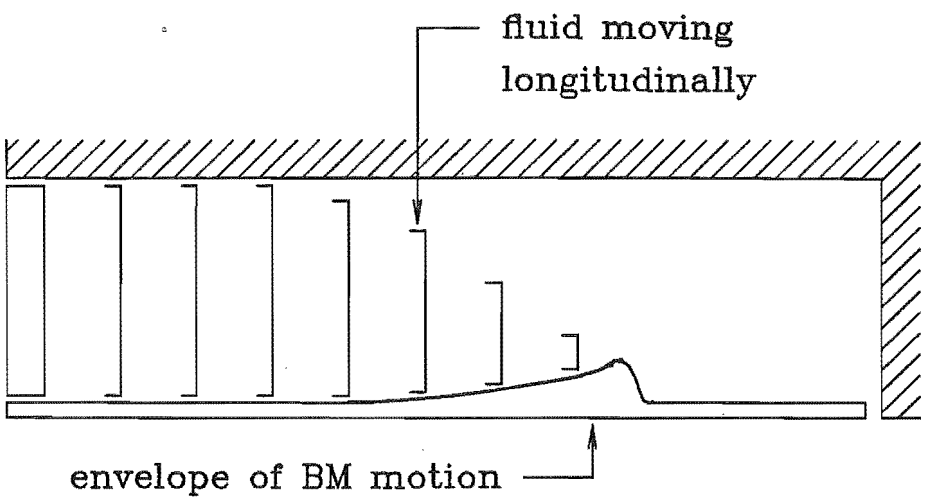

Figure 3.2: Variation of fluid wavelength within the cochlea (only the scala vestibuli is shown - the fluid motion is equal and opposite in the scala tympani). For regions far basal of the characteristic place all the fluid participates in the longitudinal flow (the "long-wave" region). Near the characteristic place, however, the wavelength becomes comparable to the scala height and so the amount of fluid moving longitudinally is reduced (the "short-wave" region).

frequency, the position of the peak is termed the "characteristic place".

3.1.3 Fluid wavelength

For regions far basal of the characteristic place, the wavelength of the travelling wave is much larger than the dimensions of the scalae. Hence the fluid motion can be considered to be essentially one-dimensional in a longitudinal direction. This is known as the "long-wave" region. Nearer the characteristic place the wavelength becomes comparable to the scalae dimensions, and hence the longitudinal movement of fluid is confined to a smaller distance above the BM. This corresponds to "short-wave" fluid behaviour. The transition from long-wave to short-wave region is shown graphically in Fig. 3.2.

This variation in fluid wavelength, which is frequency and place dependent, produces two important benefits. Firstly, if the scalae dimensions were smaller than the wavelength throughout the cochlea, the rapidly-changing BM impedance near the characteristic place would produce reflections, resulting in the generation of waves travelling in the reverse direction. Secondly, in the presence of the short-waves, the increased fluid impedance

(owing to the fluid effectively being "squeezed" through a smaller cross-sectional area) and the reduced BM impedance (owing to a reduction in the amount of fluid "riding" with the BM), result in a larger peak at the characteristic place. Both of these features are beneficial in that they maximize the energy transfer from the stapes to the sensory hair cells.

3.2 Measured Responses

This section summarizes the available response data obtained from experimental investigations on animals. The magnitude response data illustrate the remarkable sensitivity and selectivity of the mechanical response of the cochlea, whereas the phase response data confirm the presence of a travelling wave. The changes in the mechanical response, as a result of trauma, are also outlined in this section. The data referred to here are for the response to pure tone stimuli. It should be remembered that the response of the BM exhibits the same degree of selectivity for single frequency and noise stimuli (de Boer, 1973).

3.2.1 Measurement techniques

There are three main techniques used for measuring the very small mechanical movements of the BM (e.g. de Boer, 1980; Khanna, 1986): Mössbauer, Laser Interferometry, and Capacitive Probe. In the Mössbauer technique, a small gamma-ray source containing ^{52}Co is placed on the BM. An absorber (enriched in ^{52}Fe) is positioned so that the rays penetrating are detected on a scintillation counter. The rays reaching the counter are minimized when there is no relative motion between the source and the absorber, since the resonance frequencies of the two nuclides are then the same. When the source vibrates, the emitted rays are frequency modulated (owing to the Doppler effect) and therefore undergo varying absorption. The absorption-time functions so obtained are used to calculate the magnitude and phase of the source motion. In the Capacitive Probe technique, a small probe that is part of an electrical resonant circuit is brought into close proximity with the BM. Motion of the BM results in variations of capacitance between the BM and the probe (the scala tympani is drained), and hence causes changes in the circuit's resonant frequency. In Interferometric techniques a small mirror is placed on the BM and is illuminated by a coherent laser beam. Frequency and phase variations of the reflected beam, caused by motion of the mirror, are detected using interferometry. This information is used to determine the BM motion.

For all of the techniques described above it is usual to measure isovelocity curves, in which the eardrum sound pressure required to keep the velocity of the detector constant is recorded. A typical set of data is shown in Fig. 3.3. These data were obtained in the chinchilla (Robles *et al.*, 1986), and give the response of the normal and traumatized cochlea. Only data for the magnitude response of the traumatized cochlea are shown; no phase response data are available.

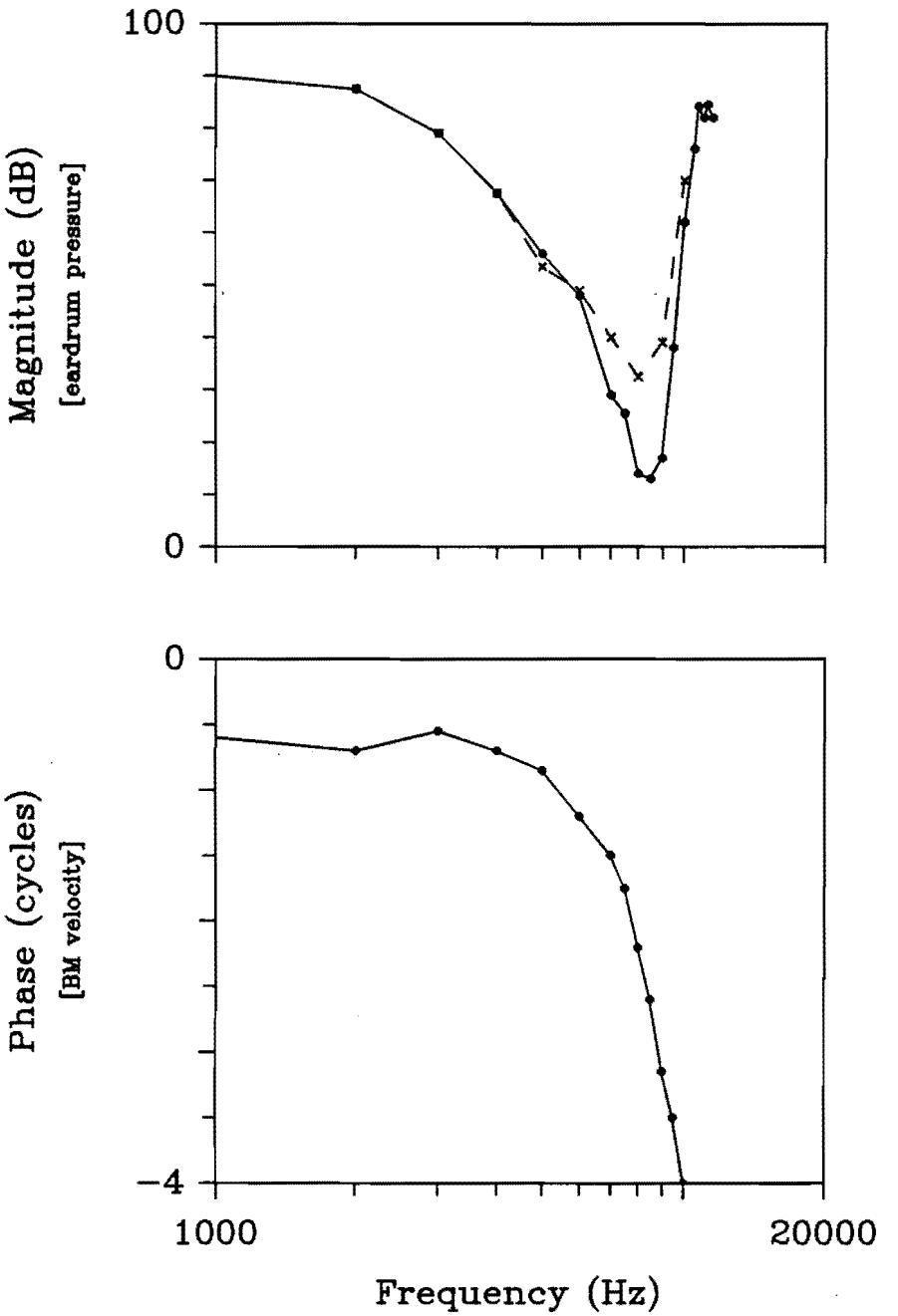

Figure 3.3: A typical set of data of the mechanical response of the cochlea (from Robles *et al.*, 1986 - animal 44). Isovelocity curves are presented, showing the eardrum pressure required to elicit a BM vibration of 0.1 $mm \cdot s^{-1}$. The response of the viable cochlea is indicated by the solid line, whilst that of the traumatized cochlea (i.e. 8 hours after the start of the experiment) is indicated by the dashed line.

13. (page 23, para. 2) "Author's explanation":

"The response to a low stimulus frequency (relative to CF) at a given point is equivalent to the response in regions far *basal* of the characteristic place for one stimulus frequency. This is why a plot of response (at one point) vs frequency looks the same as a plot of response (for one frequency) vs position - assuming that the abscissa has the correct scale in each case."

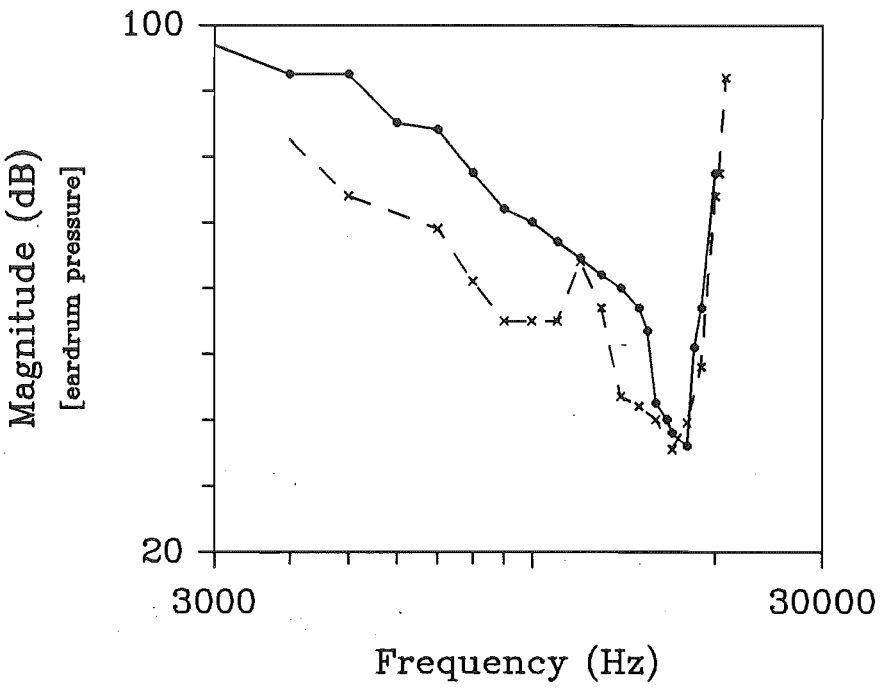

Figure 3.4: Response in the arcuate and pectinate zones of the BM (from Sellick *et al.*, 1983a - animals 116 and 90, respectively). Isovelocity curves are presented, showing the eardrum pressure required to elicit a BM vibration of 0.04 $mm \cdot s^{-1}$. The arcuate zone response is indicated by the solid line, whilst that of the pectinate zone is indicated by the dashed line. The pectinate response is more broadly tuned than the arcuate response, suggesting the presence of a mechanical second filter between the two zones.

susceptible to trauma, and that it is only when exceptional care is taken to minimize cochlea damage that high selectivity and sensitivity is observed. The data of Sellick *et al.* (1983a,b) and Robles *et al.* (1986) further support this hypothesis.

The selective vulnerability of the BM response peak (i.e. the ability to remove it, leaving the remainder of the tuning curve, including high frequency rolloff, essentially intact) suggests that its underlying mechanisms are separate from those governing the formation of the travelling wave. The likely site for this extra, metabolically-sensitive process is in the organ of Corti (see Section 2.2). If this is the case, then anatomical considerations (as outlined in Chapter 2) suggest that the response in the arcuate and pectinate zones should exhibit significant differences. In the response measurements of Sellick *et al.* (1983a,b), care was taken to note the radial position of the Mössbauer source on the BM. Figure 3.4 shows their isovelocity data of the response in the arcuate and pectinate zones of the BM. The BM response is more broadly tuned when measured with a source on the pectinate

zone compared to that measured with a source on the arcuate zone. The measured neural response resembles more closely the arcuate mechanical response than it does the pectinate response.

Evans and Wilson (1975) made concurrent BM and nerve fibre response measurements. In their data the neural response always had a large peak, whereas the BM response, measured using a capacitive probe, did not. This observation is in conflict with those of other investigators, since the large neural peak implies a cochlea free from trauma, whereas the broad mechanical response implies a traumatized cochlea. This could be a result of one of the inherent disadvantages of the Capacitive Probe technique (for a review see Khanna, 1986). The spatial resolution of this technique is severely limited by the size of the probe used. The diameter of their capacitive probe was of the same order as the width of the BM at the position of measurement (approximately 0.2 *mm*). Therefore, they were measuring the *average* BM velocity. Their results suggest that the mechanical response of the BM is different across its width, with the average response exhibiting low selectivity while the neural response is determined by a small section of the BM that exhibits a high selectivity. This hypothesis is also supported by the broad tuning curves measured (using the Capacitive Probe technique) by Le Page (1987).

The data of Evans and Wilson (1975), Sellick *et al.* (1983a) and Le Page (1987), and considerations of cochlear anatomy (see Chapter 2), all support the hypothesis (proposed in this thesis) that a *mechanical* second filter exists, from rather broad tuning in the pectinate zone to much sharper, neural-like tuning in the arcuate zone.

Chapter 4

Models

This chapter presents a brief description of a number of different types of cochlear model, and outlines the contribution they have made to the improvement of our understanding of cochlear mechanics. The formulation of electrical transmission line (ETL) cochlear models is described in detail, since the cochlear model described in Chapter 5 takes the form of an ETL. It is concluded that some of the fundamental assumptions made in the formulation of cochlear models are probably inaccurate.

4.1 Mathematical and Physical Models

On a microscopic (or *micro*mechanical) scale, the cochlea is a very complicated system with many unusual structural features. In the formulation of cochlear models, assumptions must be made concerning the relative importance of these features. If the assumptions made are accurate, the resulting model can provide new insight into the mechanics of the cochlea and can be used as a basis for determining the experimental investigations that would further improve our understanding of cochlear mechanics. A useful cochlear model must satisfy three criteria (Viergever, 1980): it must be the simplest possible, without neglecting structural features that are mechanically important; it must exhibit a realistic response; and, through its analysis, it must be capable of elucidating the important aspects of cochlear mechanics.

Different modelling techniques allure themselves to investigations of the cochlea. The most obvious distinction to be made is that between mathematical and physical models. The present trend is to formulate mathematical cochlear models and then analyse them analytically or numerically. Analytical investigations have the advantage that the solution method itself can elucidate physical properties of the model. Numerical investigations have the advantage that, in general, fewer assumptions are required in the formulation of the model. Both analysis techniques contribute significantly to our understanding of cochlear mechanics. However, in mathematical analyses there can be a tendency to regard the solution as accurately describing real cochlear operation, by forgetting the gross assumptions that are *always* required in the formulation of the model.

Most of what we know "for sure" about the basic operation of the cochlea - for instance, the formation of the travelling wave - is the result of investigations performed on physical hydrodynamic models by von Békésy (1960). However, since then the (few) such models that have appeared have had serious shortcomings. For example, the model of Cancelli *et al.* (1985) did not exhibit a realistic response, despite the incorporation of many of the cochlear partition structures as well as allowing for fully three-dimensional (3-D) fluid flow.

Another type of cochlear model, the physical ETL (e.g. Bogert, 1951; Zwicker, 1986) can be considered in the same way as physical hydrodynamic models, in that the response and stimulus appear simultaneously. This represents an important advantage over computer or analytical solutions. However, all such models to date have the disadvantages of a very simple fluid representation and an inability to incorporate mechanical coupling in the CP (techniques for overcoming these shortcomings are presented in Chapter 6).

4.2 Assumptions

The need to make assumptions in the formulation of a cochlear model is clear (for a review of the common assumptions made, see Neely (1981) or Viergever (1980, 1986)). Those assumptions which, in the opinion of the author, are considered to be accurate are:

Isolated cavity: The cochlea is considered to communicate (mechanically) with the outside world only via its two windows. The cochlear fluids have connections to the vestibule and to the endolymphatic and perilymphatic ducts. However, these are assumed to act only as reservoirs of the cochlear fluids and are thought not to have any mechanical effect. Von Békésy found the volume displacements at the round and oval windows to be approximately equal, suggesting that the flow into the other spaces is indeed negligible.

Ignore spiral coiling: The cochleae of some animals are not tightly coiled and so it is assumed that the coiling in humans and mammals is a space-saving feature. Mathematical analyses of (simplified) models support this view (Viergever, 1978a; Loh, 1983; Steele and Zais, 1985).

Ignore Reissner's membrane: Compared to the CP, Reissner's membrane is very light and flexible. Even if its motion is different from that of the BM, Reissner's membrane should not significantly influence cochlear mechanics.

Ignore scalae dimension variations: The dimensionality of the fluid flow affects the mechanical response. However, the wavelength change along the cochlear length far exceeds any scalae cross-section dimension changes and so the latter can be ignored. Gross changes in cochlear dimensions (e.g. a doubling in height) can be simulated by appropriate changes to CP parameters.

Linearity and fluid viscosity: Fluid non-linearity is negligible even at the highest intensity levels and viscosity can be ignored in macromechanical considerations (Viergever,

1980). At a micromechanical level fluid viscosity could be important, particularly in influencing the CP resistance parameters (e.g. the narrow subtectorial space dimension could result in a large arcuate resistance). For the analyses in this thesis (in Chapters 5 and 6) the resistance parameters are all quite large, and so the responses should not be significantly altered if fluid viscosity was included in the models. The cochlear partition is assumed to operate linearly near threshold (where the highest degree of selectivity and sensitivity is exhibited); non-linear effects mainly become significant for stimulus levels well above threshold. Only the linear mechanical response of the cochlea is considered in this thesis.

Stapes: It is assumed that the stapes moves as a piston and is located at the far basal end of the cochlea. In this region the fluid wavelength is much larger than the dimensions of stapes and hence its mode of excitation or its position (both within reasonable limits) should have negligible effect on the fluid waves it generates.

Helicotrema: The small diameter of the helicotrema means that it acts as a resistance between the two scalae, and only has an effect for the lowest frequencies. For the frequency range of interest (above 1 *kHz*) it can be ignored.

The following assumptions are considered to be potentially inaccurate (to the extent indicated):

Fluid compressibility: The fluid is usually assumed to be incompressible, which is definitely valid for low stimulus frequencies. However, compressibility of the fluid could influence wave mechanics for stimuli frequencies at the upper end of the audible spectrum, by the formation of standing waves in the cochlea. For these frequencies the cochlea length is approximately equal to a half wavelength, resulting in the stapes presenting an abnormal impedance to the middle ear thereby affecting measurements of eardrum pressure (Stinson, 1986; Khanna and Stinson, 1986). This questions the accuracy of selectivity and sensitivity measurements for these frequencies, which unfortunately applies to most of the available response data.

CP geometry: In almost all mathematical models, the CP is assumed to be a flat membrane with certain values of impedance across its width. In the simplest models only one impedance is defined at each position along the cochlear length. Even in 3-D fluid models the complicated geometric arrangement of the organ of Corti, the tunnel of Corti, the subtectorial space and the tectorial membrane is totally ignored. This simplification is necessary to ensure mathematical tractability, but unfortunately it is not based on experimental evidence.

Modes of vibration for the BM: In almost every modelling study, the BM is assumed to have only one mode of vibration, in that only one part of the BM (radially) is free to move. This is not in accordance with *either* its anatomical structure (see Chapter 2) *or* its measured response (see Chapter 3). The only cochlear models (known by this author) which allowed for the differing radial structure of the CP

were those of Steele and Taber (e.g Steele, 1974; Taber and Steele, 1979). From their studies they concluded that the additional modes of vibration had little effect on cochlear response. However, this conclusion is only true if the metabolically-sensitive motile process that is known to alter BM mechanics is ignored. It is understandable that Steele and Taber ignored the motile process, as at the time of the models' formulation the existence of such a process was quite uncertain. In Chapter 5 it is shown that the inclusion of a motile process in the arcuate zone (of a model with two modes of vibration for the BM) has a profound effect on the response.

4.2.1 Fluid Dimensionality

The variation of fluid wavelength along the cochlear length results in a minimization of reflections and an increase in the height of the response peak. For a cochlear model to simulate these features, a multi-dimensional fluid model must be incorporated. Current 3-D models allow for the BM spanning only a fraction of the cochlea width, which results in variations in fluid motion across the width of the cochlea. These models simulate "contraction" of the fluid wavelength in both height and width dimensions but, as mentioned above, they do not allow for the complicated structural features of the CP.

2-D models allow for variations in the fluid motion with height above the BM. Such models also simulate the transition from long-wave to short-wave behaviour. The long-wave region is as for a 3-D model but now, as the short-wave region is reached, the decreasing wavelength contracts the fluid in only one dimension (i.e. height) rather than in two dimensions (i.e. in height and width). This reduction in wavelength causes a smaller increase in the series fluid impedance, and a correspondingly less rapid reduction in the amount of fluid "riding" on the BM. The measurable result of this smaller wavelength contraction is a smaller response peak than that exhibited by 3-D models.

1-D models allow for parameter variations only along the cochlear length. This is equivalent to assuming that throughout the cochlea the wavelength is large in comparison to the cross-sectional dimensions of the scalae. Such models should be incapable of exhibiting the affects of decreasing fluid wavelength. However, if the rate of phase accumulation can be predicted, then the reduction of reflections and sharper response peak can indeed be simulated (albeit in a rather artificial fashion (Zwislocki, 1983)). For the remainder of this chapter, and all of Chapter 5, only 1-D fluid motion is considered. The affect that this simplification has on the response are shown in Chapter 6.

4.2.2 Degrees of Freedom

The formulation of new types of cochlear model has closely followed changes in the experimentally-observed response. The very highly selective and sensitive responses, first measured in 1982, strongly suggested that the underlying mechanisms were controlled by the microstructure of the CP. Before this time, the BM response could be realistically

simulated in a cochlear model with each section of the CP modelled as a second-order system, comprising a series connection of mass, compliance and resistance.

Before 1982 there were a number of models proposed which incorporated (mechanical-to-neural) second filter sharpening mechanisms to account for the huge disparity between the measured mechanical and neural responses (e.g. Duifhuis, 1976; Allen, 1977; Zwislocki and Kletsky, 1979; Neely, 1981). These models increased the CP impedance to third or fourth-order, but they were unable to mimic the later measurements showing BM mechanical response very similar to neural response. The added degree(s) of freedom had little effect on the mechanics of the BM, and so as far as the BM mechanical response was concerned such models were still second-order.

4.3 Active models

The measurement of spontaneous otoacoustic emissions (SOEs) at the eardrum (Kemp, 1979; Zurek, 1981; Martin *et al.*, 1988) proves the existence of an energy-producing process somewhere within the cochlea. It has been the trend to use these observations to support the hypothesis of active processes in cochlear tuning. This, however, is an erroneous argument. There is little to suggest that the mechanism responsible for the increase in BM response is directly related to that responsible for the generation of SOEs (a more detailed argument in support of this conclusion is presented in Section 7.3.1).

The very high selectivity and sensitivity of the BM response, and the changes in this response as a result of trauma, are also used as justifications for an active process in cochlear mechanics. In the formulation of all recent cochlear models it has been found necessary to include an active, energy-producing, process in order for the models to simulate a realistic BM response (e.g. Neely and Kim, 1983, 1986; Zwislocki, 1983; Geisler, 1986). A representative active cochlear model example is that of Neely and Kim (1986), which incorporated active processes in the form of pressure sources located at the OHCs. Over a certain narrow band of frequencies the OHCs exerted a pressure on the BM in phase with the (real part of) BM motion, thereby reducing the real part of the BM impedance. This resulted in an enhancement of BM motion for that band of frequencies, resulting in a very realistic mechanical response. The active region had to be basal of the characteristic place in order for the model to exhibit a realistic response. If it was at the characteristic place instability resulted and so, in a more refined form, the model was capable of producing SOEs (Neely, 1988). It is worth noting that the frequency domain response reported by Neely and Kim (1986) has no time domain counterpart, owing to the response being unstable (Diependaal and Viergever, personal communication). Although this deprives the results of Neely and Kim (1986) of physical significance, their model is still a good representative of the general form of active cochlear models.

Justification for active processes in cochlear tuning came from inverse approaches, in which the BM impedance function was calculated from (or fitted within a limited (realistic) parameter space so as to conform with) the measured mechanical response. These analyses

showed that, for the recent sharply-tuned responses, the real part of the BM impedance needed to be negative over a restricted region basal of the peak, in order to support the increase in travelling wave in this region (de Boer, 1983a,b,c; Viergever and Diependaal, 1986; Diependaal *et al.*, 1987). De Boer maintained that one of the key problems with a passive CP is that for a substantial rise in the response to occur there must be a corresponding decrease in the wavelength. The phase delays necessary would not correlate with those observed in the real cochlea, implying the necessity of an active process.

All active models, and inverse approaches, are open to the same criticism: that in the assumptions made in their formulation, obvious features of CP anatomy are not included. Active models do exhibit realistic response properties, but their structure does not necessarily reflect that of the cochlea. Furthermore, the conclusions drawn from the inverse approaches apply to the models used in the analysis, but do not necessarily apply to the real cochlea. It is for these reasons that the arguments used to justify the existence of active processes in cochlear tuning are not convincing. In further support of this conclusion, Chapter 5 describes a passive cochlear model that incorporates, in a crude fashion, the structure of the CP. This new cochlear model simulates realistic response selectivity, phase response and changes in response as a result of trauma.

4.4 Transmission Line Models

Von Békésy recognised the medium of the travelling waves as a non-uniform (dispersive) transmission line. The first models to capture this essential feature were the transmission line (TL) models of Zwislocki (1948), Peterson and Bogert (1950), Bogert (1951) and Fletcher (1951). One of the main assumptions necessary in the formulation of a TL model is that the fluid motion is one-dimensional. Therefore, the response peak in such models will not be as high as in multi-dimensional models, and the problem of reflections between adjacent sections can arise if the discretization is not fine enough. However, these models have a number of advantages. Firstly, the simplified fluid model means that for the same analysis complexity a more complicated CP representation can be included. Secondly, the equivalent electrical circuit can be derived (as described below) and realized using a physical circuit. The operation of this circuit can be observed in real time to real inputs (like speech and music) in a similar way to physical hydrodynamic models (e.g. Cancelli *et al.*, 1985).

4.4.1 Mechanical Transmission Line

In a TL model the cochlea is divided up lengthwise into a number of discrete sections, with each section comprising a mechanical shunt impedance representing the CP and a series fluid impedance that connects adjacent sections together. The cochlear fluid is assumed to be inviscid and (usually) incompressible. The 1-D long-wave approximation for the fluid motion means that the fluid moves as a solid lump of mass in the longitudinal direction only. Similarly, the CP element is constrained to move in the vertical direction

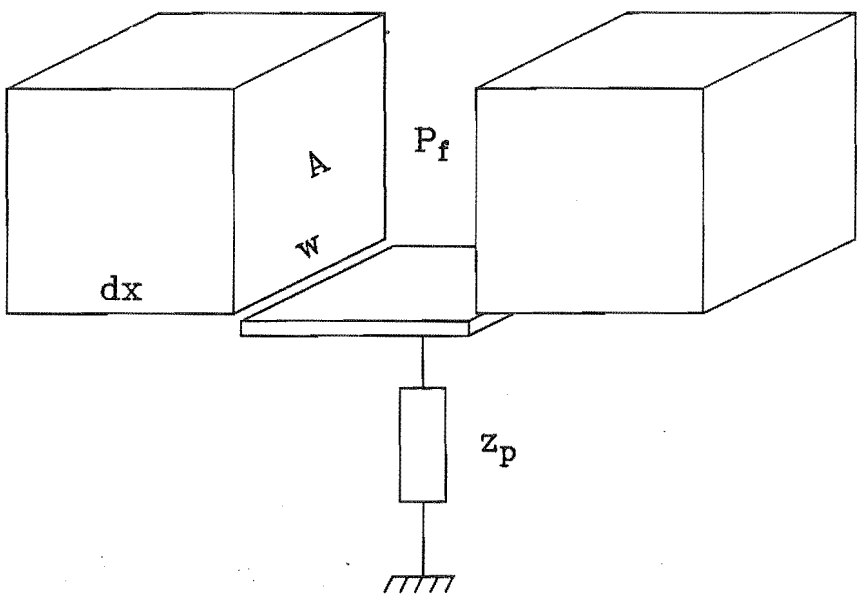

Figure 4.1: Schematic representation of one section of the cochlea, showing how the equations of motion are derived. The cochlea is assumed to be square. The impedance z_p represents the impedance of one section of the CP. The fluid between adjacent sections is constrained to move in a longitudinal direction only.

only. Owing to the symmetry that exists between the scalae vestibuli and tympani, one longitudinal fluid element can be used between each section.

A simplified representation of one section of the transmission line model is shown in Fig. 4.1. A frequency domain description is possible, owing to the linearity of the models described in this thesis. All the dependant quantities are functions of distance from stapes and complex frequency (this is assumed implicitly). Note that all velocities are point velocities. If the differential fluid pressure (scala vestibuli minus scala tympani) is P_f, v_f is the fluid velocity (in either scala - the fluid motion is equal and opposite in the two scalae), v_p is the BM velocity (motion towards the scala tympani implies a positive velocity), w is the width of the scalae, A is the cross-sectional area of the scalae, ρ is the fluid density, z_p is the CP impedance, and dx is the incremental length of the cochlea under consideration, then the equation of motion (Newton's First Law) for the fluid is given by

$$\frac{dP_f}{dx} = -\jmath\omega\rho \cdot v_f \tag{4.1}$$

where $\jmath$ is the imaginary unit ($\jmath^2 = -1$) and ω is the angular frequency. The equation of motion for the CP is

$$2P_f = -z_p \cdot v_p \tag{4.2}$$

The factor "2" appears in Eqn. 4.2 because the pressure in the two scalae is in antiphase. Consideration of fluid conservation between sections gives

$$v_p = \frac{dv_f}{dx} \cdot \frac{A}{w} \tag{4.3}$$

The quantity A/w in Eqn. 4.3 corresponds to the scala height for the case of the BM spanning the full scala width, and with the whole BM (in width) moving by the same amount. These are clearly invalid assumptions, and so it is better to define $h = A/w$, where h is the *effective* height of the scala, thereby allowing for a realistic BM width and bending mode (de Boer, 1980). Substituting Eqn. 4.3 into Eqn. 4.2 yields

$$P_f = \frac{h\, z_p}{2} \cdot \frac{dv_f}{dx} \tag{4.4}$$

In mechanical systems it is usual to express impedance as the ratio of force to velocity. However, in hydrodynamic systems such as the cochlea it is common to use pressure instead of force. Pressure is defined as the force per unit area and so the impedance per unit area must be used to ensure that point velocity is the dependent quantity. The term "specific acoustic impedance" is used to describe this form of impedance. In Eqns. 4.2 and 4.4, z_p is the specific acoustic impedance of the BM, defined as $z_p = \check{z}_p/(w \cdot dx)$, where $\check{z}_p$ is the BM point impedance.

4.4.2 Electrical Transmission Line

Two (or more) systems are analogous if their constitutive equations have the same form (Olson, 1966). The replacement of one system with its analogous system, that is more familiar and/or more readily analysed, can be beneficial to obtaining an understanding of the operation of the less familiar system. By applying dynamic analogies the quantities of the system analysed can be directly related to those of the system of interest.

A generalised ETL cochlear model has the form shown in Fig. 4.2. The series impedance is an inductance, representing the inviscid cochlear fluid. If V_f is the node voltage, i_f is the series current, L_f is the series inductance, and Z_p is the shunt impedance, then applying Kirchhoff's voltage law to the series branch gives

$$dV_f = -\jmath\omega L_f \cdot i_f \tag{4.5}$$

where dV_f is the voltage difference between adjacent sections. Kirchhoff's voltage law for the shunt branch gives

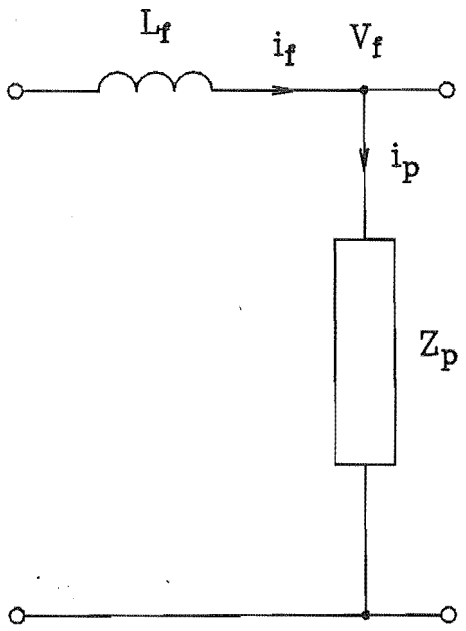

Figure 4.2: Schematic of one section of an electrical transmission line (ETL) cochlear model. The series inductor represents the inviscid fluid, and the shunt impedance represents the CP.

$$V_f = Z_p \cdot di_f \tag{4.6}$$

where di_f is the change in series current over the section, which equals the shunt current i_p. Comparing Eqn. 4.1 with Eqn. 4.5, and Eqn. 4.4 with Eqn. 4.6, yields the following analogies between the mechanical and electrical TL models:

$$\begin{aligned} V_f &\longleftrightarrow P_f \\ i_f &\longleftrightarrow v_f \\ L_f &\longleftrightarrow \rho dx \\ Z_p &\longleftrightarrow z_p \cdot \frac{h}{2dx} \end{aligned}$$

In the simplest model, z_p is a second-order system, consisting of mass, compliance, and resistance in series:

$$z_p = j\omega m_p + \frac{1}{j\omega c_p} + r_p \tag{4.7}$$

The analogous electrical circuit consists of inductance, capacitance, and resistance in series:

$$Z_p = j\omega L_p + \frac{1}{j\omega C_p} + R_p \tag{4.8}$$

where the electrical impedance parameters are obtained by scaling the mechanical (specific acoustic) impedance parameters by $h/(2dx)$. From Eqns. 4.5, 4.6 and 4.8, one section of the second-order ETL cochlear model is obtained (Fig. 4.3). As in the mechanical TL, the complete cochlear model is formed by cascading a number of these sections. The stimulus is applied to the left (basal) end of the ETL. Figure 4.4 shows what an ETL model looks like for one stimulus frequency. In all sections well basal of the resonant point, the impedance of each shunt branch is capacitive. For these sections the circuit is an LC ladder, supporting the propagation of a travelling wave with a group delay equal to $\sqrt{L_f C_p}$, resulting in a realistic monotonic phase increase. Apical of the resonant point, the shunt branch impedance is inductive and so the circuit behaves like a ladder attenuator (composed of inductances). At the resonant point, the shunt capacitance and inductance cancel each other, leaving the shunt resistance to determine the height of the resonant peak.

4.4.3 Parameters

In a(n) (E)TL model the assumption of 1-D fluid motion is paradoxical at the BM; in the real cochlea the vertical motion of the BM results in a certain quantity of fluid riding on the BM and hence increasing its effective mass. The increase is a function of both the wavelength and the area of the BM element, and is maximal when $\lambda \approx 5a$; where λ = wavelength and a = BM element area (Camp, 1970). Accurately simulating this effect in a 1-D model is not possible, owing to the frequency and place dependence of λ. However, to a good approximation the effect can be accounted for in a cochlear model with high damping by adding one-third of the total fluid mass to that of the CP (Viergever and Kalker, 1975; Sondhi, 1978), as shown in Section 6.2.3.

The phase response in basal regions of the ETL model is governed by the quantity $\sqrt{L_f C_p}$. From the mechanical to electrical analogies (see Section 4.4.2), a realistic value for L_f is determined by well known quantities: the fluid density ρ and the model discretization dx. A realistic value for C_p can then be determined from the measured phase response and/or from measurements of BM compliance (allowing for the $h/(2dx)$ scaling factor). Once C_p has been calculated, the shunt inductance L_p is determined from the CF at each point, from

$$f_{CF} = \frac{1}{2\pi\sqrt{L_p C_p}} \tag{4.9}$$

In Eqn. 4.9, L_p corresponds to the actual BM mass *plus* the added mass of the fluid that is assumed to vibrate with it.

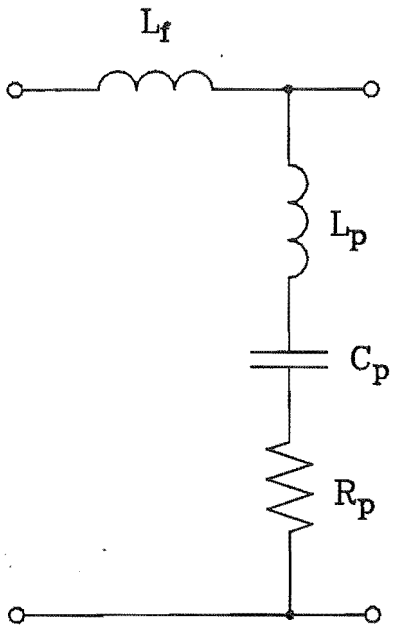

Figure 4.3: Schematic of a short length of an ETL cochlear model .

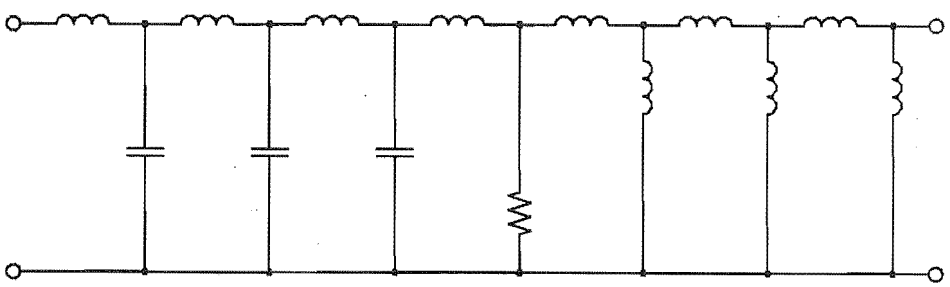

Figure 4.4: Appearance of an ETL cochlear model for one stimulus frequency. For those sections basal of the characteristic place, the shunt capacitance dominates the impedance and hence the circuit acts as an LC ladder, supporting the propagation of a travelling wave. At the resonant point, the shunt inductance cancels the capacitance, resulting in a response peak whose height is determined by the shunt resistance. Beyond the resonant point the shunt inductance dominates the impedance and the resulting inductive ladder rapidly attenuates the travelling wave .

The shunt branch of the ETL model will only exhibit a peak at resonance if it is underdamped, by having a pair of complex-conjugate poles. For this to be the case the following inequality must hold:

$$R_p < \frac{2L_p}{\sqrt{L_p C_p}} \tag{4.10}$$

The actual value of BM resistance is not known. If R_p is very small, the peak will become higher and sharper, but not broad as in the real cochlea. Furthermore, decreasing R_p increases the possibility of reflections between adjacent sections (as does a coarser discretization). Therefore, more degrees of freedom and/or active processes must be incorporated in an ETL cochlear model before it can simulate a realistic response (note that this conclusion is also true for 2-D and 3-D cochlear models).

Chapter 5

The OHCAP Model

This chapter describes a new type of cochlear model which has been developed by the author (Kolston, 1988a,c; Kolston and Viergever, 1989a; Kolston *et al.*, 1989). The special assumptions made in the formulation of the model, which are different from those made for previous cochlear models, are strongly supported by features of cochlear anatomy (see Chapter 2) and measurements of cochlear response (see Chapter 3). The model simulates realistic selectivity and phase response, and realistic changes in response as a result of trauma, without needing to incorporate active processes. Therefore, these features of the mechanical response should not be used to support the hypothesis of active processes in cochlear mechanics.

5.1 Assumptions

Many assumptions that are made in the formulation of cochlear models (as summarized in Chapter 4) can be justified on the basis of anatomical features of the real cochlea. However one frequent assumption, that the BM has only one mode of vibration in the radial direction, is not supported by anatomical evidence; the structure of the CP is quite different in its arcuate and pectinate zones (see Chapter 2). Indeed, recent experimental investigations have explicitly shown that the radial position of measurement greatly influences the measured response (see Chapter 3). Therefore, it seems reasonable to assume that an accurate cochlear model must allow for a radial variation in the BM response.

The new cochlear model presented here is called the OHCAP (Outer-Hair-Cell-Arcuate-Pectinate) model. This name is used to emphasize the two special assumptions made in its formulation: that the BM has two radial modes of vibration, corresponding to division into its arcuate and pectinate zones; and that the OHCs greatly influence the mechanics of the arcuate zone. The latter assumption is also made in the formulation of other (recent) cochlear models (remembering that in these models the BM has only one mode of vibration), and is strongly supported by experimental investigations (see Chapter 2). The difference between previous models and the OHCAP model is that in the former models the OHCs inject energy (over a limited region of the cochlea) in order to achieve

a realistic enhancement in mechanical response near the CF. In these active models, the OHCs reduce the *resistance* component of the BM impedance. In the OHCAP model, the OHC impedance is assumed to reduce only the *reactance* component of the *arcuate* impedance.

Apart from the two described above, the other assumptions made in the formulation of the OHCAP model are similar to those made in previous modelling studies (see Chapter 4). The fluid flow in the OHCAP model is assumed to be one-dimensional, enabling analysis as a transmission line model (see Section 4.4). This means that both zones have the same differential fluid pressure acting on them.

5.2 Formulation

A schematic of a cross-section of the CP is shown in Fig. 5.1 (derived from the anatomical diagram shown in Fig. 2.5). A more simplified representation of the OHCAP model can be derived by considering which of the components in Fig. 5.1 have the same motion. Shear motion in the subtectorial space supposedly determines the neural tuning, which is assumed to be the same as the arcuate tuning (this assumption is strongly supported by all recent measurements of mechanical response (e.g. Khanna and Leonard, 1982; Sellick *et al.*, 1983a,b; Robles *et al.*, 1986)). This implies that the tectorial membrane has no radial resonance (as in Fig. 5.1), with the result that the tectorial membrane, pillars of Corti, sensory hair cells, and BM arcuate zone can all be lumped into one element. The pectinate zone of the BM is represented by another element. Owing to their position in the organ of Corti, it is assumed that the motile force produced by the OHCs acts on the arcuate zone.

The lumped-component equivalent of Fig. 5.1 appears in Fig. 5.2. The components labelled m_a, c_a and r_a correspond, respectively, to the mass, compliance and resistance of the arcuate zone. The components labelled m_p, c_p and r_p correspond to the quantities in the pectinate zone. The additional impedance in the arcuate zone, owing to the presence of the OHCs, is represented by z_o. This system for the CP is more complicated than that in the example described in Section 4.4. The BM itself is given two degrees of freedom, whilst the arcuate zone of the CP has more (the number of degrees of freedom is determined by the form of the OHC motile force). One feature lacking in the OHCAP model (of Fig. 5.2) is radial mechanical coupling between the two zones. Since the BM fibres span the full CP width, such coupling is obviously present in the real CP. It is shown in Chapter 6 that the inclusion of radial coupling in the OHCAP model has a trivial effect on its response.

The electrical circuit equivalent of the mechanical system (Fig. 5.2) is derived by applying the dynamic analogies outlined in Section 4.4. The resulting circuit, which represents one section of the OHCAP model, is shown in Fig. 5.3. The components labelled L_a, C_a and R_a represent, respectively, the mass, compliance and resistance of the arcuate zone. The components labelled L_p, C_p and R_p represent the corresponding quantities in the

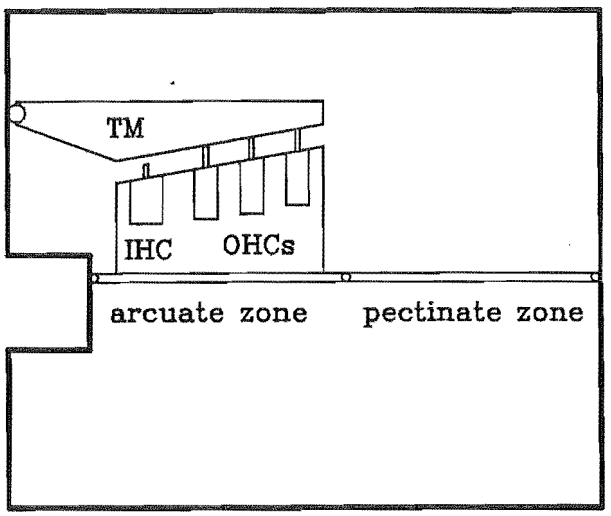

Figure 5.1: A schematic of a cross-section of the CP, derived from the anatomical diagram shown in Fig. 2.5 .

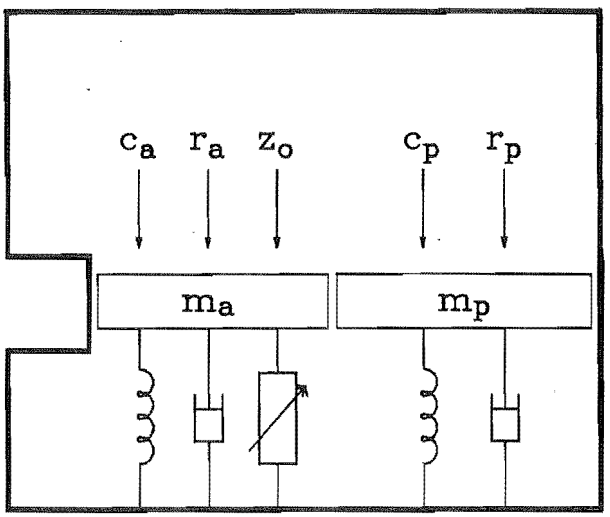

Figure 5.2: Lumped component representation of the CP. The elements representing the arcuate zone have a subscript $_a$, and those for the pectinate zone have a subscript $_p$. The mass, compliance and resistance of the arcuate zone correspond to the combined values of all the arcuate components (i.e. BM, pillars of Corti, IHC OHCs, and tectorial membrane). z_o represents the impedance of the OHC motile force which acts on the arcuate zone .

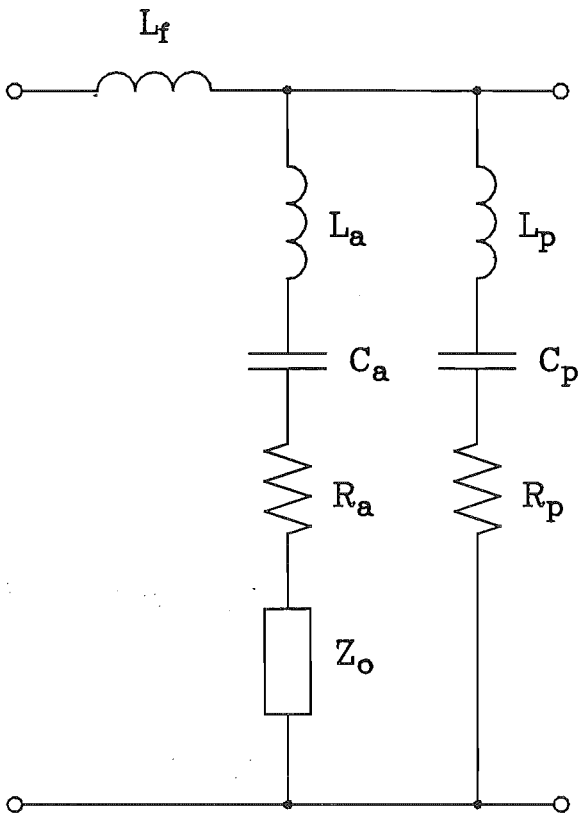

Figure 5.3: One section of the OHCAP model, in ETL form. This circuit is obtained by applying dynamic analogies to obtain the electrical circuit equivalent to the mechanical system shown in Fig. 5.2. The series inductance represents the fluid coupling between adjacent sections, whilst the two shunt branches represent the two zones of the CP. The current flowing in each branch represents the velocity of the corresponding zone.

pectinate zone. The additional impedance in the arcuate zone, owing to the presence of the OHCs, is represented by Z_o.

5.3 Operation

The most crucial feature of the OHCAP model is that the pectinate zone controls the macromechanical fluid behaviour, whilst the arcuate zone, under the control of the OHCs, controls the neural tuning.

For all stimulus frequencies less than the CF, the impedance of both CP zones is mainly imaginary and negative (i.e. is dominated by its stiffness component). The arcuate stiffness is considerably greater than the pectinate stiffness, and so the magnitude of its response is less. The phase of the motile force generated by the OHCs is arranged so that its effective impedance, Z_o, is mainly imaginary and positive (i.e. mass dominated). Therefore, the presence of the OHC reduces the imaginary component of the arcuate impedance. The amount of impedance reduction is dependent on the magnitude of Z_o. For frequencies much lower than the CF, $\mid Z_o \mid$ is small compared to the CP stiffness and hence the presence of the OHCs has little effect on the response. For stimulus frequencies near the CF, $\mid Z_o \mid$ is approximately equal to the CP stiffness resulting in a (resonance-like) cancellation of the reactance component of the arcuate impedance.

The presence of the OHCs thus produces a very large variation in the reactance component of the arcuate zone impedance, and hence a very large variation in the magnitude of the arcuate zone response. As shown in Section 5.5.3, the large reactance component at CF is associated with a large resistance component. This, however, has little effect on the response, since the resistance parameters in the OHCAP model are rather large anyway (see Table 5.2). The actual shape (or selectivity) of the arcuate response closely follows the frequency dependence of $\mid Z_o \mid$. Therefore, by using different models (or parameters) for the OHCs, different cochlear mechanical responses can be simulated. In this manner, physiologically justifiable models of the OHCs can be incorporated in the OHCAP and thereby checked to see if they produce a realistic response.

5.4 Models for the Outer Hair Cells

This section describes two models for the OHCs which can be incorporated into the OHCAP model. In the formulation of the first model it is assumed that all the filtering necessary to achieve the correct frequency dependence of Z_o is performed within the OHC itself. In the second model the geometric arrangement of the OHCs, Deiters' cells, their phalangeal processes, and the pillars of Corti is used to derive the OHC filtering requirements.

5.4.1 FOHC model

The FOHC model derives its name from the fact that all the required Filtering for the correct frequency dependence of Z_o occurs within the OHC itself. No attempt is made to justify the required filtering on the basis of OHC physiology. In the FOHC model it is assumed that the OHC is a one-port device, in that the OHC has, as its input, the motion of the arcuate zone (through bending of the OHC stereocilia) and, as its output, a motile force resulting in an effective impedance Z_o. The frequency dependence of Z_o determines the response of the FOHCAP model (which is the OHCAP model with the FOHC model incorporated in it), so that the complexity of the OHC model is governed by the type of response that is required.

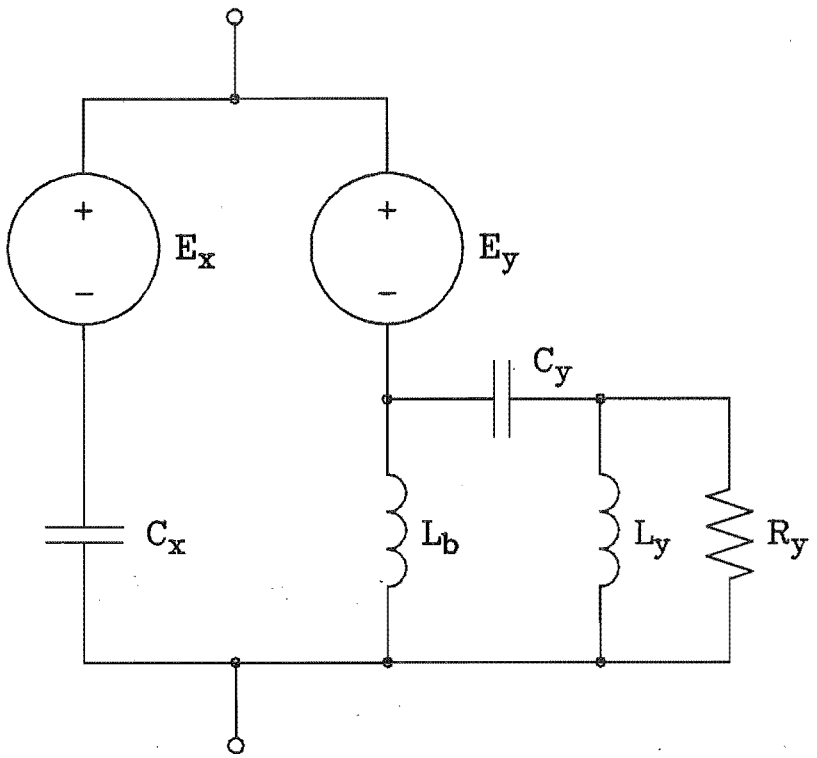

Figure 5.4: FOHC model in electrical circuit form. This circuit replaces Z_o in Fig. 5.3. The voltage sources represent the OHC motile force and are controlled by currents flowing within the circuit. Trauma is simulated in the model by reducing the gain of the voltage sources.

In order to simulate the very high peaks as observed in recent measurements, a fourth-order filter is required for the FOHC model. Figure 5.4 shows the FOHC model, in electrical circuit form. The voltage sources (force generators) are described by $E_x = -K_x \cdot V_x$ and $E_y = -K_y \cdot V_y$, where V_x is the potential difference across C_x and V_y is the potential difference across L_y. The impedance function for this network (ignoring R_y and assuming $L_b \ll L_y$) is

$$Z_o = \frac{j\omega}{\omega^2 \frac{C_x}{K_x} + \frac{\omega_b^2}{\omega^2}(1 - \frac{\omega^2}{\omega_f^2})} \tag{5.1}$$

where

$$\omega_f{}^2 = \frac{1}{L_y C_y} \quad \text{and} \quad \omega_b{}^2 = \frac{\omega_f{}^2}{K_y L_b}$$

Inclusion of R_y means that L_y is multiplied by $R_y/(R_y + j\omega L_y)$.

The operation of the FOHC model can be understood qualitatively by considering the topology of the FOHC circuit in Fig. 5.4. The FOHC model is divided into two parallel branches. The left branch acts as a mass that cancels the BM arcuate compliance. However, the presence of the right branch means that the cancellation is not complete; the amount of cancellation depends on the relative magnitudes of the two branches. For low frequencies the right branch has a relatively low impedance, thereby ensuring that the left branch has little effect on the overall arcuate impedance. Near the CF, the impedance of the right branch becomes large and so the left branch mass cancels the BM compliance, resulting in a small overall arcuate impedance and hence a large response peak.

The FOHC model operation can be understood quantitatively by considering the functional form of Eqn. 5.1. When $\omega = \omega_f$, the OHC impedance simplifies to

$$Z_o = \frac{j}{\omega C_x / K_x} \tag{5.2}$$

If parameters are chosen such that $C_x/K_x = C_a$ (C_a is the BM arcuate compliance), the reactance component of the arcuate impedance is minimized at ω_f, resulting in resonance at this frequency (i.e. the parameters are chosen so that ω_f corresponds to the CF of the pectinate zone). The minimum value of arcuate reactance is determined by the value of R_y. When $\omega \ll \omega_f$, the value of ω_b determines the amount of reactance cancellation by the FOHCs; the frequency at which the FOHCs begin to have an effect on the arcuate response is approximately equal to ω_b.

5.4.2 DOHC model

The DOHC model derives its name from the fact that the unusual geometry of the organ of Corti in the longitudinal direction (in particular the position of the Deiters' cells) is used to minimize the filtering required of the OHC. A schematic of the DOHC model is shown in Fig. 5.5, which is derived from the geometric arrangement of the OHCs, the Deiters cells, their phalangeal processes, and the pillars of Corti (see Fig. 2.8). The base of each OHC is supported by the top of a Deiters' cell, and the top of each OHC is in close proximity to a phalangeal process from an adjacent (basal) Deiters' cell. Each Deiters' cell base lies on the edge of the pectinate zone, with the first row of Deiters' cells being adjacent to the outer pillar of Corti. It is postulated that: the bottom of the OHC senses the (vertical) velocity of its supporting Deiters' cell (v_{pa} - the velocity of the more *a*pical section of the pectinate zone); the OHC performs a simple (first-order) filtering function to obtain $v_{pa'}$, the OHC-modified pectinate zone velocity; the top of the OHC senses the

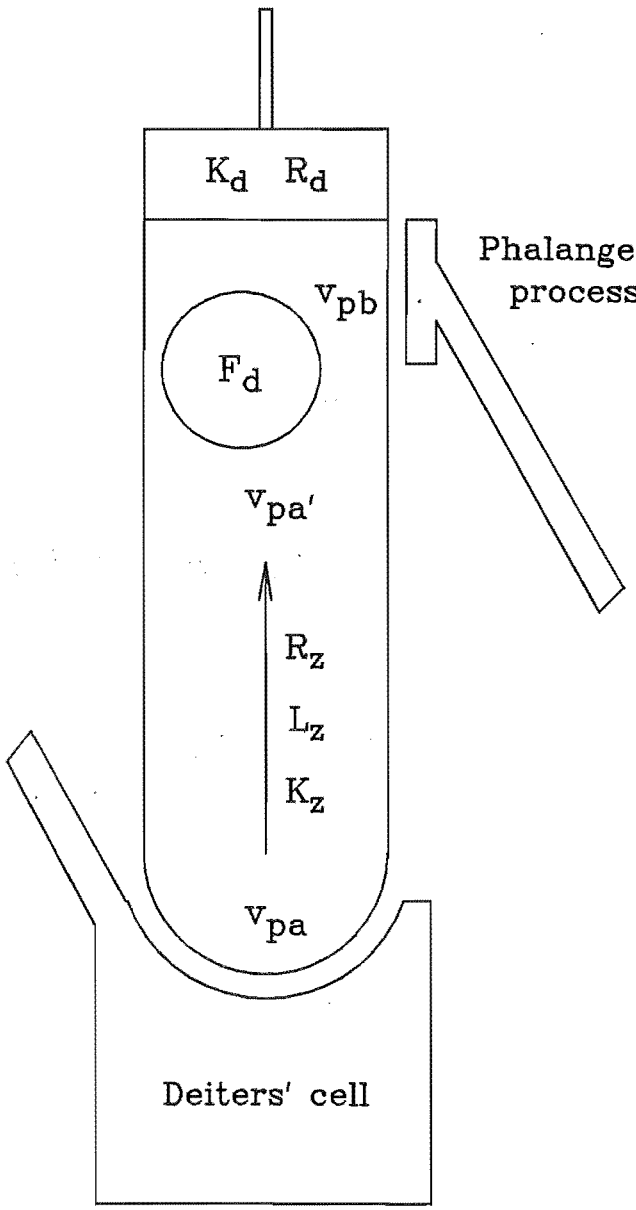

Figure 5.5: Schematic of the DOHC model. The OHC has as its input the motion of two adjacent sections of the pectinate zone. The OHC base has as an input the motion of one section of the pectinate zone, transmitted to it via its supporting Deiters' cell. This signal is filtered, before being compared with that obtained from an adjacent Deiters' cell (transmitted via the phalangeal process). This difference signal controls the motile force generator.

velocity of the adjacent Deiters' cell (v_{pb} - the velocity of the more *b*asal section of the pectinate zone); and $v_{pa'}$ and v_{pb} are used by the OHC to control its impedance. Since the OHCs are positioned within the (moving) organ of Corti, they have no absolute reference point for the monitoring of mechanical movement. The most likely reference point is the motion of the reticular lamina, which corresponds to the motion of the arcuate zone. Therefore, v_{pa} is in fact the pectinate motion minus the arcuate motion (at the same point), and v_{pb} is the adjacent (basal) pectinate motion, again minus the arcuate motion.

The OHC filter, which transforms v_{pa} to $v_{pa'}$, is designed to remove the (very small) magnitude and phase differences that exist in the responses of two adjacent sections of the pectinate zone, when the stimulus frequency is considerably less than the CF for that place. Over the frequency range of interest, the OHC filtering function is given by

$$v_{pa'} = v_{pa} \cdot K_z(j\omega L_z + R_z) \tag{5.3}$$

where v_{pa} is the velocity of the pectinate zone, L_z and R_z are the impedance parameters of the OHC filter and K_z is a real-valued constant.

The parameter values L_z, R_z and K_z are chosen so that, for stimulus frequencies much less than the CF, $v_{pa'}$ and v_{pb} have very similar magnitude and phase. When the stimulus frequency approaches the CF of both $v_{pa'}$ and v_{pb}, the phase of v_b deviates from that of $v_{pa'}$. Therefore, subtraction of v_{pb} from $v_{pa'}$ yields a signal that the OHC uses to control the motile force generator F_d:

$$F_d = K_d \cdot (v_{pa'} - v_{pb}) \tag{5.4}$$

where $v_{pa'}$ is the OHC-modified pectinate zone velocity (from Eqn. 5.3), v_{pb} is the velocity of the adjacent (basal) section of the pectinate zone, and K_d is a real-valued constant. Note that since the pectinate motion is much less than the arcuate motion, the gain parameter K_d must be very large (see Table 5.2) in order to ensure that the motile force significantly influences arcuate mechanics.

The OHC model is assumed to consist of the force generator in series with a resistance, so that the impedance function Z_o is given by

$$Z_o = R_d + F_d/v_a \tag{5.5}$$

where v_a is the velocity of the arcuate zone and R_d is a resistance. The resulting frequency dependence of Z_o is very similar to that for the FOHC model. In fact, both OHC models operate in the same manner (as described in Section 5.3).

In the DOHC model the excitation for the OHC comes from movement of its body rather than from bending of its stereocilia, the latter being the presently accepted mode of excitation. If the input to the OHC is through its body movements, its motile force generation is most likely to occur through the stereocilia, since this would keep the input and output more effectively isolated. This perhaps explains why the geometric arrangements

of the IHC and OHC stereocilia are so different: the IHC stereocilia provide the input to a forward transduction process, that merely senses mechanical motion; whereas the OHC stereocilia produce the force output of a backward transduction process. The OHC stereocilia bundle would need to be substantially stiffer than that of the IHC. This is indeed the case, since the former stereocilia are arranged in a "V" shape, whereas the latter stereocilia are in a straight line (see Section 2.2). Considerations of the organ of Corti microstructure also suggest that the OHC motility manifests itself via the bending impedance of the stereocilia, rather than via OHC body length changes (Kolston and Viergever, 1989b). Such motile stereocilia bending has been experimentally observed *in situ* (Zenner *et al.*, 1988).

5.5 Response

5.5.1 Analysis techniques

For all the responses shown here the OHCAP model is linear and passive (see Section 5.5.3), and so analysis in the frequency domain is permissible. The OHCAP model was analysed using two numerical solution techniques. For the FOHCAP model, the program "BMRSP1" from de Boer (1980) was modified to allow for two radial modes of BM vibration. In the DOHCAP model the response of the arcuate zone is dependent on that of the pectinate zone, and hence (the modified version of) de Boer's program is unsuitable. The DOHCAP model was analysed in its ETL form using the general circuit analysis program SPICE (Nagel, 1975). Using SPICE is a very inefficient form of analysis since it does not utilize the special topology of the ETL. However, it has the advantage that there are very few constraints on either the model configuration or on the model parameter values (in that discontinuities can be easily incorporated).

In a TL model the number of sections required to minimize reflections is largely determined by the resistance of the CP (see Section 4.4) and the impedance change between sections. In the OHCAP model, the CP resistance is quite large and the stiffness gradient is quite small (see Table 5.2), and hence the number sections required to minimize reflections is quite small. For the FOHCAP model a relatively large number of sections (200 per *cm*) could be used owing to the efficient analysis technique employed. The relatively small number of sections used for the DOHCAP model (50 per *cm*) raised the question of the effect that coarse discretization would have on the operation of the DOHC model. The transformation (v_{pa} - $v_{pa'}$) and subtraction ($v_{pa'}$ - v_{pb}) in the DOHC model applies to ''adjacent'' sections of the cochlea. In the real cochlea the distance between adjacent OHCs is approximately 10 μm (Thorne and Gavin, 1984) and so a cochlea model would require several thousand sections for it to truly reflect the OHC spacing. It was assumed that the model results obtained using a coarse discretization would reflect those obtained if a fine discretization was used. This assumption was checked by comparing, on a local scale, the transformation and subtraction applied to two sections 10 μm apart, and to two sections 200 μm apart. The only significant difference between the two results was

the presence of slight bumps in the response for the coarser discretization (the overall response shapes were the same).

5.5.2 Parameters

The choice of a realistic parameter set is very important if a cochlear model is to be considered a good approximation of the real cochlea. As discussed in Section 4.4, realistic parameters for the fluid and (in the case of the OHCAP model) for the mass and stiffness of the pectinate zone are available.

It seems reasonable to assume that the arcuate stiffness is considerably greater than the pectinate stiffness (see Chapter 2). This is largely the result of two factors: the BM fibres forming a dense mat in the arcuate zone; and the high degree of torsional rigidity afforded by the pillars of Corti and the phalangeal processes of the Deiters cells (both result in a high degree of longitudinal coupling). The ratio of arcuate-to-pectinate stiffness required in the OHCAP model is largely determined by the required response peak height (or tip-to-tail ratio). For example, for a 40 dB peak the arcuate stiffness must be 100 times greater than the pectinate stiffness. As outlined in Chapter 2, von Békésy (1960) and Miller (1985) measured significant stiffness differences in the arcuate and pectinate zones. Their measurements do not account for the huge differences assumed in the OHCAP model (see Table 5.2). However, both investigations were performed on damaged cochleae (e.g. no OHCs present), and so differences of several orders of magnitude may indeed be present in the normal cochlea.

The value of arcuate mass is not very important (in terms of the response produced), since it is the frequency dependence of Z_o, combined with arcuate stiffness, that dominates the value of arcuate reactance. The value of resistance in the real CP is hardly known. In the OHCAP model the resistance only affects the shape of the response peak *at* the CF. The rise in response well before the CF is unaffected by the resistance and so, to minimize reflections, relatively large CP resistance values were chosen.

Realistic values for the OHC parameters are not known. The filtering performed by the OHCs could be a combination of mechanical, electrical and chemical processes, so it may not even be possible to gauge realistic values from their physical size (except that, for example, a mass value of $10^3\ g \cdot cm^{-2}$ could be deemed to be unrealistic!).

5.5.3 Typical response

The FOHCAP model response (BM velocity versus stapes velocity) for a typical parameter set is shown in Fig. 5.6 (this is similar to a typical DOHCAP model response). As described in Section 5.3, for all stimulus frequencies less than the CF the pectinate motion greatly exceeds that of the arcuate zone, resulting in the pectinate zone controlling the phase response. To illustrate how the presence of the OHCs affects the impedance (and hence motion) of the arcuate zone, Fig. 5.7 shows the reactance component of the arcuate and pectinate zone impedances, with and without the OHCs. In Fig. 5.7 the lines

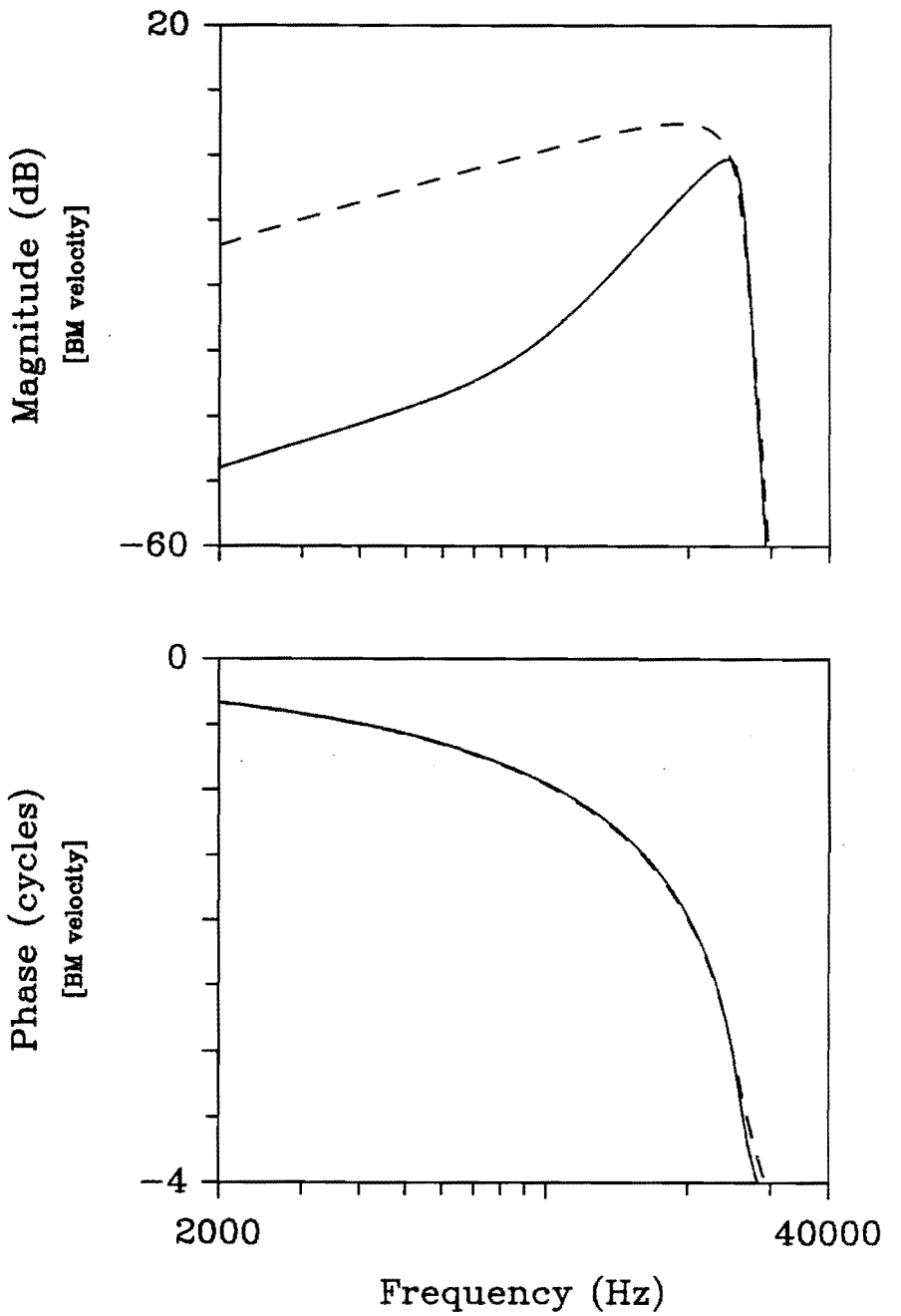

Figure 5.6: Typical response (BM velocity versus stapes velocity) of the FOHCAP model. The arcuate zone response is indicated by the solid line and the pectinate zone response is indicated by the dashed line. The response 3.5 *mm* from the stapes is shown; the response in more basal regions differs in that the arcuate peak is lower and the pectinate response exhibits a slower rolloff above CF (both differences are a result of the greater effects of CP resistance in apical regions).

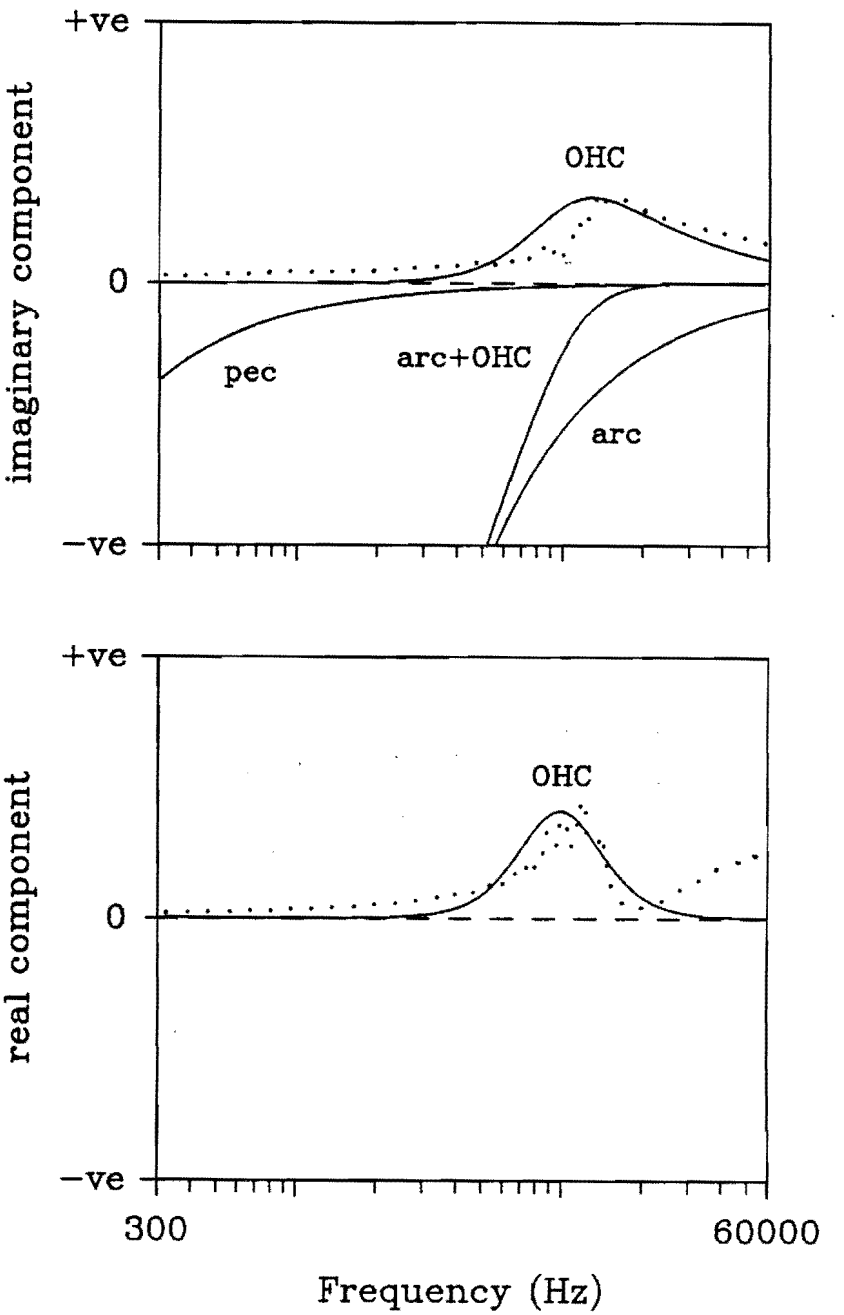

Figure 5.7: Impedances in the OHCAP model. The solid lines indicate the real and imaginary components of the FOHCAP model impedances, for the response shown in Fig. 5.6. The corresponding impedances of the DOHCAP are similar; the dotted lines indicate the impedance of the DOHC model, for the response shown in Fig. 5.13 (the frequency scale is as for the response figure).

are labelled as follows: "pec" indicates the pectinate impedance; "arc" indicates the BM arcuate impedance without the OHCs; "OHC" indicates the OHC impedance; and "arc+OHC" indicates the net arcuate impedance for the complete model (equalling "arc" plus "OHC"). For frequencies slightly less than the CF, the motile force generation by the OHCs effectively adds mass to the arcuate zone, cancelling the stiffness and so reducing the net reactance component of the impedance. This results in a rising arcuate zone response over this frequency range.

Also shown in Fig. 5.7 is the real component of the OHC impedance. For all stimulus frequencies this is positive (and largest at the CF), proving that the OHCAP model is passive. The presence of the resistor R_d in the DOHC model accounts for the non-zero value of DOHC resistance for low frequencies. The bumps in the DOHC model impedance (particularly near the CF) are a result of the relatively small number of sections used.

One of the most important features of the OHCAP model is the differing impedances of the arcuate and pectinate zones. As can be seen in Fig. 5.7, the arcuate and pectinate impedances are approximately the same at the CF, but for all lower stimulus frequencies the pectinate stiffness (being the lower of the two) governs the net stiffness for each section of the model. Therefore, the pectinate zone controls the propagation of the travelling wave, making the wave very similar (in terms of magnitude and phase) to that in a conventional second-order TL model. As shown in Fig. 5.6, the tuning in the pectinate zone is correspondingly broad whereas, owing to its greater impedance and the presence of the OHCs, the arcuate response is sharply tuned. Therefore, the OHCAP model contains a mechanical second filter, from the broad tuning in the pectinate zone to the sharp tuning in the arcuate zone - the arcuate zone "taps" off the energy flowing in the pectinate zone, in a manner that is frequency and place specific. Since the phase response (in both zones) is determined by the pectinate zone impedance, it can be altered relatively independently of the arcuate magnitude response. Because of this, the OHCAP model can simultaneously exhibit realistic selectivity and phase response, and realistic response changes resulting from trauma. This has not been achieved in any other type of passive cochlear model (with realistic parameters).

5.5.4 Comparisons with experimental data

In order to ascertain the accuracy of a cochlear model, its response must be compared to that measured experimentally. The OHCAP model parameters used for the comparisons with experimental data are given in Tables 5.1 and 5.2 (where "PSA" = Parameter Set A"; "DPSA" applies to the DOHCAP model; etc.). Note that the equations describing the OHC models are presented in electrical network form (Eqns. 5.1-5.4). However, in all tables in this thesis mechanical parameters (in cgs units) are listed - the mechanical and electrical parameters are related by the usual dynamic analogies (see Section 4.4.2).

The input to the OHCAP model is the stapes velocity. Therefore, for comparison with data measured relative to the sound pressure at the eardrum, a middle ear model must be added. The inclusion of a middle ear model does not significantly alter the response near

the peak, but it does determine the slope of the magnitude response for low frequencies. For all the comparisons (other than for the data of Sellick *et al.*, 1983a) the middle ear model had the following (stapes displacement vs eardrum pressure) transfer function: magnitude flat at $4.5 \cdot 10^{-7}$ $cm^3 \cdot dyn^{-1}$) up to 1.5 *kHz*, falling at 20 *dB/decade* above 1.5 *kHz*; phase equal to zero up to 0.5 *kHz*, falling at 0.5 *cycles/decade* above 0.5 *kHz*. This transfer function is similar to that described by Zwislocki (1962, 1963).

The data of Sellick *et al.* (1983b), showing BM displacement versus stapes displacement (corresponding to the isovelocity data of Sellick *et al.*, 1983a), exhibit a magnitude response which rises at > 10 *dB/decade* for low stimulus frequencies. This feature of their data does not conform with a BM whose impedance is dominated by stiffness for low frequencies. The low frequency response slope should be approximately 6 *dB/decade*, in conformity with the BM data of Wilson and Johnstone (1975), Rhode (1978); the isovelocity data of Sellick *et al.* (1982) and Robles *et al.* (1986); the isodisplacement data of Khanna and Leonard (1982, 1986); and analyses of cochlear models (e.g. de Boer, 1980). Therefore, the physical significance of the low frequency slope of the Sellick *et al.* (1983a,b) data is unclear. To achieve this slope in the OHCAP model, the middle ear model response magnitude rose at 20 *dB/decade* above 1.5 *kHz*. No attempt is made to justify this middle ear model on the basis of anatomy.

All the isomotion graphs shown on the following pages have the same format. The experimental data are in the form of eardrum sound pressure (relative to 0 *dB* SPL = $2 \cdot 10^{-4} dyn \cdot cm^{-2}$) required to obtain a certain BM isomotion (isodisplacement or isovelocity) level. The graphs show magnitude and/or phase of the arcuate and/or pectinate zone responses with and/or without trauma (the actual combination of these features depends upon the available experimental data). The OHCAP model response is shown using lines whilst the experimental data are shown using discrete points. For most of the experimental data, the radial position of measurement was not explicitly stated - it is assumed that the more sharply-tuned data were obtained in the arcuate zone (as is the case for the data of Sellick *et al.*, 1983a).

The sensitivity of the OHCAP model is less than that measured experimentally. Therefore, to enable comparisons of selectivity and response changes resulting from trauma, the magnitude response graphs have been normalized (except in the comparisons with the data of Sellick *et al.* (1983a), for which a phenomenological middle ear model was used). The amount of normalization applied to the OHCAP response in each graph is

Scalae parameters	
Scala length	3.5 cm
Effective scala height (h)	0.1 cm
Fluid density (ρ)	1.0 $g \cdot cm^{-3}$

Table 5.1: OHCAP model scalae parameters used in the comparisons with experimental data.

DOHCAP:	DPSA	DPSB	
m_a	$7.0 \cdot 10^{-2}\ g \cdot cm^{-2}$	$7.2 \cdot 10^{-2}$	
m_p	$1.8 \cdot 10^{-1}\ g \cdot cm^{-2}$	$7.2 \cdot 10^{-2}$	
c_a	$2.0 \cdot 10^{-11}\ \exp^{2.8x}\ cm^3 \cdot dyn^{-1}$	$6.0 \cdot 10^{-11}\ \exp^{2.8x}$	
c_p	$8.0 \cdot 10^{-11}\ \exp^{2.8x}\ cm^3 \cdot dyn^{-1}$	$2.0 \cdot 10^{-9}\ \exp^{2.8x}$	
r_a	$1.0 \cdot 10^{3}\ dyn \cdot s \cdot cm^{-3}$	$1.0 \cdot 10^{2}$	
r_p	$5.0 \cdot 10^{2}\ dyn \cdot s \cdot cm^{-3}$	$2.0 \cdot 10^{2}$	
m_z	$7.0 \cdot 10^{-4}\ g \cdot cm^{-2}$	$1.4 \cdot 10^{-3}$	
r_d	$5.0 \cdot 10^{2}\ dyn \cdot s \cdot cm^{-3}$	$2.0 \cdot 10^{1}$	
r_z	$1.0 \cdot 10^{2}\ dyn \cdot s \cdot cm^{-3}$	$1.0 \cdot 10^{2}$	
k_z	$8.8 \cdot 10^{-3}\ cm^3\ dyn^{-1}\ \cdot s^{-1}$	$9.2 \cdot 10^{-3}$	
k_d	$3.0 \cdot 10^{4}\ dyn \cdot s \cdot cm^{-1}$	$5.0 \cdot 10^{5}$	
FOHCAP:	**PSA**	**PSB**	**PSC**
m_a	$4.0 \cdot 10^{-3}\ g \cdot cm^{-2}$	$5.0 \cdot 10^{-3}$	$4.0 \cdot 10^{-3}$
m_p	$4.0 \cdot 10^{-3}\ g \cdot cm^{-2}$	$1.2 \cdot 10^{-2}$	$4.0 \cdot 10^{-3}$
c_a	$1.0 \cdot 10^{-11} \exp^{3.7x}\ cm^3 \cdot dyn^{-1}$	$1.1 \cdot 10^{-10} \exp^{3.7x}$	$3.3 \cdot 10^{-11} \exp^{3.7x}$
c_x	$1.0 \cdot 10^{-9} \exp^{3.7x}\ cm^3 \cdot dyn^{-1}$	$1.1 \cdot 10^{-9} \exp^{3.7x}$	$3.3 \cdot 10^{-9} \exp^{3.7x}$
$c_{p,y}$	$1.7 \cdot 10^{-9} \exp^{3.7x}\ cm^3 \cdot dyn^{-1}$	$1.1 \cdot 10^{-9} \exp^{3.7x}$	$3.3 \cdot 10^{-9} \exp^{3.7x}$
r_a	$1.0 \cdot 10^{3}\ dyn \cdot s \cdot cm^{-3}$	$3.0 \cdot 10^{2}$	$3.0 \cdot 10^{1}$
r_p	$1.5 \cdot 10^{2}\ dyn \cdot s \cdot cm^{-3}$	$3.0 \cdot 10^{1}$	$2.0 \cdot 10^{1}$
m_b	$1.0 \cdot 10^{-4}\ g \cdot cm^{-2}$	$1.0 \cdot 10^{-4}$	$1.0 \cdot 10^{-4}$
m_y	$8.0 \cdot 10^{-3}\ g \cdot cm^{-2}$	$1.3 \cdot 10^{-2}$	$4.0 \cdot 10^{-3}$
r_y	$1.0 \cdot 10^{5}\ dyn \cdot s \cdot cm^{-3}$	$4.0 \cdot 10^{5}$	$9.0 \cdot 10^{4}$
k_x	$1.0 \cdot 10^{2}\ dyn \cdot s^{-2} \cdot cm^{-3}$	$1.0 \cdot 10^{1}$	$1.0 \cdot 10^{2}$
k_y	$8.0 \cdot 10^{4}\ cm^2 \cdot g^{-1}$	$9.0 \cdot 10^{4}$	$5.0 \cdot 10^{5}$
FOHCAP:	**PSD**	**PSE**	**PSF**
m_a	$5.0 \cdot 10^{-3}$	$4.0 \cdot 10^{-2}$	$2.0 \cdot 10^{-2}$
m_p	$5.0 \cdot 10^{-3}$	$4.0 \cdot 10^{-2}$	$2.0 \cdot 10^{-2}$
c_a	$3.3 \cdot 10^{-12} \exp^{3.7x}$	$3.3 \cdot 10^{-11} \exp^{3.7x}$	$3.3 \cdot 10^{-12} \exp^{3.7x}$
c_x	$3.3 \cdot 10^{-9} \exp^{3.7x}$	$3.3 \cdot 10^{-10} \exp^{3.7x}$	$3.3 \cdot 10^{-9} \exp^{3.7x}$
$c_{p,y}$	$3.3 \cdot 10^{-9} \exp^{3.7x}$	$3.3 \cdot 10^{-10} \exp^{3.7x}$	$3.3 \cdot 10^{-9} \exp^{3.7x}$
r_a	$3.0 \cdot 10^{1}$	$2.0 \cdot 10^{2}$	$1.0 \cdot 10^{2}$
r_p	$2.0 \cdot 10^{1}$	$3.0 \cdot 10^{2}$	$1.0 \cdot 10^{2}$
m_b	$1.0 \cdot 10^{-4}$	$1.0 \cdot 10^{-4}$	$1.0 \cdot 10^{-4}$
m_y	$5.0 \cdot 10^{-3}$	$3.0 \cdot 10^{-2}$	$2.0 \cdot 10^{-2}$
r_y	$9.0 \cdot 10^{4}$	$9.0 \cdot 10^{4}$	$9.0 \cdot 10^{4}$
k_x	$1.0 \cdot 10^{3}$	$1.0 \cdot 10^{1}$	$1.0 \cdot 10^{3}$
k_y	$5.0 \cdot 10^{6}$	$2.0 \cdot 10^{4}$	$7.0 \cdot 10^{7}$

Table 5.2: OHCAP model CP parameters used in the comparisons with experimental data (x = distance from stapes).

quoted. Except where otherwise noted, the phase data show BM motion into the scala tympani relative to stapes rarefaction.

Figures 5.8 and 5.9 show that the FOHCAP model simulates well the data of Khanna and Leonard (1982, 1986). Both sets of data have a pronounced dip at 3-3$\frac{1}{2}$ *kHz* which is not simulated by the model - the dip is assumed to be an artifact of the experimental procedure. For the data of Khanna and Leonard (1986), it is assumed that the more broadly tuned responses were measured in the pectinate zone, and that the sharply tuned response originated from the arcuate zone. The FOHCAP model response in both zones matches this data very well (including the sensitivity - the normalization factor is only 6 *dB*). The measured responses exhibit a pronounced plateau just above CF; this is only evident in the pectinate zone response of the FOHCAP model.

The two sets of data from Sellick *et al.* (1982), shown in Figs. 5.10 and 5.11, are matched quite well by the FOHCAP model. The traumatized FOHCAP model response shown in the former figure deviates from the data for frequencies above CF. However, the model exhibits a realistic sensitivity change with trauma. The normal and traumatized model responses shown in the latter figure are more realistic, although the response below CF in this figure is not very good.

The only available data for which the radial position of measurement was recorded are those of Sellick *et al.* (1983a). Both the FOHCAP and DOHCAP model (Figs. 5.12 and 5.13, respectively) match this data well, particularly with respect to the response magnitude in the two zones. The bumps in the DOHCAP model response are a result of the relatively small number of sections used in the simulations.

The work of Robles *et al.* (1986) provides data for the magnitude response in normal and traumatized cochleae, and the phase response in normal cochleae. Both the FOHCAP and DOHCAP models (Figs. 5.14 and 5.15, respectively) match this data reasonably well, although the selectivity of the DOHCAP model traumatized response is rather poor. The unusual phase jump of π radians in the phase response data is not simulated by the OHCAP model. The physical significance of this feature of the data is not known. In order to simulate trauma, the change required in FOHC force generator gain parameters of the FOHCAP model is considerably less than that required in the DOHCAP model. This implies that the latter model is less sensitive to parameter variations; an interesting result, since the filtering action of the DOHC model relies on the structural integrity of the organ of Corti.

As seen in Figs. 5.8 through 5.15, the OHCAP model is able to match a wide (and varied) range of experimental data (on the basis of response selectivity, response phase and changes in response as a result of trauma) using realistic parameter sets. It would be informative to know if other cochlear models could match such a wide range of experimental data with a similar degree of correlation.

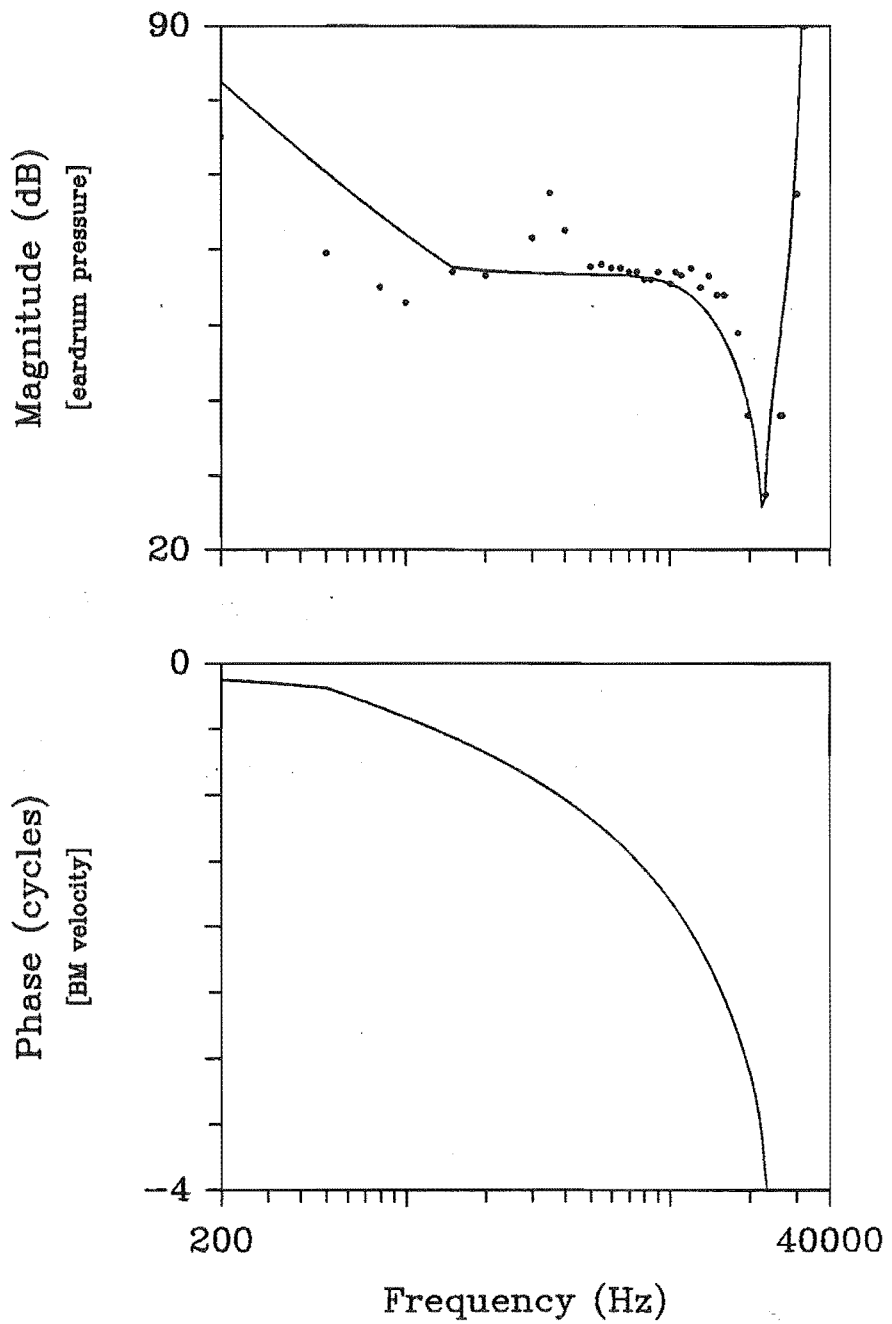

Figure 5.8: Comparison of FOHCAP model arcuate zone response (using PSA, 3.5 *mm* from the stapes) with the experimental data of Khanna and Leonard (1982 - animal 3/26/81). Isodisplacement level: 1 Å. Normalization used for FOHCAP response: 40 *dB*.

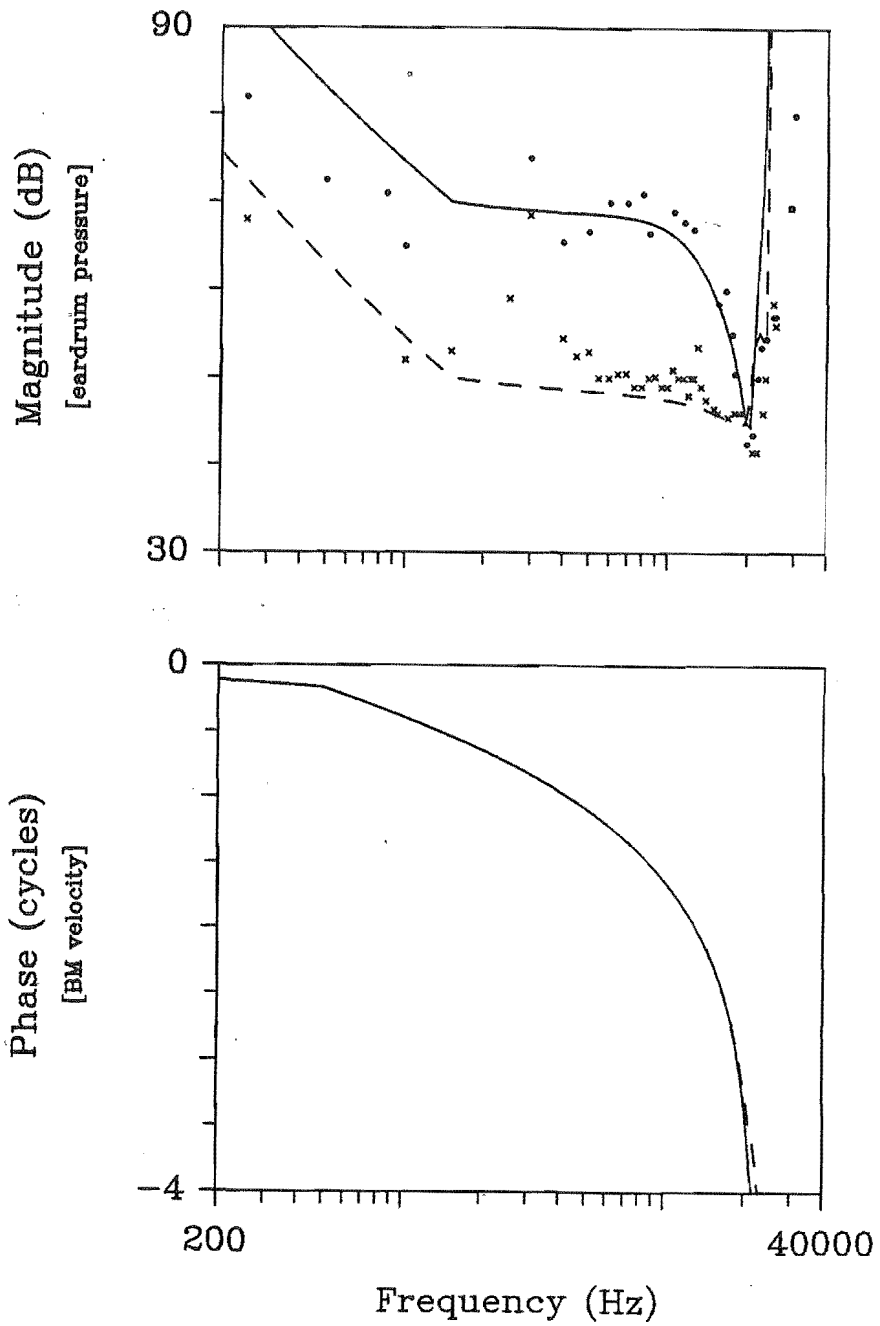

Figure 5.9: Comparison of FOHCAP model response (using PSB, 3.5 *mm* from the stapes) with the experimental data of Khanna and Leonard (1986). Isodisplacement level: 1 Å. Normalization used for FOHCAP response: 6 *dB*. The arcuate response is indicated by dots (animal 8/28/80) and the pectinate response is indicated by crosses (animal 4/2/81).

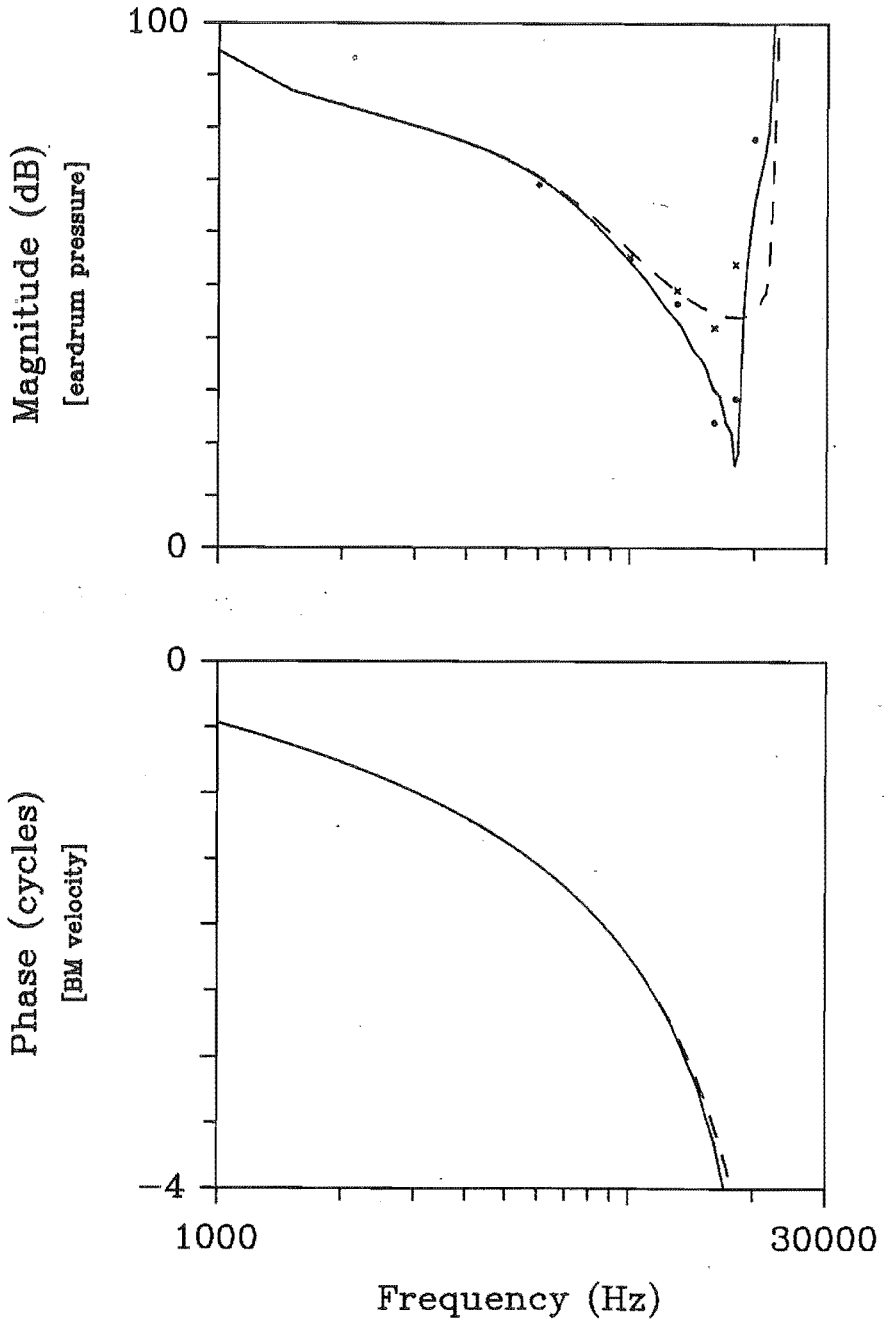

Figure 5.10: Comparison of FOHCAP model arcuate response (using PSC, 3.5 *mm* from the stapes) with the experimental data of Sellick *et al.* (1982 - animal 29). Isovelocity level: 0.04 $mm \cdot s^{-1}$. Normalization used for FOHCAP response: 35 *dB*. The response in the viable cochlea is indicated by dots; the traumatized response (action-potential threshold down 20 *dB*) by crosses. The trauma was simulated in the FOHCAP model by reducing the force generator gain parameters by 5%.

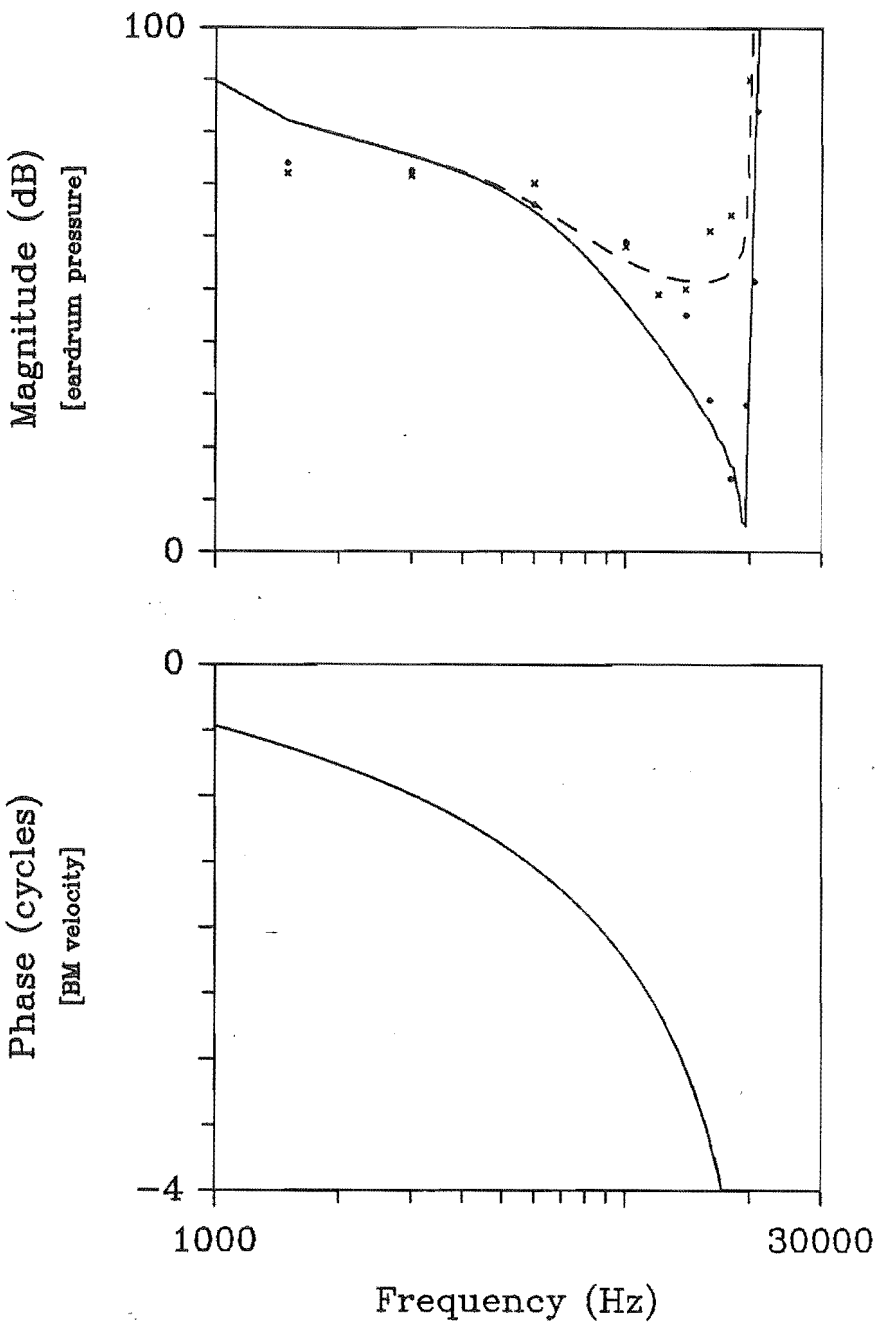

Figure 5.11: Comparison of FOHCAP model arcuate response (using PSD, 3.5 *mm* from the stapes) with the experimental data of Sellick *et al.* (1982 - animal 35). Isovelocity level: 0.04 $mm \cdot s^{-1}$. Normalization used for FOHCAP response: 60 *dB*. The response in the viable cochlea is indicated by dots; the traumatized response (action-potential threshold down 45 *dB*) by crosses. The trauma was simulated in the FOHCAP model by reducing the force generator gain parameters by 20%.

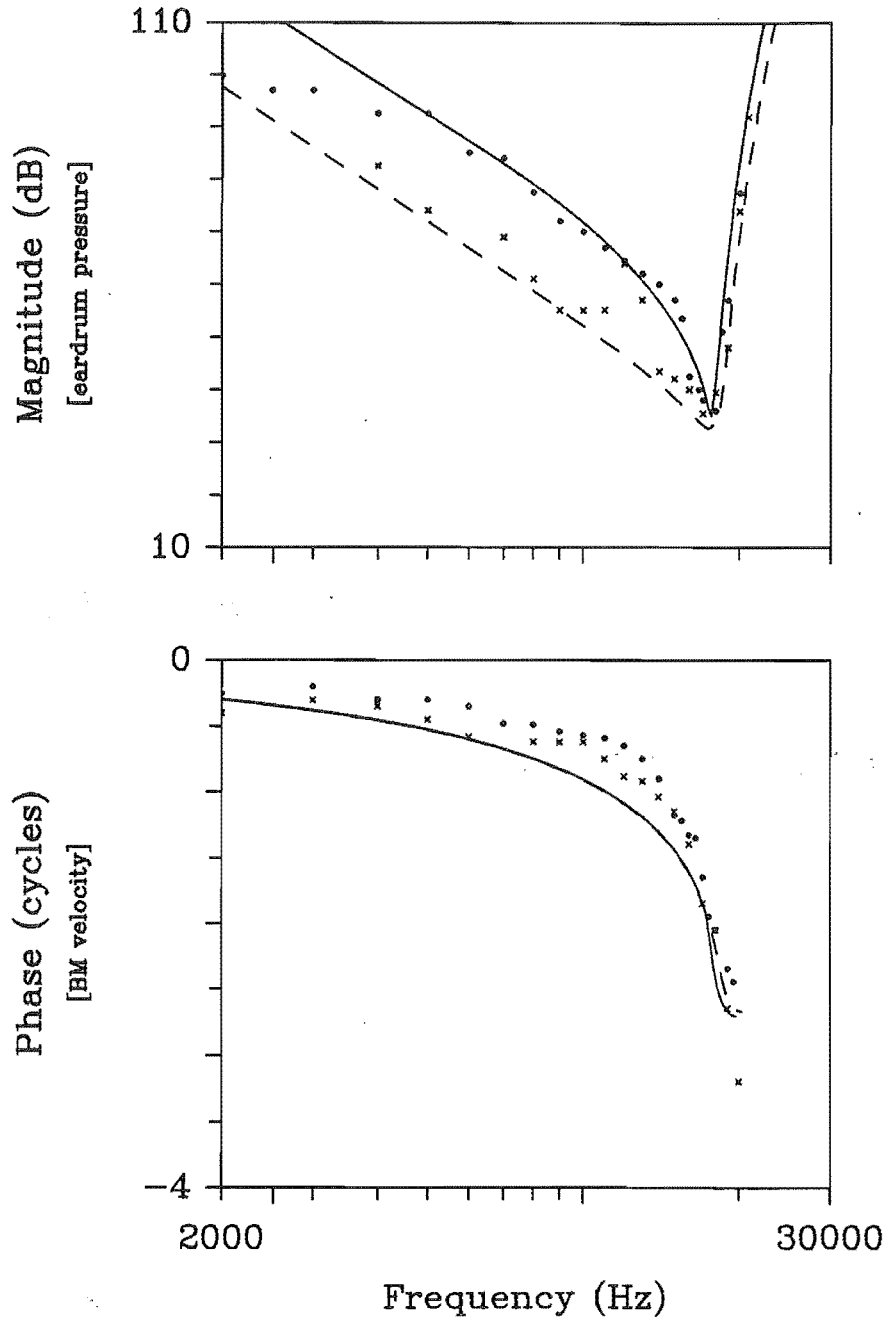

Figure 5.12: Comparison of FOHCAP model response (using PSE, 4.6 mm from the stapes) with the experimental data of Sellick *et al.* (1983a). Isovelocity level: 0.04 $mm \cdot s^{-1}$. The arcuate response is indicated by the dots (animal 116) and the pectinate response is indicated by the crosses (animal 90).

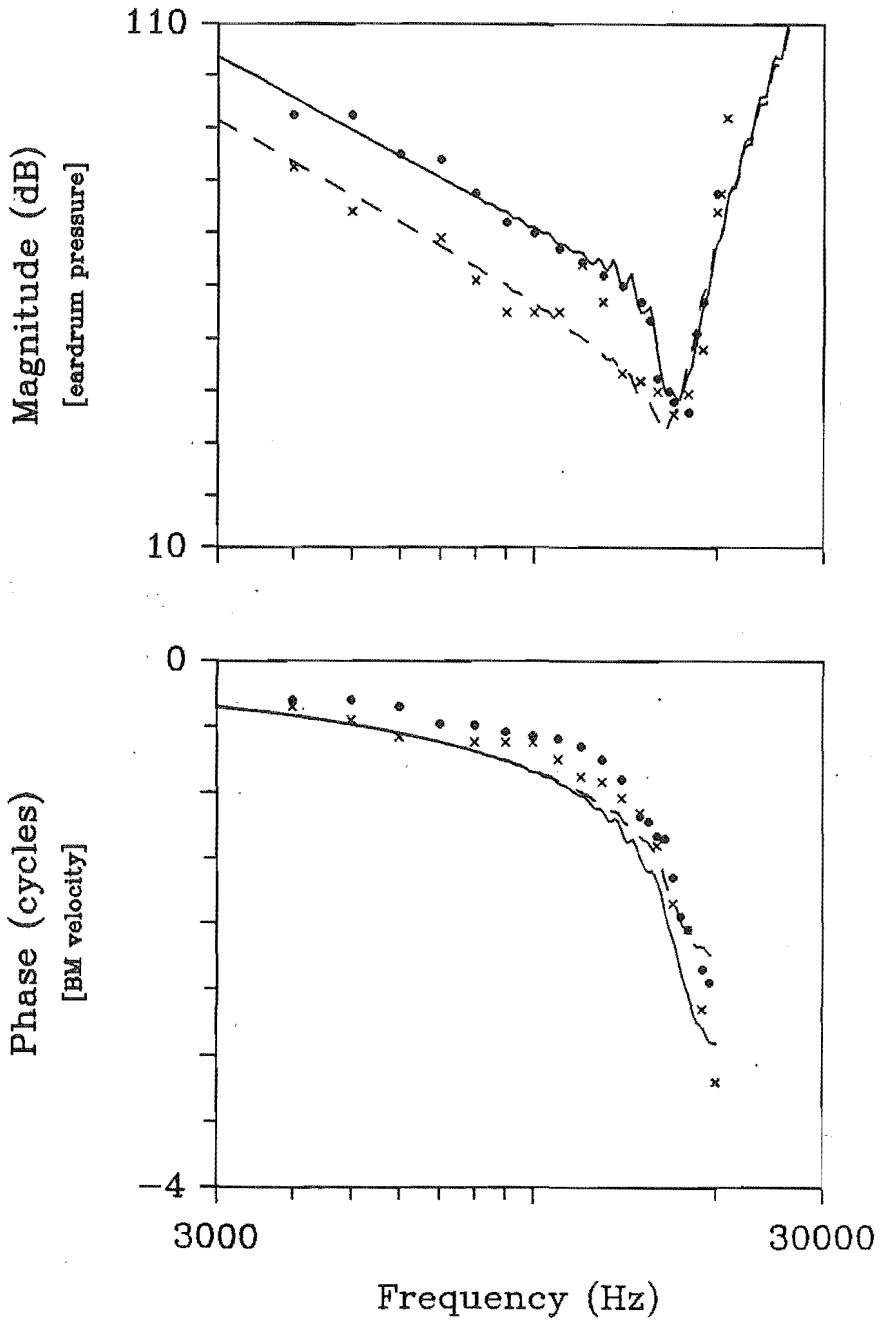

Figure 5.13: Comparison of DOHCAP model response (using DPSA, 6.6 *mm* from the stapes) with the experimental data of Sellick *et al.* (1983a). Isovelocity level: 0.04 $mm \cdot s^{-1}$. The arcuate response is indicated by the dots (animal 116) and the pectinate response is indicated by the crosses (animal 90).

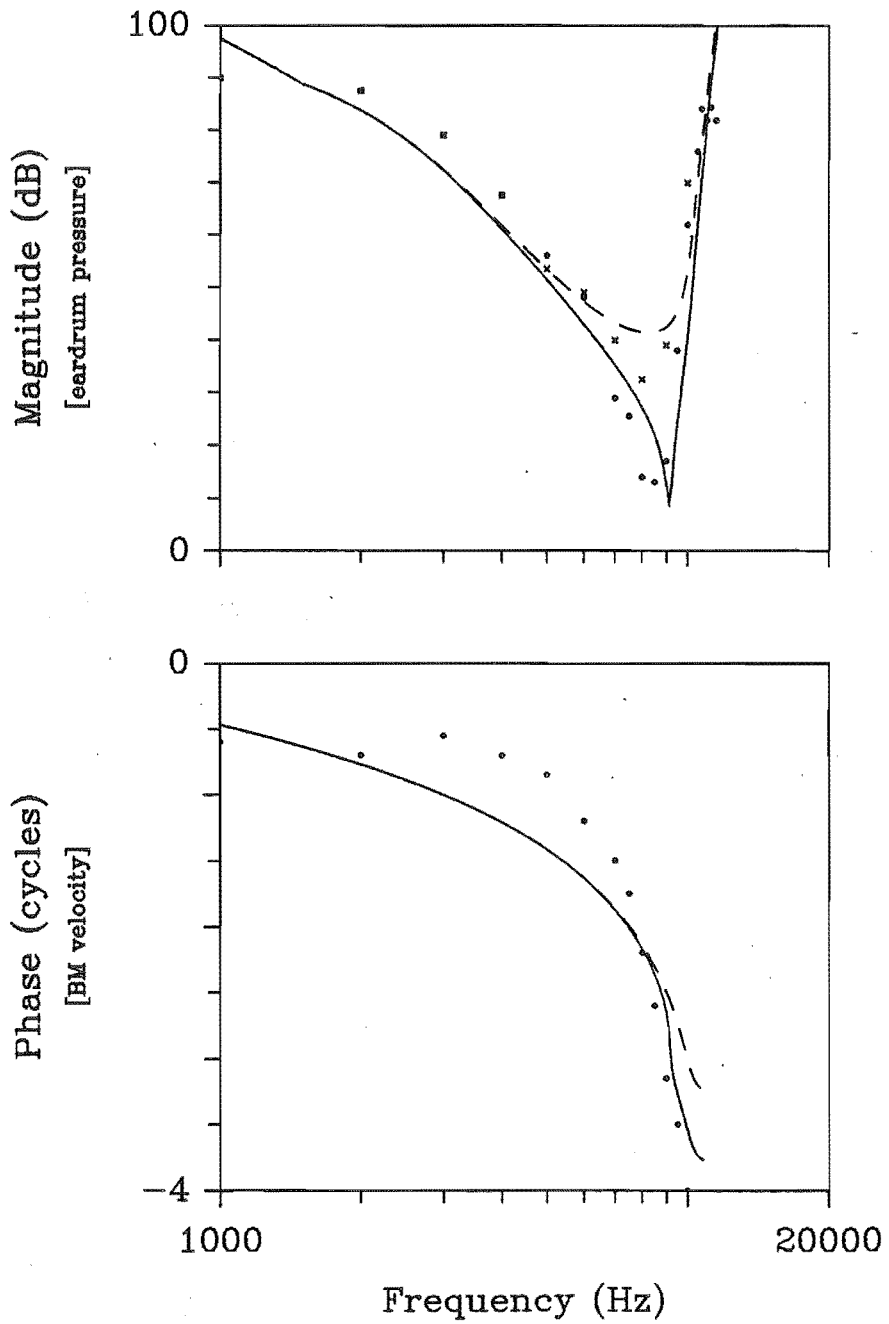

Figure 5.14: Comparison of FOHCAP model arcuate response (using PSF, 3.5 *mm* from the stapes) with the experimental data of Robles *et al.* (1986 - animal 44). Isovelocity level: 0.1 $mm \cdot s^{-1}$. Normalization used: 60 *dB*. The response in the viable cochlea is indicated by dots; the traumatized response (obtained 8 hours after the start of the experiment) by crosses. The trauma was simulated in the FOHCAP model by reducing the force generator gain parameters by 1%.

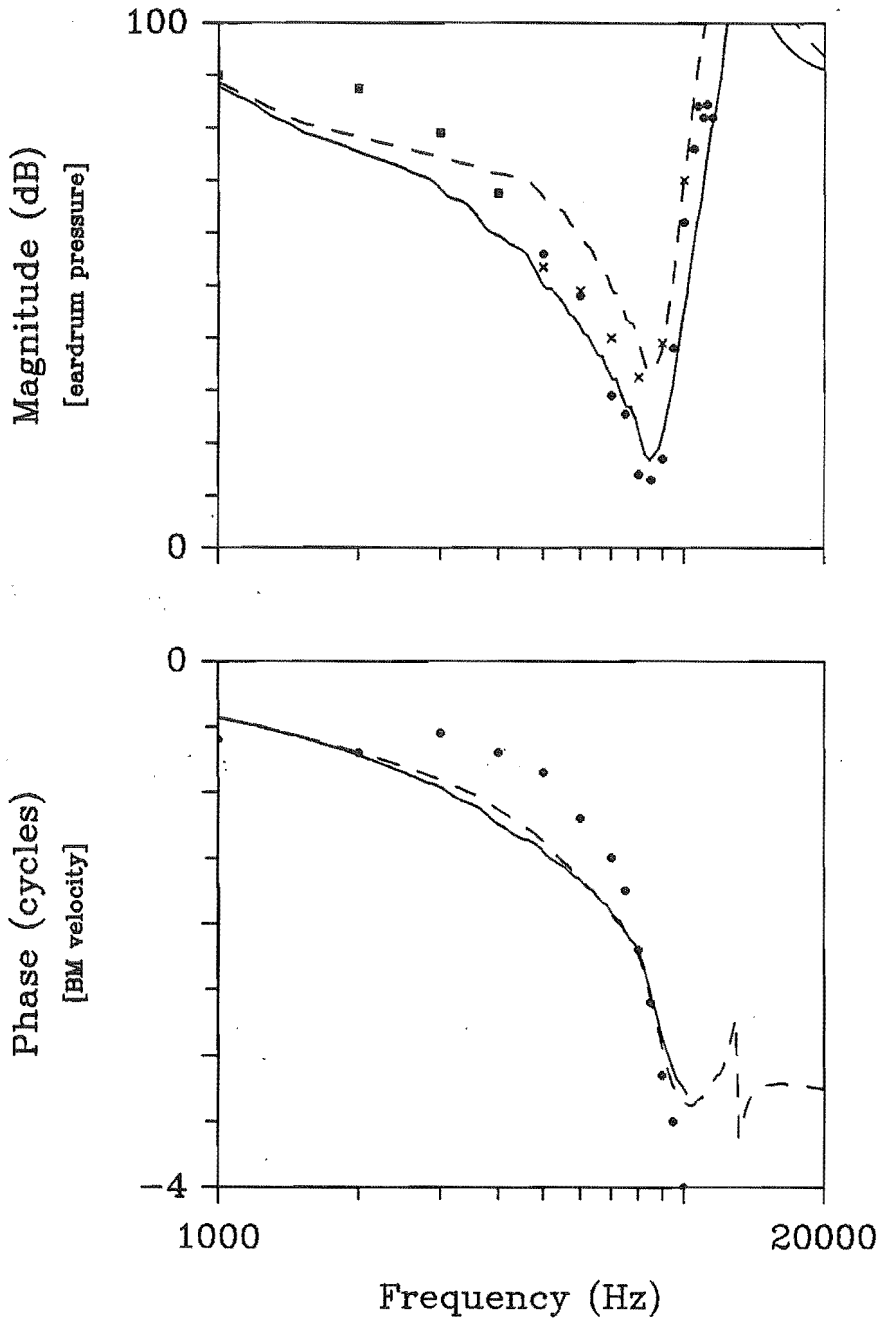

Figure 5.15: Comparison of DOHCAP model arcuate response (using DPSB, 3.2 *mm* from the stapes) with the experimental data of Robles *et al.* (1986 - animal 44). Isovelocity level: 0.1 $mm \cdot s^{-1}$. Normalization used: 65 *dB* The response in the viable cochlea is indicated by dots; the traumatized response (obtained 8 hours after the start of the experiment) by crosses. The trauma was simulated in the DOHCAP model by reducing the force generator gain parameter K_d by 80%.

Chapter 6

Extensions to ETL Cochlear Models

Electrical Transmission Line cochlear models, when realized as physical circuits, have important advantages over computer modelling techniques. The physical ETL model can simulate the functional behaviour of the cochlea in real time to real stimuli, such as speech or music. This enables direct observations of its operation and response, and rapid testing of the effects that different components have on its behaviour. A real circuit more accurately reproduces natural variations in parameter values, and it comes complete with the ubiquitous thermal noise.

Compared to physical hydrodynamic models, the physical ETL model has the advantage that observation of its behaviour is very straightforward, without requiring the use of specialized transducers. One shortcoming of using the mechanical-to-electrical analogy, as is required in the formulation of an ETL, is that limitations in the allowable topological structure of an electrical circuit can prevent the inclusion of important features of cochlear anatomy.

This chapter describes two new modelling techniques that can be used to improve the realism of ETL cochlear models. Using these techniques, mechanical coupling in the CP and multi-dimensional fluid motion can be incorporated in an ETL model. To illustrate the use of the modelling techniques, mechanical coupling (between the arcuate and pectinate zones of the BM) and 2-D fluid are added to the FOHCAP model, and the fluid motion in a 2-D second-order ETL model is investigated. It is shown that adding mechanical coupling and 2-D fluid to the (F)OHCAP model has a predictable effect on its response.

Note that the Appendix of this thesis describes a technique for modelling stick-slip friction in an electrical circuit. It is possible that such friction could affect cochlear fluid micromechanics, and so this technique could be used to incorporate such friction in an ETL cochlear model. This, however, has not been attempted; instead, in the Appendix two test examples are used to illustrate the validity of the technique.

6.1 Mechanical Coupling

It can be deduced from anatomical considerations and experimental observations that the amount of longitudinal coupling in the CP is different in its arcuate and pectinate zones (see Chapter 2). This coupling results in an effective increase in the arcuate impedance, making the impedance significantly larger than that in the pectinate zone (as is assumed in the parameters used for the OHCAP model in Chapter 5). Any cochlear model that allows for different motion in the two CP zones (such as the OHCAP model) should also include mechanical coupling in a radial direction since the BM fibres span the full CP width. This was not done for the OHCAP model responses shown in Chapter 5.

This section describes a technique for including both types of mechanical coupling in a ETL cochlear model. The example of longitudinal coupling in a simple (E)TL is used in the formulation of equations. With slight modifications, these equations also apply to radial coupling. The effects of adding radial coupling to the FOHCAP model are shown.

6.1.1 Description

Two sections of a second-order TL model with longitudinal mechanical coupling are shown in Fig. 6.1, The components m_{p_i}, c_{p_i} and r_{p_i} represent, respectively, the mass, compliance and resistance of the ith section of the BM (the other components of the CP are ignored). The components c_c and r_c represent, respectively, the compliance and resistance parameters for the coupling. The equation of motion for the BM, without coupling, is (from Eqn. 4.2)

$$P_{f_i} = v_{p_i} \cdot (\jmath\omega m_{p_i} + \frac{1}{\jmath\omega c_{p_i}} + r_{p_i}) \tag{6.1}$$

where P_{f_i} is the differential fluid pressure and v_{p_i} is the BM velocity. With no mechanical coupling the motion of the BM is solely determined by its local impedance (i.e. the impedance at a certain point). However, when mechanical coupling is included the local impedance is influenced by the impedance of all the other sections of the BM. This can be incorporated by making adding a force to each section which is controlled by the relative motion between adjacent sections. The inclusion of such a force means that the local impedance is now increased. If the coupling force is to represent compliance and resistance coupling, Eqn. 6.1 becomes

$$P_{f_i} = v_{p_i} \cdot (\jmath\omega m_{p_i} + \frac{1}{\jmath\omega c_{p_i}} + r_{p_i}) + (v_{p_{i+1}} - v_{p_i}) \cdot \left[r_{c_{i+1}} + \frac{1}{\jmath\omega c_{c_{i+1}}} \right] + (v_{p_i} - v_{p_{i-1}}) \cdot \left[r_{c_i} + \frac{1}{\jmath\omega c_{c_i}} \right] \tag{6.2}$$

The inclusion of longitudinal mechanical coupling means that the BM elements are now coupled in two ways: through the structural BM coupling and through the horizontal motion of the fluid mass element Z_{f_i}. To allow for this coupling (which is in orthogonal

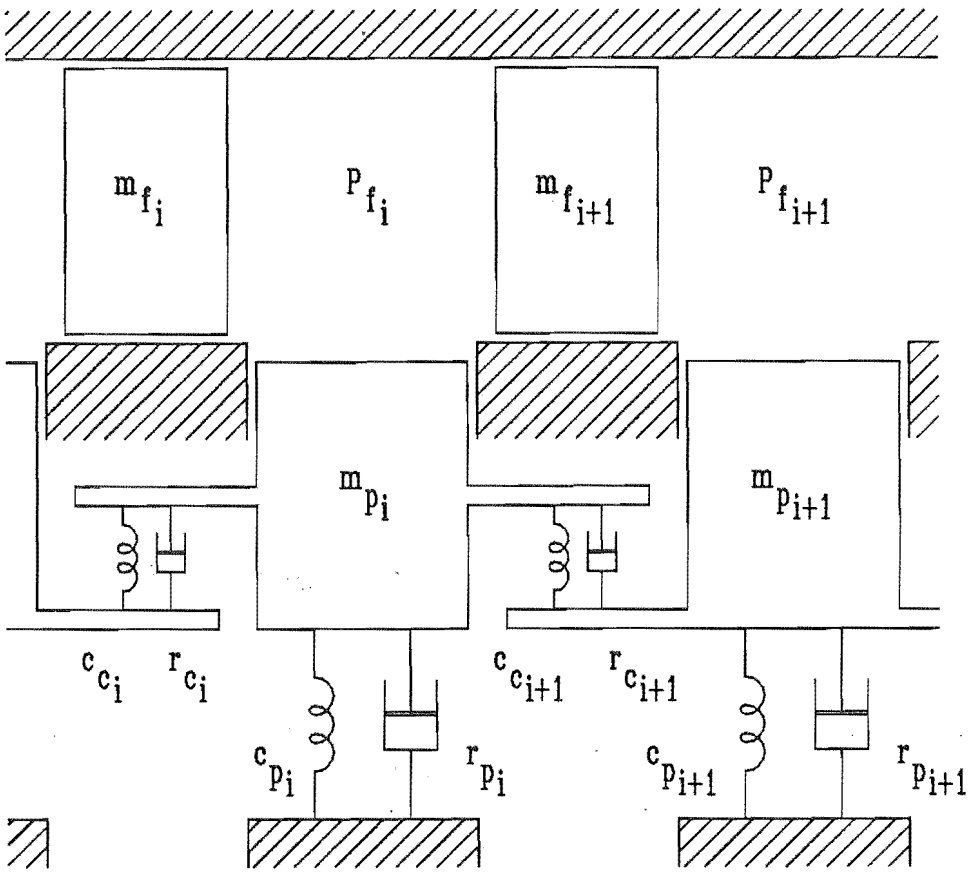

Figure 6.1: Transmission line model with longitudinal mechanical coupling. The elements with subscript p_k represent the local BM impedance at the $_{k-th}$ section and the elements with subscript c_k represent coupling between adjacent sections.

directions) in the ETL model, it is necessary to have a model for a "floating" spring and dashpot. By applying the usual dynamical analogies, the electrical circuit equivalent to Eqn. 6.2 is obtained as

$$V_{f_i} = i_{p_i} \cdot (j\omega m_{p_i} + \frac{1}{j\omega C_{c_i}} + r_{p_i}) + (i_{p_{i+1}} - i_{p_i}) \cdot \left[r_{c_{i+1}} + \frac{1}{j\omega C_{c_{i+1}}} \right] + (i_{p_i} - i_{p_{i-1}}) \cdot \left[r_{c_i} + \frac{1}{j\omega C_{c_i}} \right] \tag{6.3}$$

It was found that implementation of the latter two terms in Eqn. 6.3 requires the use of two ideal transformers in each section to isolate the coupling elements from the BM

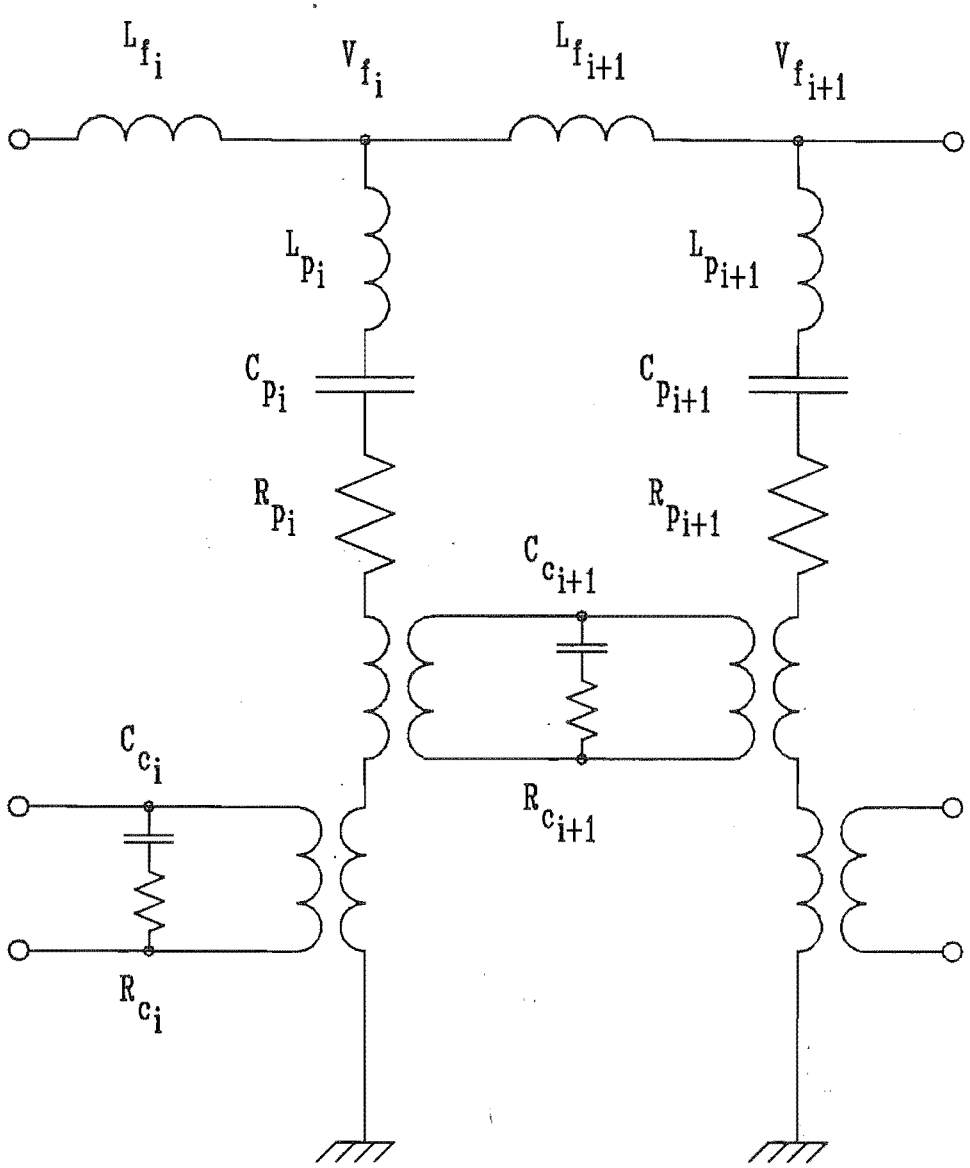

Figure 6.2: ETL model with longitudinal mechanical coupling. The BM sections are interconnected in two ways: via the longitudinal motion of the fluid, and via the structural CP coupling. This interconnection in two dimensions means that transformers are necessary to isolate the coupling capacitor and resistor from the rest of the circuit.

elements. The resulting circuit, equivalent to the mechanical TL in Fig. 6.1, is shown in Fig. 6.2.

The effect of including the transformers (in Fig. 6.2) can be understood by considering the response for different values of coupling impedance. If the coupling impedance is large very little current can flow in the centre branch. Therefore, the same current will flow in adjacent shunt branches of the model, which is equivalent to adjacent sections of the BM having the same velocity. Conversely, if the coupling impedance is small any difference in adjacent shunt branch currents will effectively be dissipated by the centre branch. In this case the transformers are essentially uncoupled, enabling adjacent sections of the BM to act independently of each other.

6.1.2 Effect of radial coupling on OHCAP model response

Radial coupling is simulated in the OHCAP model by adding a transformer/capacitor/resistor network between each of the arcuate and pectinate branches in the ETL model. The coupling is a result of the BM fibres spanning the full CP width. Therefore, it seems reasonable to make the radial coupling impedance equal to the local pectinate impedance. Figure 6.3 shows the effect of adding this amount of radial coupling to the FOHCAP model, using the parameters given in Table 6.1. The response 3.5 *mm* from the stapes is

Scalae parameters	
Scala length	3.5 cm
Scala height (h)	0.1 cm
Fluid density (ρ)	1.0 $g \cdot cm^{-3}$
Partition parameters	
m_a	$2.0 \cdot 10^{-2}$ $g \cdot cm^{-2}$
m_p	$2.0 \cdot 10^{-2}$ $g \cdot cm^{-2}$
c_a	$2.0 \cdot 10^{-12} \exp^{2.8x}$ $cm^3 \cdot dyn^{-1}$
c_x	$2.0 \cdot 10^{-9} \exp^{2.8x}$ $cm^3 \cdot dyn^{-1}$
$c_{p,y}$	$2.0 \cdot 10^{-9} \exp^{2.8x}$ $cm^3 \cdot dyn^{-1}$
r_a	$1.0 \cdot 10^{2}$ $dyn \cdot s \cdot cm^{-3}$
r_p	$3.0 \cdot 10^{2}$ $dyn \cdot s \cdot cm^{-3}$
m_b	$1.0 \cdot 10^{-4}$ $g \cdot cm^{-2}$
m_y	$3.0 \cdot 10^{-2}$ $g \cdot cm^{-2}$
r_y	$9.0 \cdot 10^{3}$ $dyn \cdot s \cdot cm^{-3}$
k_x	$1.0 \cdot 10^{3}$ $dyn \cdot s^{-2} \cdot cm^{-3}$
k_y	$5.0 \cdot 10^{7}$ $cm^2 \cdot g^{-1}$

Table 6.1: FOHCAP model parameters (cgs units) used for showing the effect of adding radial coupling.

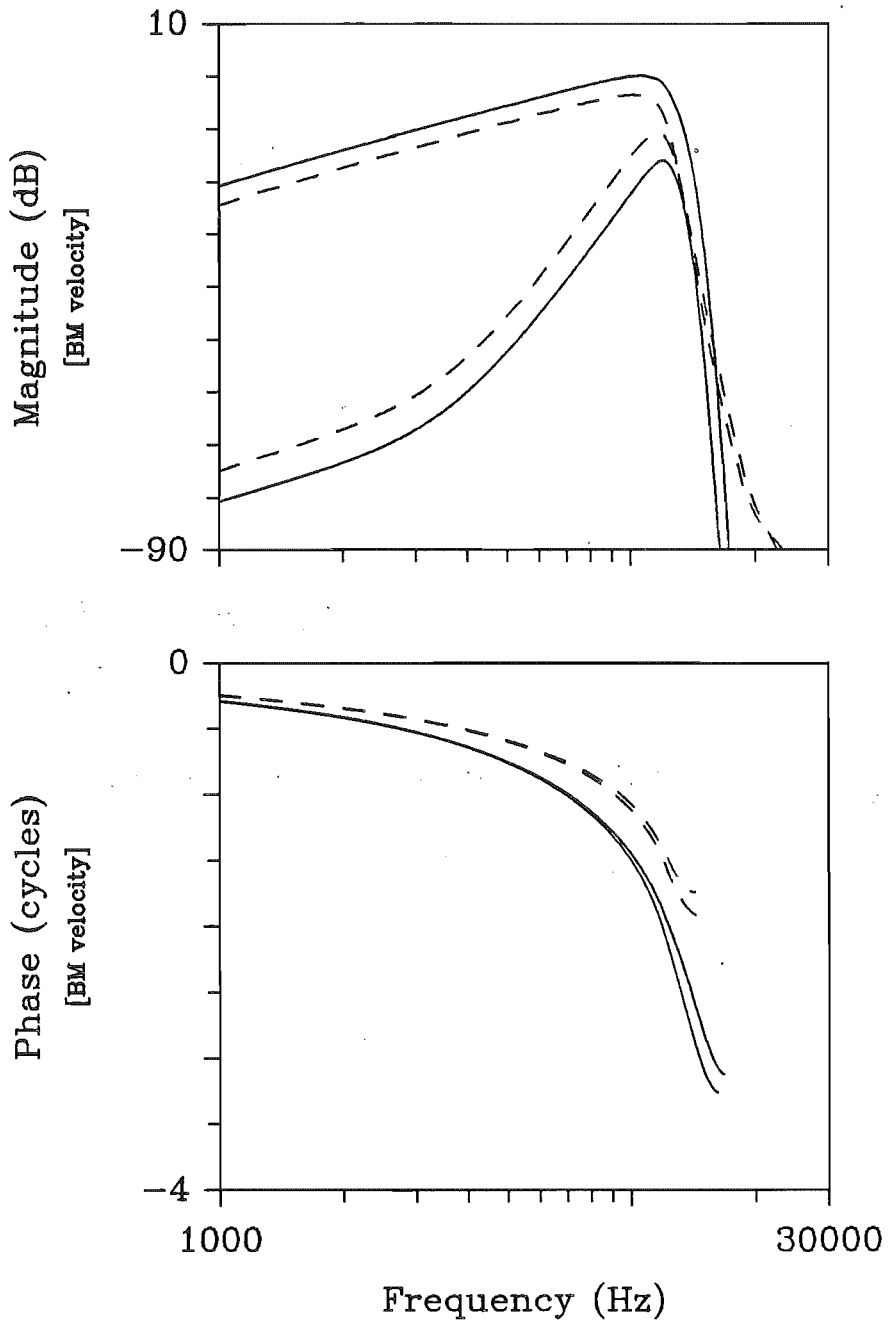

Figure 6.3: Effect of adding radial mechanical coupling to the FOHCAP model. The response of the uncoupled response is indicated by the solid lines, and that of the coupled model is indicated by the dashed lines. The coupling impedance was equal to the local impedance of the pectinate zone. The main effect of adding the coupling is that the arcuate motion increases and the pectinate motion decreases.

shown. The main effects of adding radial coupling are an increase in arcuate motion and a decrease in pectinate motion. This is as expected since the pectinate motion is greater than the arcuate motion, and so coupling between the two zones brings the motion of both zones closer to the average motion. The selectivity of the arcuate and pectinate responses is unchanged.

6.2 Multi-dimensional Fluid Modelling

The one-dimensional fluid approximation inherent in the formulation of (E)TL cochlear models means that the variation of fluid motion above the BM is not allowed for. The incorporation of a 2-D (or even 3-D) fluid representation would be particularly advantageous in the physical ETL model, because then the (macromechanical and/or micromechanical) fluid flow would be observable in real time (as is the case in physical hydrodynamic cochlear models).

6.2.1 Description

In a (E)TL cochlear model the cochlea is divided up into discrete sections. A discrete model gives very similar results to those obtained with the CP treated as a continuum, if the change in parameters (and hence motion) is small between adjacent sections. This approximation can also be applied when modelling the fluid.

Consider a Lagrangian representation of an inviscid fluid, in which it is considered to be made up of a number of particles whose only property is that of inertia (i.e. mass). If gravity forces are ignored, the equation of motion for a fluid particle in the direction of a streamline (which indicates the mean direction of a number of particles at the same instant of time), is (from Fig. 6.4)

$$P\,dA - (P + \frac{\partial P}{\partial s}ds)dA = \rho\,dA\,ds \cdot \alpha \tag{6.4}$$

where P is the pressure in the fluid, dA is the fluid element cross-sectional area, ds is the length of the fluid element, ρ is the fluid density, and α is the acceleration of the fluid element. Eqn. 6.4 is easily simplified to obtain Euler's equation for an inviscid fluid without gravity forces:

$$\frac{1}{\rho} \cdot \frac{\partial P}{\partial s} + \alpha = 0 \tag{6.5}$$

The acceleration of the fluid element is $\alpha = dv/dt$. In general the velocity is a function of position and time, so the acceleration is

$$\alpha = \frac{\partial v}{\partial s} \cdot \frac{ds}{dt} + \frac{\partial v}{\partial t} \tag{6.6}$$

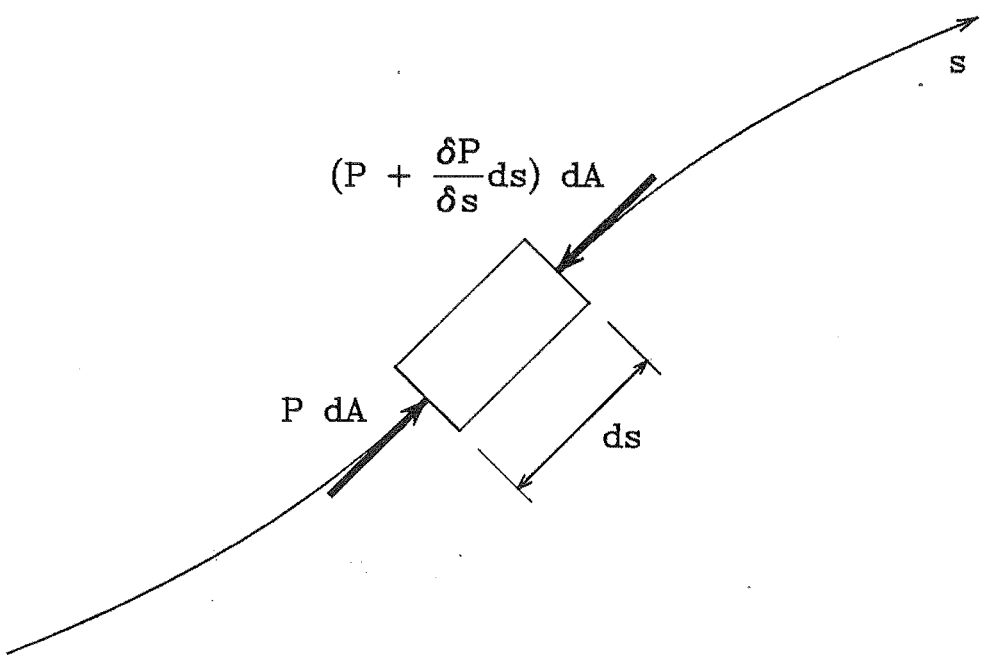

Figure 6.4: Particle motion on a streamline (ignoring gravity forces) in an inviscid fluid.

If the fluid motion is sufficiently non-steady, the acceleration's time dependence is much greater than its position dependence. This is true for sound stimuli to the cochlea (Viergever, 1978b; 1980). Eqn. 6.6 therefore simplifies to $\alpha = \partial v/\partial t$ which, upon substitution into Eqn. 6.5, yields

$$\frac{\partial P}{\partial s} + \rho \frac{\partial v}{\partial t} = 0 \tag{6.7}$$

Eqn. 6.7 applies to a streamline pointing in an arbitrary direction. However, such a streamline can be resolved into orthogonal components so that, as shown in Fig. 6.5, the fluid region can be modelled by a network of fluid elements, each constrained to move in only one dimension. In Fig. 6.5 the area bounded by each of the four masses and the solid walls is assumed to be filled with an incompressible, massless fluid. Since each fluid element acts like a pure mass, in an electrical circuit the fluid can be represented by a grid of inductors.

The above analysis assumes a streamline in 2-D only. Three-dimensional fluid motion could also be modelled, by using a 3-D inductor network; but this has not been attempted.

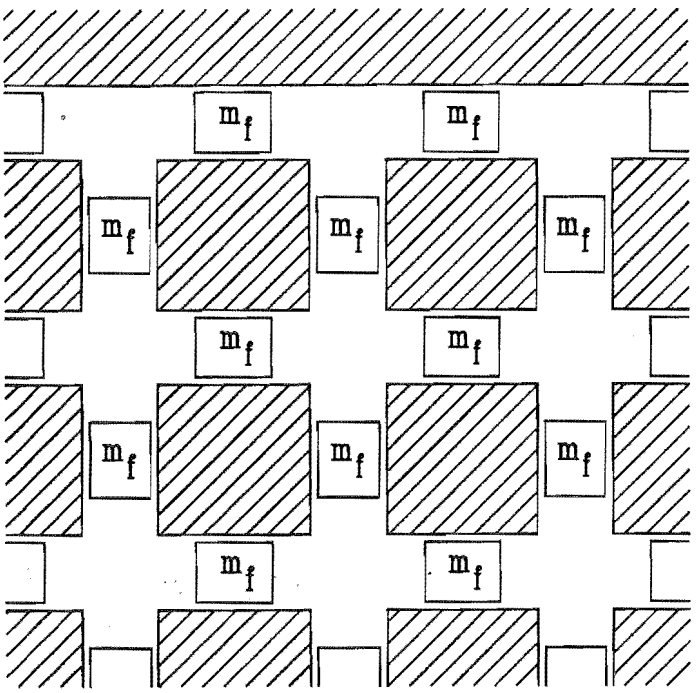

Figure 6.5: Two-dimensional approximation of an inviscid fluid. Each mass element is constrained to move in one dimension, with the area bounded by each of the four masses and the solid walls filled with an incompressible, massless fluid.

It is also possible to make the fluid compressible using Bogert's (1951) method (for a 1-D ETL model), by adding shunt capacitors at each node of the inductor grid. Compressibility of the cochlear fluids could be important for high frequency stimuli (Lighthill, 1981; Section 4.2), but the inclusion of shunt capacitors has not been attempted.

6.2.2 Two-dimensional fluid motion

The inclusion of a 2-D fluid representation in the (E)TL model is accomplished by replacing the line of series inductors with a grid of inductors. Each inductor in the grid represents a small block of fluid, the value of which is dependent upon the discretization. If the discretization is uniform in x and uniform in y (but not necessarily the same in x and y dimensions), the inductor values are given by

$$L_h = \frac{\rho\, dx}{\Delta z} \quad \text{and} \quad L_v = \rho\, h \cdot 2\,\Delta z$$

where L_h is the value of the horizontal inductors, L_v is the value of the vertical inductors, dx is the incremental cochlear length, h is the height of the scalae, and Δz is the fractional height represented by each fluid element.

Figure 6.6 shows the magnitude and phase of fluid pressure and BM velocity for a second-order ETL model using the parameters given in Table 6.2. The stimulus frequency was 1.6 *kHz*. The responses are shown as a function of distance from the stapes and height above the BM (both dimensions are normalized). The fluid response is presented using contour plots with unequal scales in the length and height dimensions to improve clarity. The magnitude contours are spaced at 10 *dB* intervals and the phase contours are spaced at $\frac{1}{4}$ cycle intervals. For all the responses shown, the vertical dimension (i.e. the fluid) was represented by 16 sections.

The transition from long-wave to short-wave fluid motion (see Section 3.1.3) can be clearly seen in both the magnitude and phase responses. Far basal of the characteristic place, the fluid pressure (both magnitude and phase) is approximately constant with height above the BM. This implies that the wavelength is large relative to the cochlear height (long-wave region). Nearing the characteristic place, the fluid pressure magnitude and phase accumulation both become less away from the BM, corresponding to the short-wave region. Beyond the short-wave region the phase does not vary along the cochlear length, but it does vary with height (in multiples of one cycle). This implies that the BM motion has the same phase along the cochlear length, resulting in all the fluid motion being perpendicular to the BM as shown by the parallel phase contours. The close "bunches" of several phase contours indicates the presence of a standing wave in the vertical direction. The standing wave has a very small amplitude, as indicated by the small curvature in the magnitude contours in this region. Note that this fluid motion is somewhat different from that shown by Neely (1981). In his responses, adjacent phase contours near the char-

Scalae parameters	
Scala length	3.5 cm
Effective scala height (h)	0.1 cm
Fluid density (ρ)	1.0 $g \cdot cm^{-3}$
Partition parameters	
BM mass	$5.0 \cdot 10^{-2}$ $g \cdot cm^{-2}$
BM compliance	$2.0 \cdot 10^{-10}$ $\exp^{2.8x}$ $cm^3 \cdot dyn^{-1}$
BM resistance	$1.0 \cdot 10^{2}$ $dyn \cdot s \cdot cm^{-3}$

Table 6.2: ETL model parameters (cgs units) used for showing two-dimensional fluid motion in a simple cochlear model.

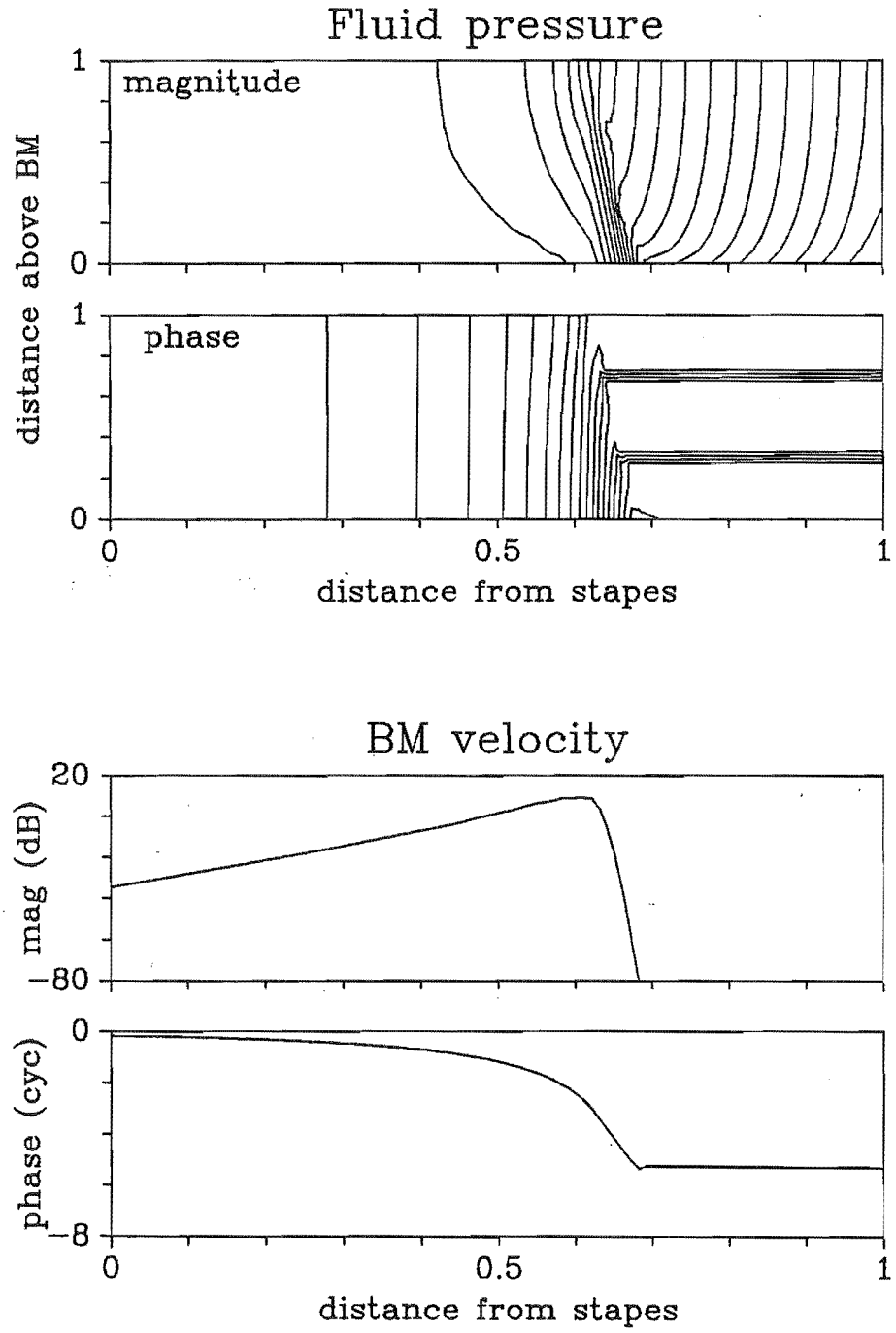

Figure 6.6: Two-dimensional fluid motion in an ETL cochlear model, for normal scala height ($h = 0.1cm$). The contours are spaced at intervals of 10 dB (for the magnitude) and $\frac{1}{4}$ cycle (for the phase).

acteristic place were shown to converge at some point above the BM, with few contours apical of this position. Since different phase contours cannot physically join up in this way, Fig. 6.6 shows the correct fluid motion.

The variation of fluid wavelength in the cochlea is dependent on the scalae dimensions. Figure 6.7 shows the fluid motion in the ETL model when the height of the scalae is increased to 0.5 *cm*. The fluid flow now varies dramatically with height above the BM. The upper part of the fluid does not participate in the formation of the travelling wave, as indicated by the virtual absence of phase contours in this region. Both responses show that the fluid is being "sucked" into a pronounced magnitude minimum, suggesting the formation of an eddy. The BM response displays a pronounced plateau just apical of the characteristic place. It is suggested that this is a result of the initial fluid pressure (see Section 3.1.2) having a greater affect in the apical regions than is the case with normal scalae height.

Figure 6.8 shows the fluid motion in the ETL model when the height of the scalae is reduced to 0.02 *cm*. There is very little difference in both the magnitude and phase of fluid pressure with height above the BM, indicating the fluid flow to be close to one-dimensional over the whole length of the cochlea. The low scalae height results in an increase of the axial fluid impedance, resulting in an increase in phase accumulation (see Section 4.4.3).

In his physical models, von Békésy (1960) found that decreasing the scalae height had a greater affect on BM motion than increasing the scalae height. This observation is confirmed in Figs. 6.6-6.8.

6.2.3 Effect of 2-D fluid on OHCAP model response

The effect of adding 2-D fluid to the FOHCAP model is shown in Fig. 6.9, using the parameters given in Table 6.1. The responses of a 1-D and a 2-D model are shown. The shape of the response peaks exhibited by both models is very similar, owing to the relatively large resistance parameters used in the OHCAP model. The main effect of adding 2-D fluid is that the CF is slightly reduced. This difference between the responses of the models is similar to that exhibited in second-order cochlear models with high damping (e.g. Viergever, 1980). This similarity is expected, as it is the (second-order) pectinate zone of the FOHCAP model which governs the model's macromechanical fluid motion (see Section 5.3). Also shown in Fig. 6.9 is the response of the 1-D model with one-third of the fluid mass added to the BM. The 1-D model response is now virtually identical to that of the 2-D model, validating this (slight) parameter modification in a 1-D cochlear model with high damping (see Section 4.4.3).

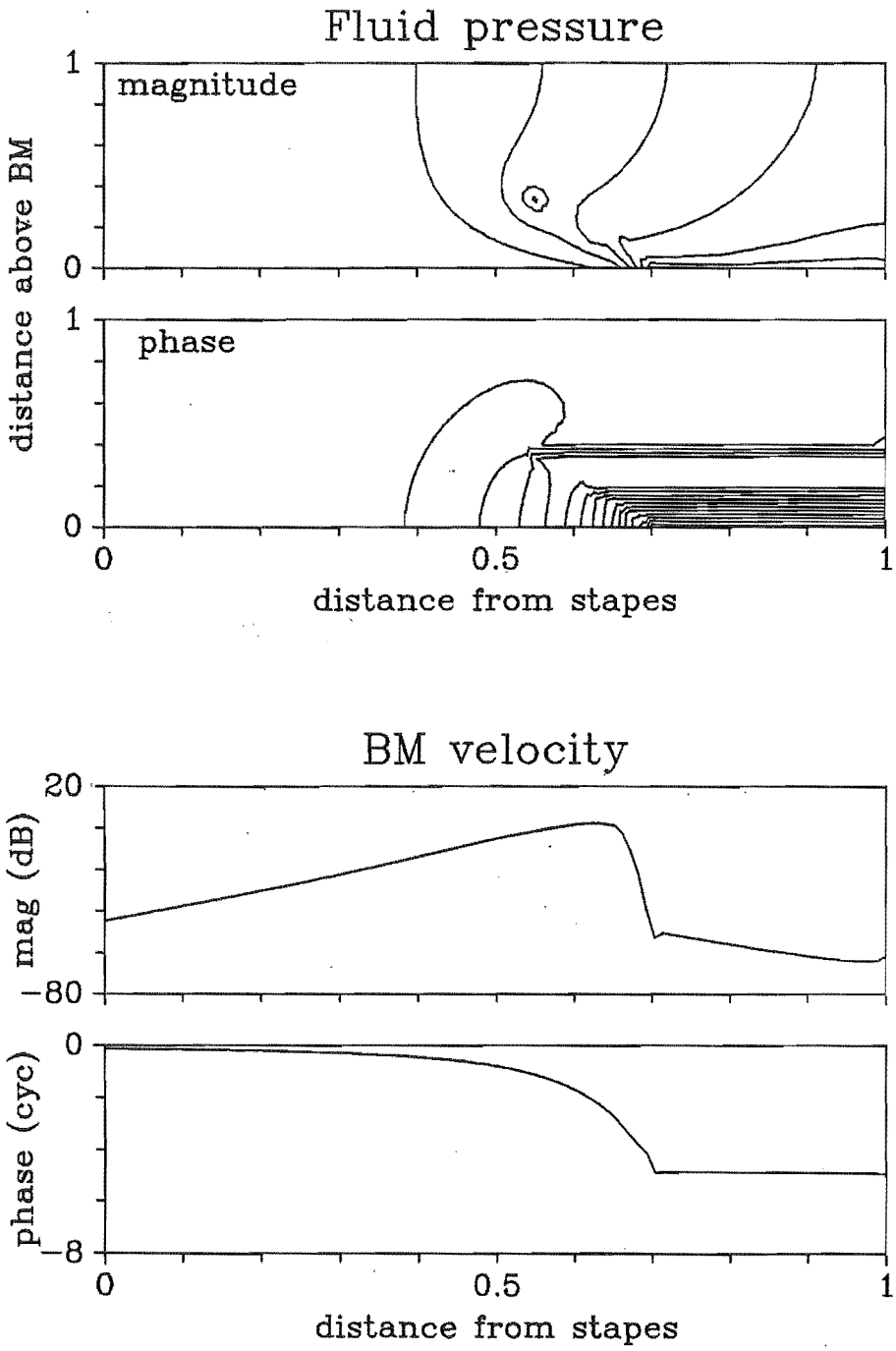

Figure 6.7: Two-dimensional fluid motion in an ETL cochlear model with high scalae ($h = 0.5cm$). Only the fluid adjacent to the BM affects the mechanics.

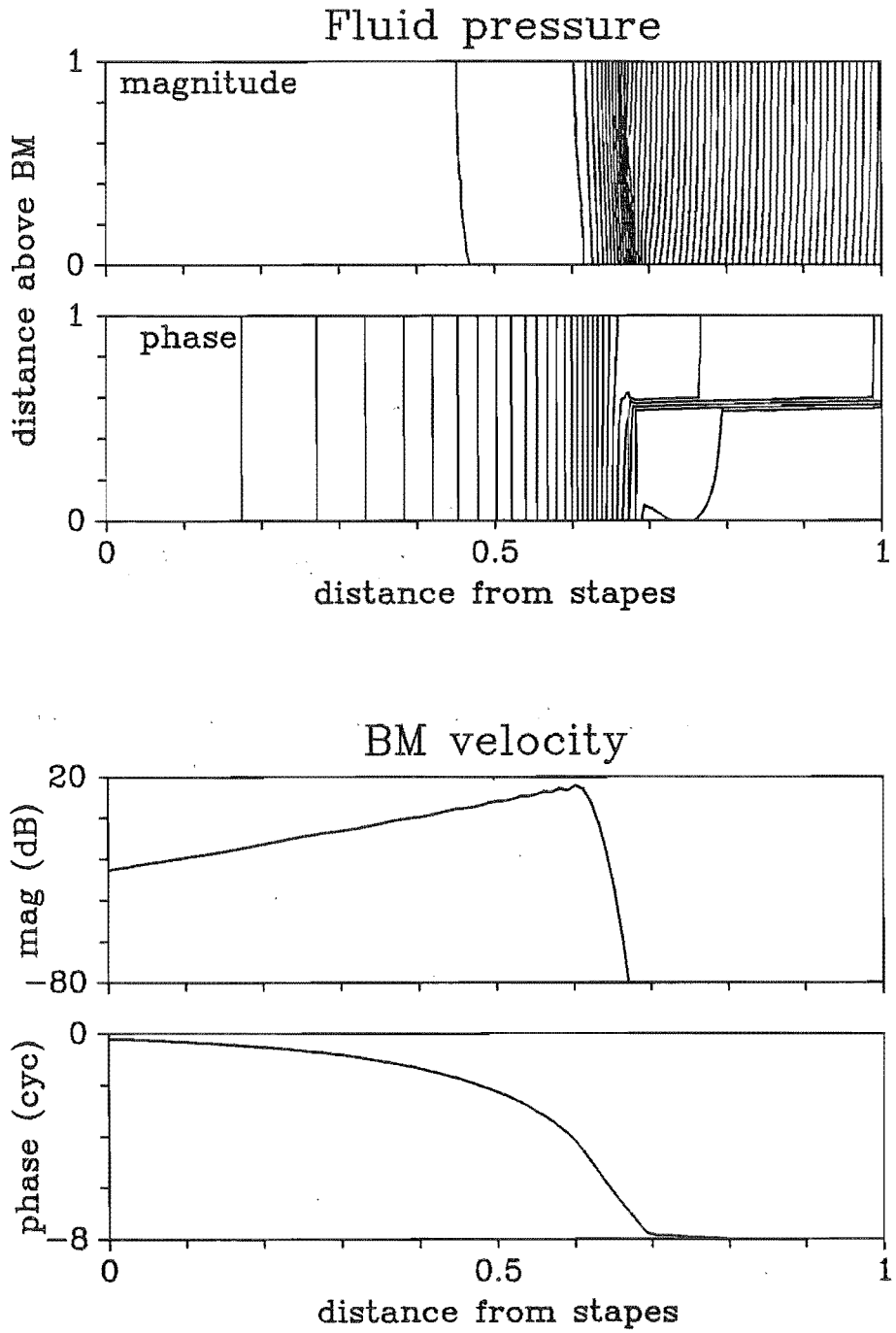

Figure 6.8: Two-dimensional fluid motion in an ETL cochlear model with low scalae ($h = 0.02cm$). The fluid response is very similar to that obtained in a 1-D model.

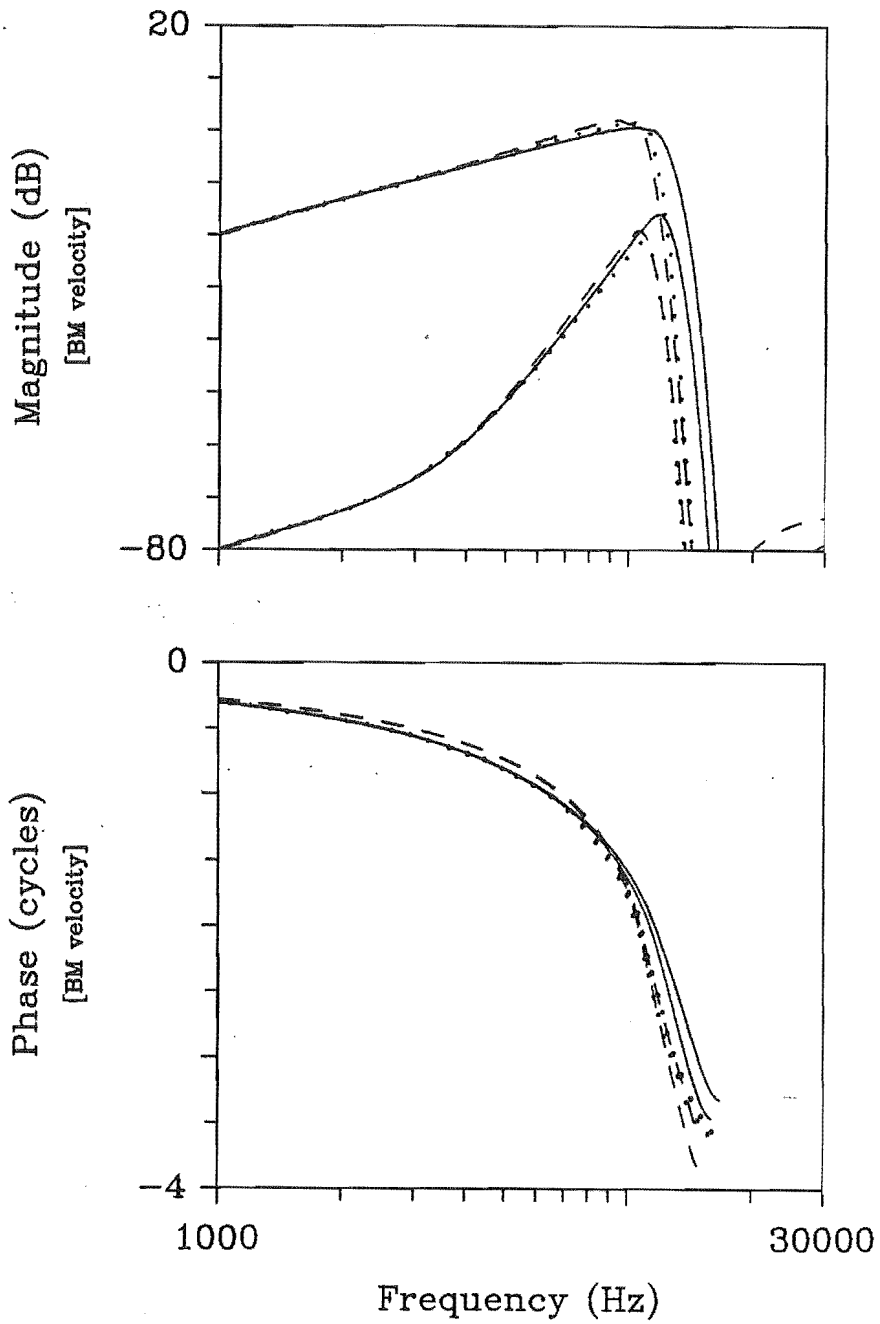

Figure 6.9: Response of FOHCAP model with 1-D and 2-D fluid. The responses of the 1-D and 2-D model are indicated, respectively, by the solid and dashed lines. The differences in response are as for a simple second-order cochlear model with high BM damping. The dotted line shows the response of the 1-D model with one-third of the fluid mass added to the BM.

Chapter 7

Discussion

The most important original contribution of this thesis is the description of a new type of cochlear model. The special features of the model (in both its structure and its response) raise questions regarding the accuracy of some currently accepted hypotheses concerning cochlear mechanics. This chapter presents a critical appraisal of the model.

7.1 Anatomical support for the OHCAP model

The assumption of differing motion in the arcuate and pectinate zones of the CP is solidly based on considerations of the CP's structure. It seems strange that very few modelling investigations properly take into account the gross structural differences between the two zones.

One of the most attractive features of the DOHCAP model is that it suggests a function for the unusual spatial arrangement of the various components of the organ of Corti. The most debatable assumption made in its formulation, that the OHCs receive stimulation from their outer surface rather than from the bending of their stereocilia, requires further investigation. Among the questions that arise from the DOHCAP model are: is it feasible that the outer surface of the OHCs could receive stimuli from the Deiters' cells and their phalangeal processes; are the phalangeal processes sufficiently stiff; and can the OHCs produce a force that is proportional to the difference between two inputs? The answer to these questions obviously requires a closer look at the physiology of the organ of Corti.

It should be noted that the FOHC and DOHC models presented in Chapter 5 are only two examples of the many possible OHC models which, when added to the OHCAP model, result in it exhibiting a realistic response.

7.2 Advantages of a passive model

OHCAP model is a passive cochlear model, in that the only source of energy is the stapes. The presence of the OHCs enhances the motion of the BM, but this is achieved without the OHCs adding any energy; the motile force they produce reduces the net stiffness of the BM and not its damping. The assumptions made in the formulation of the OHCAP model ensure that the OHCs are able to redistribute the energy coming in from the stapes, by effectively tapping off the pectinate zone motion in a frequency and place specific manner, so as to produce arcuate motion that reflects sharp neural-like tuning.

There are a number of important reasons for achieving a realistic response using the (passive) OHCAP model, rather than using active models. Firstly, active cochlear models are inherently in danger of becoming unstable, since they are extremely sensitive to parameter variations (which exist in a biological system such as the cochlea). This problem can be rectified by introducing large non-linearities, but this causes further problems such as dynamic range limiting (Neely, 1988). The response of the OHCAP model is also sensitive to parameter variations (the effects of trauma are simulated by small changes to the gain parameters of the force generators - see Section 5.5.4), but its stability is not.

Secondly, and more importantly, both assumptions made in the formulation of the OHCAP model are *essential* in order for a realistic passive cochlear model to simultaneously exhibit realistic selectivity and phase response. This provides a nice explanation as to why nature has devised a cochlea which has such a large difference in mechanical structure in the two zones of the CP.

7.3 Arguments supporting active models

7.3.1 Acoustic emissions

The presence of spontaneous otoacoustic emissions strongly supports the existence of active biomechanical mechanisms that inject energy along the length of the cochlea. However, the author suggests that the mechanisms involved with the generation of SOEs are not directly related to cochlear tuning. This hypothesis is supported by a number of observations. Firstly, the extremely narrow bandwidth of SOE's suggests that they originate from isolated (i.e. discrete) regions along the cochlear length (Manley, 1983), and not from extended zones as required in active cochlear models. Secondly, there is a strong correlation between the site of SOE production and irregularities in the structure of the organ of Corti (e.g. the presence of four rows of OHCs rather than the usual three (Martin *et al.*, 1988) or a loss of "orderliness" in the OHCs or in the arrangement of their stereocilia (Manley, 1983)). Thirdly, in the relatively few observations in which SOEs have been detected in animals, emitted responses are often situated on the borders of regions associated with significant threshold shifts and consequently appear to be related to abnormal cochlear processes (Ruggero *et al.*, 1984).

These observations suggest that the SOEs are a manifestation of improper organ of Corti structure, rather than reflecting an integral process of cochlear tuning. Assuming that the SOEs are produced by the OHCs, this could be simulated in the OHCAP model by altering one or more of the OHC parameters (or altering slightly the structure of the OHC model) so as to produce an impedance that has a negative real part. In this case, the model is locally active and so has the potential to generate SOEs.

7.3.2 Experimentally-measured tuning data

In all previous cochlear models it has been found that active processes are required in order for the model to exhibit realistic sensitivity, selectivity, and changes in response as a result of trauma. The OHCAP model exhibits realistic selectivity and phase response, and realistic changes in both selectivity and sensitivity as a result of trauma (see Section 5.5). Therefore, these latter features of the response of the real cochlea should not be used as justifications for the hypothesis of active processes in cochlear mechanics.

The sensitivity of the OHCAP model is less than that of the data obtained from the real cochlea. This is a fundamental problem with the model, and one that may ultimately rule out its complete acceptance. However, there are a number of aspects concerning the experimental data that should be kept in mind. Firstly, if the hypotheses made in the formulation of the OHCAP model are valid, the smaller impedance of the pectinate zone makes it more susceptible to loading from the source placed on it during experimental measurements. In their measurements, Sellick *et al.* (1983b) concluded that "the Mössbauer source is loading the BM and the measured tuning curves may not be representative of the unloaded travelling wave". This was particularly true for large sources in the pectinate zone, and so the presence of the Mössbauer source could be affecting the measured sensitivity.

Secondly, accurate measurement of sound pressure at the eardrum is very difficult. It has been shown that a major portion (up to 95%) of the acoustic wave entering the ear can be reflected off the eardrum (Khanna and Stinson, 1985). The reflected wave interferes with the incident wave, resulting in standing waves in the ear canal. The reflected wave is large if the stapes impedance is abnormally large, which could be the case near CF since for high frequencies the cochlea length is approximately equal to a half wavelength. This all means that considerable variations of sound pressure can exist near the eardrum, and so the measured air pressure (by a probe microphone) may not accurately represent the true sound pressure acting as an input to the middle ear (and cochlea). If the microphone is placed in a position when a minimum of sound pressure occurs, the apparent sensitivity of the cochlea will be increased. This effective increase could amount to as much as 25 *dB* (Khanna and Leonard, 1986), resulting in a large uncertainty in the cochlea's actual sensitivity.

Thirdly, the measured sensitivity implies that, at threshold, the BM motion resulting from stapes stimulus is 30 *dB* below its motion caused by thermal noise. This suggests that an understanding of cochlear mechanics near threshold requires the use of quantum-

mechanical descriptions (Bialek, 1983). Bialek calculated that a perfect amplifier (in the quantum mechanical sense) is required to explain this sensitivity, and so conventional cochlear models cannot be used.

Even if the above uncertainties relating to the measured sensitivity are found to be unimportant, this would not invalidate important conclusions that can be drawn from the OHCAP model: for example, that realistic mechanical response selectivity and phase response, and realistic changes in response as a result of trauma, can all be simulated in a passive cochlear model with realistic parameters.

Chapter 8

Conclusion

It is appropriate to end this thesis with a few comments regarding the current state of our understanding of cochlear mechanics, as suggested by the work contained in this thesis.

It is claimed in this thesis that inaccurate assumptions have been made in the formulation of all cochlear models (assumptions that were necessary before construction and analysis of the models could be attempted). If true, this in itself does not render the models worthless; the main problem is that too much faith is placed in the conclusions drawn from analyses of these models. For example, if a cochlear model needed active processes in order for it to exhibit a realistic response, then it was assumed that these active processes must also be present in the real cochlea: the use of inverse methods has proved that a cochlear model having only one degree of freedom in a radial direction cannot exhibit a realistic response without incorporating active processes. The results obtained from studying the OHCAP model are in complete agreement with these findings, since the OHCAP model allows for two degrees of freedom in the radial direction and so is not bound by the conclusions made from the inverse studies. This illustrates that the results from inverse methods are only true for a certain type of cochlear model, and may not be true for the real cochlea. More generally, the results from any cochlear model investigation only apply in the framework of the assumptions made in the model's formulation.

Another recurring problem in cochlear mechanics is that the observations made during experimental measurements are often taken out of context. One of the main themes of this thesis is that the CP has gross (and mechanically important) structural differences across its width which result in differing structural parameters and differing motion. These differences must be considered when comparing, for example, experimental measurements of the isotropy in the CP.

The OHCAP model illustrates how making different assumptions in the formulation of a cochlear model can result in *completely* different conclusions regarding the *fundamental* processes of cochlear mechanics. This suggests that all our models are too simple to be considered as accurately representing what is going on in the cochlea. This conclusion, naturally, also applies to the OHCAP model. The author does not consider the OHCAP model to be an accurate representation of the cochlea. It seems that people in general

should become more critical of the results obtained from cochlear modelling studies.

The lack of experimental data is largely responsible for our present (lack of) understanding of cochlear mechanics. It can be concluded that the available response data is woefully insufficient, and should not be used as a strong basis for the support or otherwise of theories concerning cochlear mechanics. This constitutes the most important limiting factor in our quest for an accurate understanding of the mechanics of the cochlea.

Until recently, the organ of Corti has been treated as one unit when considering its mode of action, in spite of a very complex design. It could well be that aspects of cochlear mechanics that result in the exquisite cochlear response are intimately related to the three-dimensional nature of the CP and the fluids in which it is positioned. We will not find this out until measurements are made to check whether the assumptions made in present cochlear models are accurate. Particular measurements that must be made include:

- Motion of the arcuate and pectinate zones of the BM, preferably relative to stapes motion rather than relative to eardrum pressure.
- Motion of the structures constituting the organ of Corti.
- Observations of OHC motility *in vivo* (or at least *in situ*).
- Structural parameters of the organ of Corti, particularly the rigidity of the Deiters' cells and their phalangeal processes.

Such measurements may highlight the importance that the three-dimensional structure of the CP has on cochlear mechanics. If so, we will have to develop more powerful analysis methods for our mathematical models, or else place more emphasis on the construction and analysis of physical (hydrodynamic and electric) cochlear models.

Appendix

An Electrical Model of Stick-slip Friction

This Appendix describes a technique for modelling stick-slip friction, enabling it to be incorporated in an ETL cochlear model.

Cochlear fluid non-linearity, manifesting itself in the form of eddies, has only been observed in physical models (von Békésy, 1960; Tonndorf, 1958). It is uncertain whether or not these eddies occur in the ear, because of the high friction in its much narrower scalae. However, in narrow channels the starting friction may be quite large and so stick-slip friction (Blok, 1940) may play an important role in the production of eddies or in the mechanics of the subtectorial space. This hypothesis is supported by the observations of Tonndorf's models, in which the eddies appeared rather abruptly when the stimulus magnitude reached a value sufficient to overcome the starting friction of the fluid.

This section describes a technique by which stick-slip friction can be incorporated in a (non-linear) ETL cochlear model. Owing to the linear nature of the cochlear models described in this thesis, it is not possible to incorporate stick-slip friction in them. Therefore, to illustrate the validity of the technique, examples from solid mechanics are used.

A.1 Description

Stick-slip friction affects mechanical systems in which the unlubricated surfaces of two solids are in contact under a condition of sliding or tendency to slide. A friction force tangent to the surface of contact is developed both during the interval leading up to the impending slippage and while slippage takes place. The maximum static friction force is usually greater than the kinetic friction force, resulting in a "stick-slip" form of motion (Fig. A.1).

The transition region is defined as the portion of the friction force versus velocity curve (stick-slip friction curve) where the friction force is changing from the static value to the

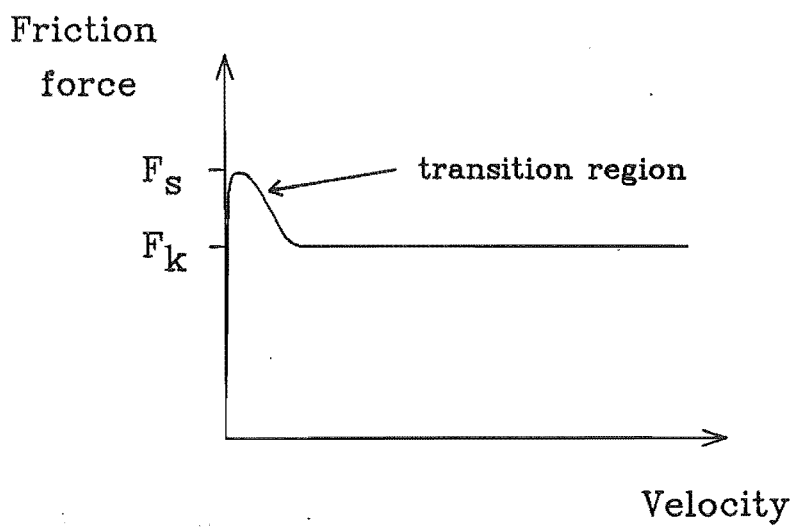

Figure A.1: A typical stick-slip friction characteristic. When stick-slip friction acts between two surfaces in a mechanical system, the starting friction F_s exceeds the kinetic friction F_k. The transition zone refers to the velocity range over which stick-slip friction acts.

kinetic value. Note that the stick-slip friction characteristic is an odd function. The shape of the transition region is different depending upon the type of surfaces involved in the motion, and whilst many modelling techniques have been proposed and used previously, a flexible and easily applied technique appeared to be outstanding.

Kolston (1988b) found that by deriving the electrical circuit equivalent to the mechanical system of interest and then implementing a special circuit component in SPICE (Nagel, 1975), it was possible to alter one region of the simulated stick-slip friction curve without affecting other regions. This is because different components of the stick-slip electrical circuit component determined the different parameters (e.g.; static to kinetic friction ratio, type of transition region) virtually independently.

The usual mechanical-to-electrical analogies are used (as in Section 4.4.2), which means that an electric circuit component is required that has a voltage versus current characteristic as shown in Fig. A.1 The circuit is shown in Fig. A.2. The current sources are controlled by the input current. Two parallel pairs of diodes are used, the pairing being necessary to ensure that the V/I characteristic is an odd function. The diode V/I characteristics are such that when the diode current is non-zero, the voltage drop

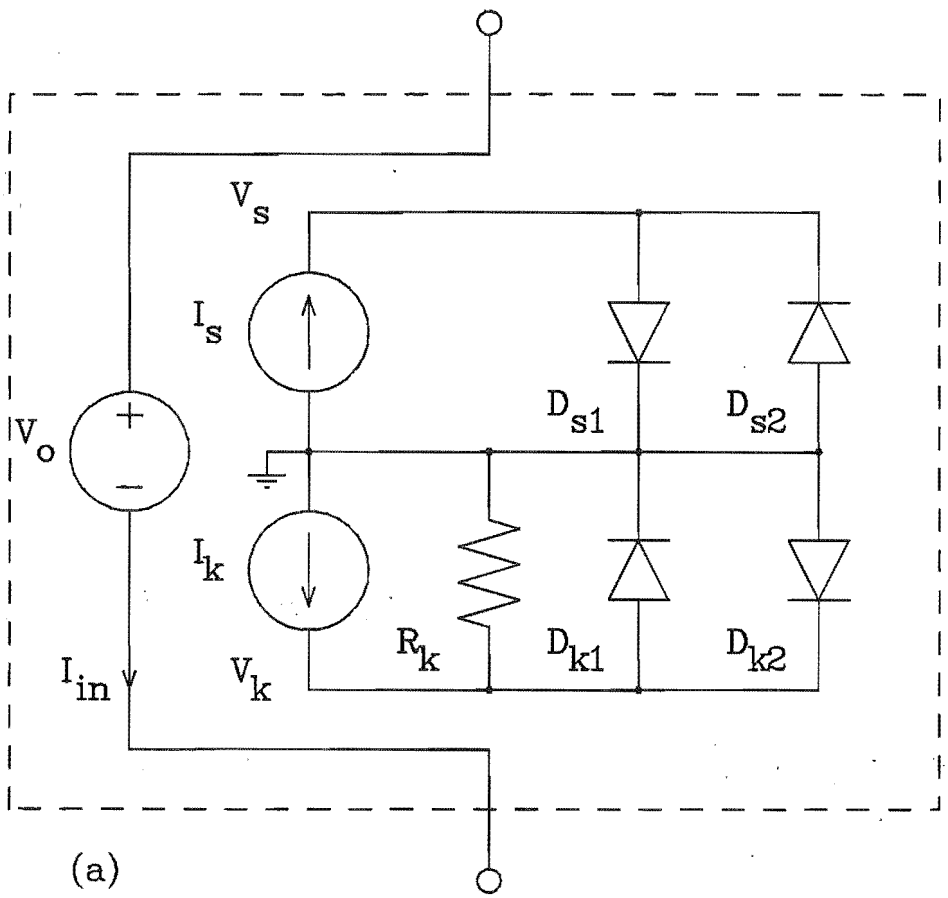

Figure A.2: The electrical stick-slip friction model: *(a)* actual circuit, *(b)* model symbol. The current sources are described by: $I_s = K_s \cdot I_{in}$ and $I_k = K_k \cdot I_{in}$. The voltage source is described by: $V_o = K_o \cdot (V_s - V_k)$. The back-to-back diodes ensure that the V/I characteristic is an odd function. For the examples described in Section A.2, the following parameters were used: $K_s = 30.0$, $K_k = 3.0$, $K_o = 20.0$ ($K_o = 10.0$ for the example with interacting stick-slip friction forces), and $R_k = 1$ (i.e. is a linear resistor).

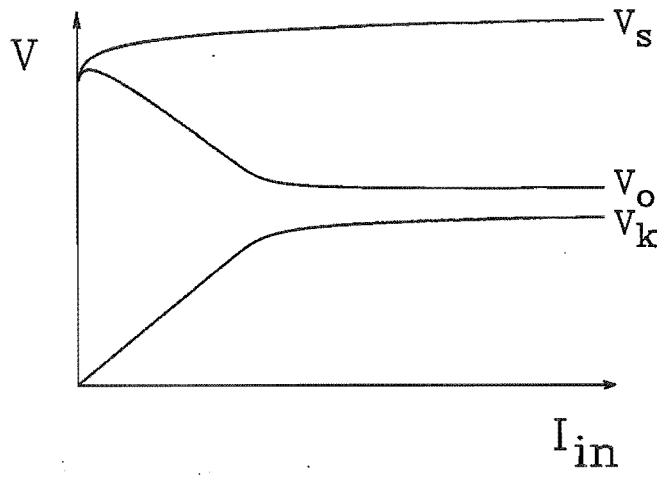

Figure A.3: How the transition region characteristic is obtained. On the application of input current (I_{in}) V_s rises rapidly to its saturation value, whereas V_k rises more slowly owing to the presence of resistor R_k in the lower part of the circuit. Subtracting V_k from V_s produces the required output voltage variation .

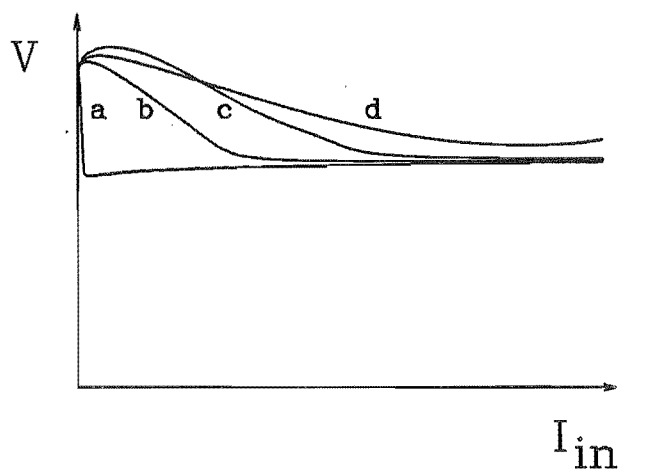

Figure A.4: Some possible friction characteristics: (a) Blok; (b) Cockerham and Cole; (c) Bo and Pavelescu; (d) Banerjee .

is approximately constant, independent of input current. This diode saturation region is modelled in SPICE using an exponential function, and results in a stick-slip friction characteristic which has no discontinuity at the transition to constant kinetic friction. The presence of resistor R_k alters V_k so that, unlike V_s, there is an input current range over which V_k rises up to the constant (saturated) value. Note that using the SPICE diode model ensures that the friction force is zero for zero velocity, and equal to the static friction force value for any infinitesimally small velocity. That is, the force versus velocity slope is effectively infinite between the positive and negative static friction force values.

The transition region shape is determined by R_k. This resistor is modelled using a current-controlled-voltage source. The resistor can be described by a polynomial of up to degree 20, and so many different types of transition region are possible. Note that the whole stick-slip friction V/I characteristic could be modelled using a polynomial current-controlled-voltage-source, but this would not give the sharp characteristic possible using the circuit shown. Also, the different sections of the characteristic could not be independently adjusted. The coefficient K_o determines the magnitude of F_s and F_k, whilst the ratio of the diode saturation voltages determine the ratio F_s to F_k. The output voltage source V_o is equal to V_s minus V_k, and produces the required characteristic as shown in Fig. A.3.

The real physical stick-slip friction characteristic is still the subject of some debate (Klamechi, 1985). The Blok (1940) model was based on an instantaneous drop in friction force in the transition region. Cockerham and Cole (1976) suggested a linear transition region while Bo and Pavelescu (1981) used an exponential friction model. Banerjee's model (1968) assumed that outside the transition region the kinetic friction force increases with velocity. Fig. A.4 shows that all these curves can be modelled using the technique described here, by altering the coefficients describing R_k.

A.2 Test examples

The validity of the technique is shown with the aid of two examples. It can be applied to any (hydro-) mechanical system that has an analogous electrical circuit suitable for SPICE simulation (such as the OHCAP model).

First consider a simple spring-mass system driven at a constant velocity. Fig. A.5 shows the system and its analogous electrical circuit. The presence of stick-slip friction causes the mass to stop periodically as shown in Fig. A.6. Increasing the drive velocity whilst keeping other parameters constant will reduce the time for which the mass is stationary. The form of the transition region has little effect on the motion when the stick-slip friction is large as in this case.

Another example is shown in Fig. A.7, where m_1 slides on m_2, which in turn slides on the ground. A velocity input is provided at the spring c_1. Fig. A.8 shows the response of the system starting at rest to a step in the input velocity which returns to zero at 0.1 s. This motion is similar to that shown by Karnopp (1985) when the same system (with different parameters) is similarly excited. For the present results $F_s = 1.5\ F_m$, with a

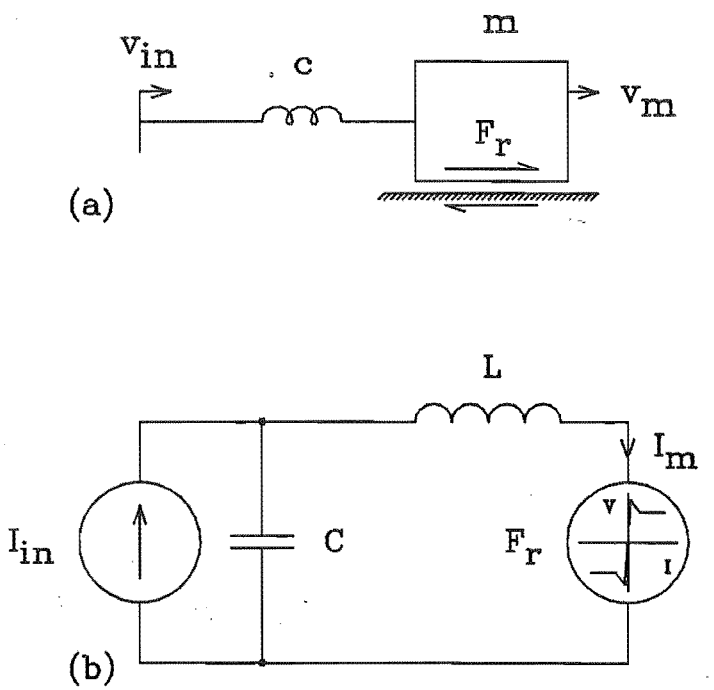

Figure A.5: Simple spring-mass system: *(a)* mechanical system, *(b)* equivalent electrical circuit. Parameters used: $L = 0.5$ and $C = 0.5$. Diode emission coefficients (their other parameters took the default SPICE values): $D_s = 4.0$ and $D_s = 1.0$.

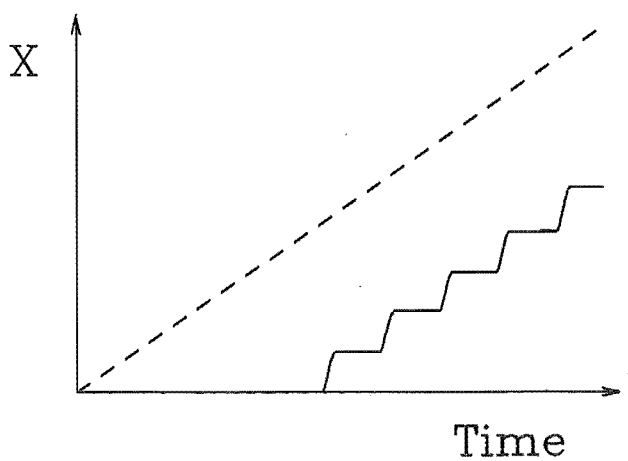

Figure A.6: Response of the simple spring-mass system. The displacement of the stimulus is indicated by the dashed line, and the displacement of the mass is indicated by the solid line. The presence of stick-slip friction results in the mass lagging the stimulus and periodically stopping .

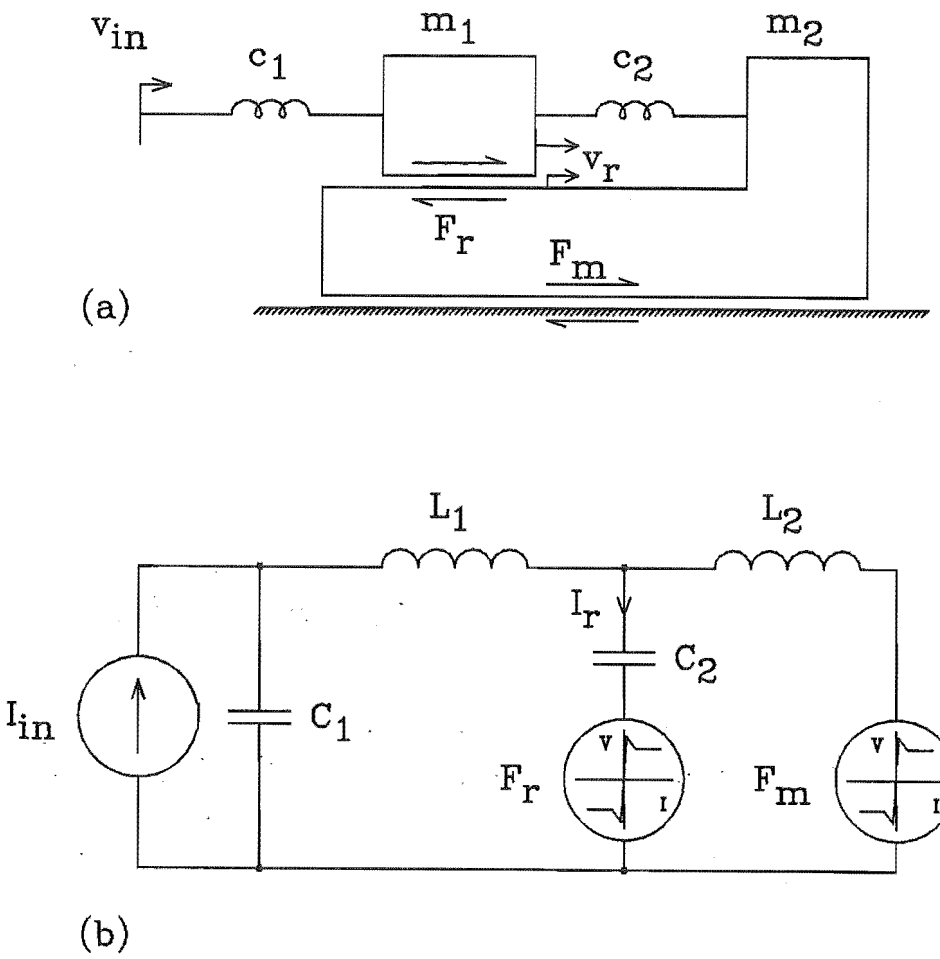

Figure A.7: System with interacting stick-slip forces: *(a)* mechanical system, *(b)* equivalent electrical circuit. Parameters used: $L_1 = 0.1$, $L_2 = 0.1$, $C_1 = 0.01$, $C_2 = 0.005$, and $K_o = 10.0$. Diode emission coefficients (their other parameters took the default SPICE values): $D_s = 0.7$ and $D_s = 1.4$.

linear transition region. At several times during the motion one can observe sticking with zero velocity, a subsequent rise of the friction force to its breakaway value, and then a drop to the kinetic value, all as expected intuitively.

The two examples described above illustrate the effects that stick-slip friction can have on the response of simple mechanical systems. The stick-slip model (Fig. A.2) can also be added to more complicated systems, such as an ETL cochlear model. The analysis of more complicated systems using SPICE is as straightforward as for the examples given here, except that more computer processor time and memory is required.

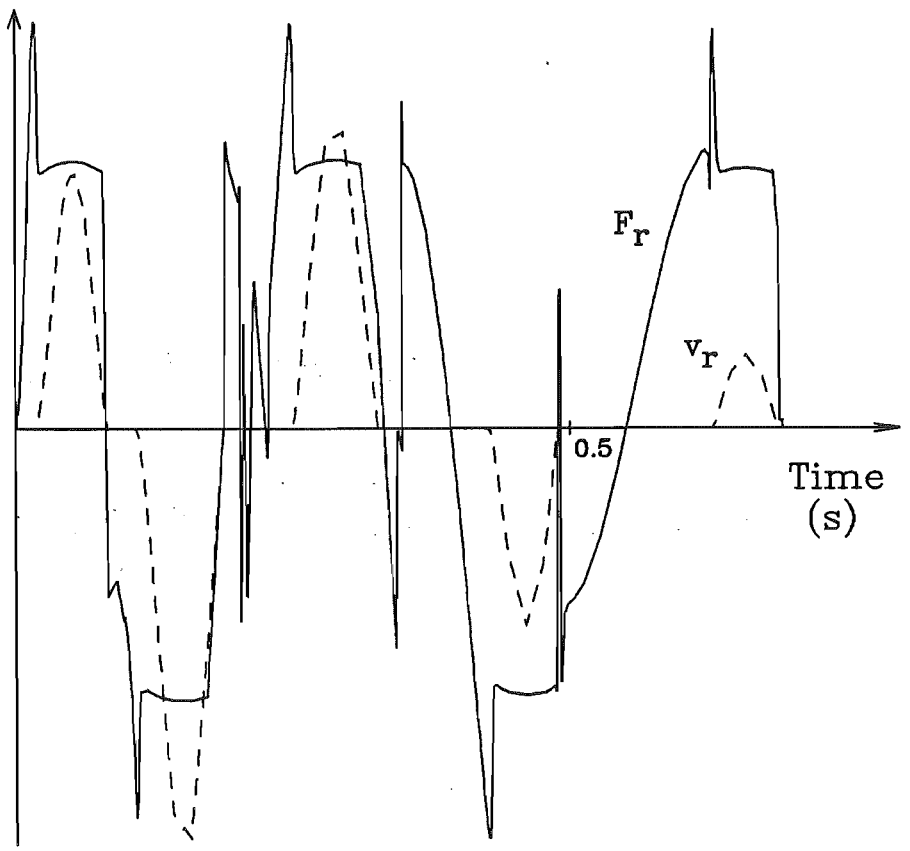

Figure A.8: Response of the system with interacting stick-slip forces. The solid line indicates the friction force between the two masses, and the dashed line indicates their relative velocity. At several times during the motion one can observe sticking with zero velocity, a subsequent rise of the friction force to its breakaway value, and then a drop to its kinetic value.

References

Allen, J.B. (1977). Cochlear micromechanics - a mechanism for transforming mechanical to neural tuning within the cochlea. J. Acoust. Soc. Am., 62, 930-939.

Banerjee, A.K. (1968). Influence of kinetic friction on critical velocity of stick-slip motion. Wear, 12, 107-116.

Bialek, W. (1983). Thermal and quantum noise in the inner ear. In *Mechanics of Hearing*, edited by E. de Boer and M.A. Viergever, (Delft University Press), pp 185-192.

Blok, H. (1940). Fundamental mechanical aspects of boundary lubrication. SAE Trans., 46, 54-68.

Bo, L.C. and Pavelescu, D. (1982). The friction-speed relation and its influence on the critical velocity of stick-slip motion. Wear, 82, 277-289.

Bogert, B.P. (1951). Determination of the effects of dissipation in the cochlear partition by means of a network representing the basilar membrane. J. Acoust. Soc. Am., 23, 145-151.

Camp, L. (1970). *Underwater Acoustics.* Wiley-Interscience, New York.

Cancelli, C., D'Angelo, S., Masili, M., and Malvano, R. (1985). Experimental results in a physical model of the cochlea. J. Fluid Mech., 153, 361-388.

Cockerham, G. and Cole, M. (1976). Stick-slip stability by analogue simulation. Wear, 36, 189-198.

de Boer, E. (1973). On the principle of specific coding. ASME J. Dynamic Systems, Measurement, and Control, 95, 265-273.

de Boer, E. (1980). Auditory physics. Physical principles in hearing theory. I. Phys. Rep., 62, 89-174.

de Boer, E. (1983a). No sharpening? A challenge for cochlear mechanics. J. Acoust. Soc. Am., 73, 567-573.

de Boer, E. (1983b). On active and passive cochlear models - Toward a generalized analysis. J. Acoust. Soc. Am., 73, 574-576.

de Boer, E. (1983c). Power amplification in an active model of the cochlea - Short-wave case. J. Acoust. Soc. Am., 73, 577-579.

Diependaal, R.J., de Boer, E., and Viergever, M.A. (1987). Cochlear power flux as an indicator of mechanical activity. J. Acoust. Soc. Am., 82, 917-926.

Duifhuis, H. (1976). Cochlear nonlinearity and second filter: Possible mechanism and implications. J. Acoust. Soc. Am., 59, 408-423.

Evans, E.F. and Wilson, J.P. (1973). Frequency selectivity of the cochlea. In *Basic Mechanisms of Hearing*, edited by A.G. Möller, (Academic Press, New York), pp 519-551.

Evans, E.F. and Wilson, J.P. (1975). Cochlear tuning properties: Concurrent basilar membrane and single nerve fiber measurements. Science, 190, 1218-1221.

Fletcher, H. (1951). On the dynamics of the cochlea. J. Acoust. Soc. Am., 23, 637-645.

Geisler, C.D. (1986). A model of the effect of outer hair cell motility on cochlear vibrations. Hearing Research, 24, 125-131.

Helmholtz, H.L.F. (1863). Die Lehre von den Tonempfindungen als physiologische Grundlage für die Theorie der Musik. First ed. Brunswick, Vieweg. Eng. trans. by A.J. Ellis, 1885. *On the Sensation of Tone*, reprinted by Dover, 1954.

Iurato, S. (1962). Functional implications of the nature and submicroscopic structure of the tectorial and basilar membranes. J. Acoust. Soc. Am., 34, 1386-1395.

Johnstone, B.M. and Boyle, A.J.F. (1967). Basilar membrane vibration examined with the Mössbauer technique. Science, 158, 390-391.

Karnopp, D. (1985). Computer simulation of stick-slip friction in mechanical dynamic systems. ASME J. of Dynamic Systems, Measurement, and Control. 107, 100-103.

Kemp, D.T. (1979). Evidence of mechanical nonlinearity and frequency selective wave amplification in the cochlea. Arch. Oto-Rhino-Laryngol., 224, 37-45.

Khanna, S.M. (1986). Homodyne interferometry for basilar membrane measurements. Hearing Research, 23, 9-26.

Khanna, S.M. and Leonard, D.G.B. (1982). Basilar membrane tuning in the cat cochlea. Science, 215, 305-306.

Khanna, S.M. and Leonard, D.G.B. (1986). Relationship between basilar membrane tuning and hair cell condition. Hearing Research, 23, 55-70.

Khanna, S.M. and Stinson, M.R. (1985). Specification of the acoustical input to the ear at high frequencies. J. Acoust. Soc. Am., 77, 577-589.

Klamechi, B.E. (1985). A catastrophe theory description of stick-slip motion in sliding. Wear, 101, 325-332.

Kohllöffel, L.U.E. (1972). A study of basilar membrane vibrations. III. The basilar membrane frequency response curve in the living guinea pig. Acustica, 27, 82-89.

Kolston, P.J. (1988a). Micromechanics remove the need for active processes in cochlear tuning. In *Basic Issues in Hearing*, edited by H. Duifhuis, J.W. Horst and H.P. Wit, (Academic Press, London), pp 74-79.

Kolston, P.J. (1988b). Modeling stick-slip friction using electrical circuit analysis. ASME J. of Dynamic Systems, Measurement, and Control, 110, 440-443.

Kolston, P.J. (1988c). Sharp mechanical tuning in a cochlear model without negative damping. J. Acoust. Soc. of Am., 83, 1481-1487.

Kolston, P.J. and Viergever, M.A. (1989a). Realistic basilar membrane tuning does not require active processes. In *Cochlear Mechanisms - Structure, Function and Models*, edited by J.P. Wilson and D.T. Kemp, (Plenum Press, London), pp 415-424.

Kolston, P.J. and Viergever, M.A. (1989b). How do the outer hair cells influence cochlear mechanics? Submitted for publication.

Kolston, P.J., Viergever, M.A., de Boer, E., and Diependaal, R.J. (1989). Realistic mechanical tuning in a micromechanical cochlear model. J. Acoust. Soc. of Am., 86 (In Press).

Le Page, E.L. (1987). Frequency-dependent self-induced bias of the basilar membrane and its potential for controlling sensitivity and tuning in the mammalian cochlea. J. Acoust. Soc. Am., 82, 139-154.

Lighthill, J. (1981). Energy flow in the cochlea. J. Fluid Mech., 106, 149-213.

Lim, D.J. (1980). Cochlear anatomy related to cochlear micromechanics. A review. J. Acoust. Soc. Am., 67, 1686-1695.

Loh, C.H. (1983). Multiple scale analysis of the spirally coiled cochlea. J. Acoust. Soc. Am., 74, 95-103.

Manley, G.A. (1983). Frequency spacing of acoustic emissions: A possible explanation. In *Mechanisms of Hearing*, edited by W.R. Webster and L.M. Aitkin, (Monash University Press, Clayton, Australia), pp 36-39.

Martin, G.K., Lonsbury-Martin, B.L., Probst, R., and Coates, A.C. (1988). Spontaneous otoacoustic emissions in a non-human primate. I. Basic features and relations to other emissions. Hearing Research, 33, 49-68.

Miller, C.E. (1985). Structural implications of basilar membrane compliance measurements. J. Acoust. Soc. Am., 77, 1465-1474.

Mountain, D.C. (1980). Changes in endolymphatic potential and cross-olivocochlear-bundle stimulation alter cochlear mechanics. Science, 210, 71-72.

Nagel, L.W. (1975). SPICE2: A computer program to simulate semiconductor circuits. Memo no. ERL-M520, University of Berkeley, California.

Neely, S.T. (1981). Fourth-order partition dynamics for a two-dimensional model of the cochlea. Academic Thesis, Washington University, Missouri, USA.

Neely, S.T. (1988). Transient responses in an active, nonlinear model of cochlear mechanics. In *Basic Issues in Hearing*, edited by H. Duifhuis, J.W. Horst and H.P. Wit, (Academic Press), pp 106-115.

Neely, S.T., and Kim, D.O. (1983). An active cochlear model showing sharp tuning and high sensitivity. Hearing Research, 9, 123-130.

Neely, S.T. and Kim, D.O. (1986). A model for active elements in cochlear biomechanics. J. Acoust. Soc. Am., 79, 1472-1480.

Olson, H.F. (1966). *Solutions of Engineering Problems by Dynamic Analogies.* van Nostrand, New Jersey.

Peterson, L.C. and Bogert, B.P. (1950). A dynamical theory of the cochlea. J. Acoust. Soc. Am., 22, 369-381.

Rhode, W.S. (1971). Observations of the vibration of the basilar membrane in squirrel monkeys using the Mössbauer technique. J. Acoust. Soc. Am., 49, 1218-1231.

Rhode, W.S. (1978). Some observations on cochlear mechanics. J. Acoust. Soc. Am., 64, 158-176.

Ruggero, M.A., Kramek, B., and Rich, N.C. (1984). Spontaneous otoacoustic emissions in a dog. Hearing Research, 13, 293-296.

Robles, L., Ruggero, M.A., and Rich, N.C. (1986). Basilar membrane mechanics at the base of the chinchilla cochlea. I. Input-output functions, tuning curves, and response phases. J. Acoust. Soc. Am., 80, 1364-1374.

Sellick, P.M., Patuzzi, R., and Johnstone, B.M. (1982). Measurement of basilar membrane motion in the guinea pig using the Mössbauer technique. Hearing Research, 72, 131-141.

Sellick, P.M., Patuzzi, R., and Johnstone, B.M. (1983a). Comparison between the tuning properties of inner hair cells and basilar membrane motion. Hearing Research, 10, 93-100.

Sellick, P.M., Yates, G.K., and Patuzzi, R. (1983b). The influence of Mössbauer source size and position on phase and amplitude measurements of the guinea pig basilar membrane. Hearing Research, 10, 101-108.

Sondhi, M.M. (1978). Method for computing motion in a two-dimensional cochlear model. J. Acoust. Soc. Am., 63, 1468-1477.

Spoendlin, H. (1969). Innervation patterns in the organ of Corti of the cat. Acta. Otolaryng., 67, 239-254.

Steel, K.P. (1983). The tectorial membrane of mammals. Hearing Research, 9, 327-359.

Steele, C.R. (1974). Behavior of the basilar membrane with pure tone excitation. J. Acoust. Soc. Am., 55, 148-172.

Steele, C.R. and Zais, J.G. (1985). Effect of coiling in a cochlea model. J. Acoust. Soc. Am., 77, 1849-1852.

Stinson, M.R. (1986). Spatial distribution of sound pressure in the ear canal. In *Peripheral Auditory Mechanisms*, edited by J.B. Allen, J.L. Hall, A. Hubbard, S.T. Neely and A. Tubis, (Springer, Munich), pp 13-20.

Taber, L.A. and Steele, C.R. (1979). Cochlear model including three-dimensional fluid and four modes of partition flexibility. J. Acoust. Soc. Am., 70, 426-436.

Thorne, P.R. and Gavin, J.B. (1984). The accuracy of hair cell counts in determining distance and position along the organ of Corti. J. Acoust. Soc. Am., 76, 440-442.

Tonndorf, J. (1958). Harmonic distortion in cochlear models. J. Acoust. Soc. Am., 30, 929-937.

Viergever, M.A. and Kalker, J.J. (1975). A two-dimensional model for the cochlea. I. The exact approach. J. Engin. Math., 9, 353-365.

Viergever, M.A. (1978a). Basilar membrane motion in a spiral-shaped cochlea. J. Acoust. Soc. Am., 64, 1048-1053.

Viergever, M.A. (1978b). On the physical background of the point-impedance characterization of the basilar membrane in cochlear mechanics. Acustica, 39, 292-296.

Viergever, M.A. (1980). Mechanics of the inner ear - a mathematical approach. Academic thesis, Delft University of Technology, The Netherlands.

Viergever, M.A. (1986). Cochlear macromechanics - a review. In *Peripheral Auditory Mechanisms*, edited by J.B. Allen, J.L. Hall, A. Hubbard, S.T. Neely and A. Tubis, (Springer, Munich), pp 63-72.

Viergever, M.A. and Diependaal, R.J. (1986). Quantitative validation of cochlear models using the Liouville-Green approximation. Hearing Research, 21, 1-15.

Voldrich, L. (1978). Mechanical properties of the basilar membrane. Acta Otolarygol., 86, 331-335.

Voldrich, L. (1983). Experimental and topographic morphology in cochlear mechanics. In *Mechanics of Hearing*, edited by E. de Boer and M.A. Viergever, (Delft University Press), pp 163-168.

von Békésy, G. (1928). Zur theorie des Hörens; Die Schwingungsform der Basilarmembran. Physik, 29, 793-810.

von Békésy, G. (1960). *Experiments in Hearing.* McGraw-Hill, New York.

Wilson, J.P. and Johnstone, J.R. (1975). Basilar membrane and middle ear vibration in the guinea pig measured with the capacitance probe. J. Acoust. Soc. Am., 57, 705-723.

Wright, A. (1984). Dimensions of the cochlear stereocilia in man and the guinea pig. Hearing Research, 13, 89-98.

Zenner, H.P., Reuter, G., Plinkert, P.K., and Gitter, A. (1988). Outer hair cells possess acetylcholine receptors and produce motile responses in the organ of Corti. In *Cochlear Mechanisms - Structure, Function and Models*, edited by J.P. Wilson and D.T. Kemp, (Plenum Press, London).

Zurek, P.M. (1981). Spontaneous narrowband acoustic signals emitted by human ears. J. Acoust. Soc. Am., 69, 514-523.

Zwicker, E. (1986). A hardware cochlear nonlinear preprocessing model with active feedback. J. Acoust. Soc. Am., 80, 146-153.

Zwislocki, J. (1948). *Theorie der Schneckenmechanik* (Thesis), Acta. Otolaryngol. Suppl. LXXII, pp 50-51.

Zwislocki, J.J. (1962). Analysis of the middle ear function. Part I: Input impedance. J. Acoust. Soc. Am., 34, 1514-1523.

Zwislocki, J.J. (1963). Analysis of the middle ear function. Part II: Guinea pig ear. J. Acoust. Soc. Am., 35, 1034-1040.

Zwislocki, J.J. (1983). Sharp vibration maximum in the cochlea without wave reflection. Hearing Research, 9, 103-111.

Zwislocki, J.J. and Kletsky, E.J. (1979). Tectorial membrane: A possible effect on frequency analysis in the cochlea. Science, 204, 639-641.

New references

Mountain, D.C. (1985). Active filtering by hair cells. In *Peripheral Auditory Mechanisms,* edited by J.B. Allen, J.L. Hall, A. Hubbard, S.T. Neely and A. Tubis (Springer, Munich), pp 179-188.

Lim, D.J. (1986). Functional structure of the organ of Corti: a review. In *Cellular Mechanisms in Hearing,* edited by Å. Flock and J. Wersäll (Elsevier, Amsterdam), pp 117-146.

Yost, W.A. and Nielsen, D.W. (1977). *Fundamentals of Hearing.* Holt, Rinehart and Winston, New York.